INTERNATIONAL STUDIES IN ENGINEERING

EDITORS

PROF. DR. COŞKUN ÖZALP

PROF. DR. SELAHATTİN BARDAK

March 2024

SERÜVEN YAYINEVİ

Genel Yayın Yönetmeni / Editor in Chief • C. Cansın Selin Temana

Kapak & İç Tasarım / Cover & Interior Design • Serüven Yayınevi

Birinci Basım / First Edition • © Mart 2024

ISBN • 978-625-6644-80-9

Serüven Yayınevi / Serüven Publishing
Türkiye Adres / Turkey Address: Kızılay Mah. Fevzi Çakmak 1. Sokak
Ümit Apt No: 22/A Çankaya/ANKARA
Telefon / Phone: 05437675765
web: www.seruvenyayinevi.com
e-mail: seruvenyayinevi@gmail.com

Baskı & Cilt / Printing & Volume
Sertifika / Certificate No: 47083

INTERNATIONAL STUDIES IN ENGINEERING

March 2024

Editors

PROF. DR. COŞKUN ÖZALP

PROF. DR. SELAHATTİN BARDAK

CONTENTS

CHAPTER 1

ANALYSIS OF TEC PREDICTION PERFORMANCE OF THE LATEST VERSION OF THE IRI MODEL (IRI-2020) OVER A TURKISH STATION

Salih ALCAY[1]
Sermet OGUTCU[2]
Gurkan OZTAN[3]

1 Necmettin Erbakan University, Geomatics Engineering Department, Konya, Turkey, salcay@erbakan.edu.tr
2 Necmettin Erbakan University, Geomatics Engineering Department, Konya, Turkey
3 Nigde Omer Halisdemir University, Bor Vocational School, Department of Land Registry and Cadastre, Bor, Nigde

1. INTRODUCTION

The ionosphere is an atmospheric region extending from about 50 km to 1000 km above the Earth's surface. The density of free electrons and ions that exist in the ionosphere affects high-frequency electromagnetic waves (Fagre et al. 2019). Since free electrons are lighter than free ions, they affect the propagation more. Thus, Total Electron Content (TEC) is an important ionospheric parameter that plays a significant role in positioning, communication, and navigational applications (Tariq et al. 2020). The electron density of the ionosphere changes due to regular (diurnal variations, seasonal changes, solar cycle, etc.) and irregular (geomagnetic activities, solar radiation storms, solar flares, Travelling Ionospheric Disturbances, etc.) variabilities. The accurate characterization of the ionosphere is a challenging task and the variations of the ionosphere and its effects on various applications need due attention.

To monitor the behavior of the ionosphere several data sources such as GNSS, Jason, Swarm, Cosmic RO, etc. are used. In addition to these data sources, various empirical models are also preferred in ionospheric studies. Among them International Reference Ionosphere (IRI) (Bilitza 2001), the Nequick model (Di Giovanni and Radicella 1990), and the IRI PLAS model (Gulyaeva and Bilitza, 2012, Arikan et al., 2015, Zakharenkova et al., 2015) are regularly being improved and updated.

The IRI is the most widely used standard empirical model for Earth's ionosphere. It was developed by COSPAR (Committee on Space Research) and URSI (International Union of Radio Science) working groups (Bilitza and Xiong, 2020). The latest version is IRI-2020. The performance of IRI has been assessed by many researchers in a comparative approach utilizing different versions of the model (Marew et al. 2024, He et al. 2023, Wang et al. 2023, Jenan et al. 2022, Liu et al. 2022, Alcay 2021, Pignalberi et al. 2021, De Dieu Nibigira et al. 2021, Tariq et al. 2020, Cehen et al. 2020, Arikan et al. 2019, Alcay et al. 2017, Inyurt et al. 2017, Zakharenkova et al. 2015, Luo et al. 2014, Nigussie et al. 2013). However, a minimal number of studies have been conducted on the performance of the latest IRI model. Among the most recent ones, Marew et al. (2024) evaluated the performance of IRI-2016 and IRI 2020 models in terms of TEC prediction over the equatorial region for geomagnetially active and quiet periods. It is found that although both versions are poor at predicting storm effect, IRI-2020 shows better agreement with the observed TEC during the geomagnetic active period. He et al. (2023) evaluated the Wuhan University GIM-TEC and IRI-2020 model TEC over the China region from 2008 to 2020. The comparison indicated that IRI-2020 TEC is lower than GIM TEC and the discrepancy is more obvious in low-latitude regions and during high solar conditions.

In this study, the TEC prediction performance of the IRI-2020 model was examined by comparing GPS TEC data. For this purpose, diurnal, seasonal, and yearly characteristics of IRI-2020 TEC over the KNYA (Turkey) station were validated.

The paper is arranged as follows: Details of the IRI-2020 model and GPS TEC are provided in the following section. The third section presents the diurnal, seasonal, and yearly results with a comparative approach. Then, the concluding points are provided in the final section.

2. DATA AND METHODS

2.1 IRI-2020

The IRI empirical model is the official standard ionosphere model developed and updated by COSPAR and URSI based on many ground and space-based data sources (Bilitza and Xiong, 2021). IRI provides various parameters including electron/ion temperature, ion composition, TEC, etc. for altitudes 50 km to 2000 km. The first IRI model was released in 1978, and then several improved versions have been released over the years (Bilitza et al. 2017, Alcay et al. 2017). The recent version of the model is IRI-2020. Bilitza et al. (2022) provides the new features of the recent version of the model. The details of the major updates of the model in terms of TEC and electron density based on Bilitza and Xiong (2021) and Friedrich et al. (2018) are provided in Marew et al. (2024).

2.2 GPS TEC

GPS TEC data can be obtained using both code and carrier phase observations. There are various software packages widely used in studies. In this study, ionolabtecv1.39 software was used to derive TEC values (http://www.ionolab.org/). Using this program, slant TEC (STEC) data are obtained for each satellite and then converted into VTEC values using a mapping function (Arikan et al. 2003, Nayir et al., 2007, Sezen et al., 2013). Details of this program in terms of TEC estimation are given in Arikan et al. (2003, 2004) and Nayir et al. (2007).

3. RESULTS AND DISCUSSION

To validate the TEC prediction of the IRI-2020 model, the location of a station from the northern hemisphere mid-latitude was used. The location and geographical coordinates of the station are provided in Figure 1 and Table 1, respectively.

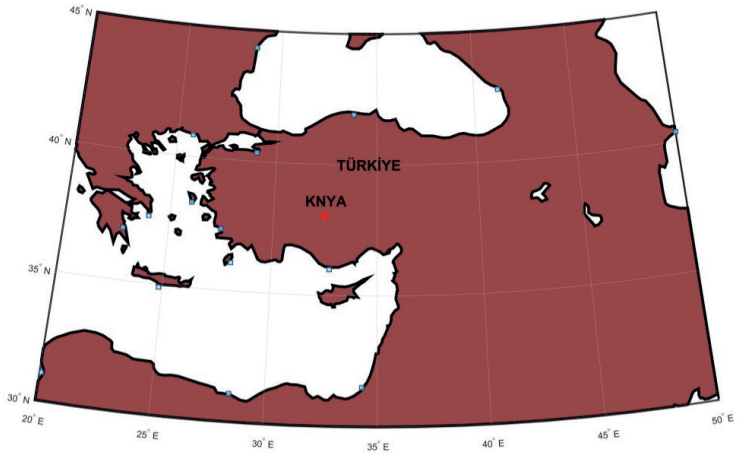

Figure 1. *The location of the KNYA station in Turkey*

Table 1. *Geographical coordinates of the KNYA sation*

Station Code	Country	City	Geographic Coordinates		
			Latitude ϕ (° ‘ “)	Longitude λ (° ‘ “)	Height h (m)
KNYA	TÜRKİYE	Konya	38 01 19.746753	32 30 18.840983	1205,6816

IRI-2020 TEC values were derived using NASA's Community Coordinated Modeling Center (CCMC) website (https://kauai.ccmc.gsfc.nasa.gov/instantrun/iri). In order to use GPS TEC values for validation, 1-year observation of KNYA CORS TR station was used. GPS TEC values were estimated using ionolabtecv1.39 software belonging to the Ionospheric Research Laboratory (IONOLAB) (http://www.ionolab.org/). Since the IRI model provides better results for geomagnetically quiet days, active days were removed from the comparison. Thus, the days when the kp index was above 5 were not taken into account (https://omniweb.gsfc.nasa.gov/).

To examine the diurnal performance of the model, seven consecutive geomagnetically quiet days (1-7 January 2023) were selected. The diurnal variation of the IRI-2020 TEC and GPS TEC derived on an hourly basis over KNYA stationare presented in Figure 2. The top, second, and third panels belong to kp, Dst, and F10.7 indices, respectively. Since 2023 is within the solar active period F10.7 values are above 140 sfu (Figure 2). The kp and dst indices, which indicate the magnitude of geomagnetic activity, show that this period is quiet however they reach threshold values on January 4, 2023. In the bottom panel of Figure 2, both IRI-2020 TEC and GPS TEC values are provided. It is seen that both results exhibit a similar trend. The mean of the absolute

differences is 3.2 TECU. The discrepancies are less than 10 TECU and larger values belong to noon hours. In addition, IRI-2020 TEC mostly overestimated the observed TEC during daylight hours. However, the differences tend to decrease during the slightly active period (January 4, 2023), when GPS TEC values increase.

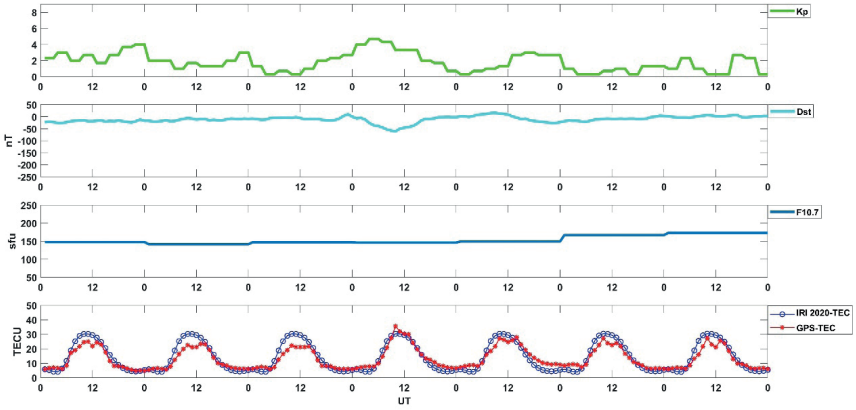

Figure 2. *Diurnal variation of TEC using IRI-2020 and GPS over KNYA station on January 1-7, 2023*

Besides the diurnal evaluation, the seasonally averaged TEC variability over the KYNA station for geomagnetically quiet days was derived on a three-hour basis and given in Figures 3-6. In the figures, the top panels show seasonal averaged TEC values corresponding to IRI-2020 model. The middle ones are observed TEC obtained from GPS observations. The bottom panels illustrate the TEC differences between GPS and model-based TEC. Due to the lack of GPS TEC data between 4 August to 20 September, this period was excluded from the comparison. Figure 3 gives the seasonal averaged IRI-2020 TEC and GPS TEC values and also TEC differences for December 2022 and January/February 2023. It is seen that model-based TEC and GPS TEC values are highly consistent and discrepancies are less than 5 TECU. Figure 4 gives the results corresponding to March-April-May period. Although both IRI-2020 TEC and GPS TEC results show similar trend, discrepancies are a little larger compared to the December-January-February results. The differences are mostly less than 7 TECU but reach ~10 TECU at 12 UT.

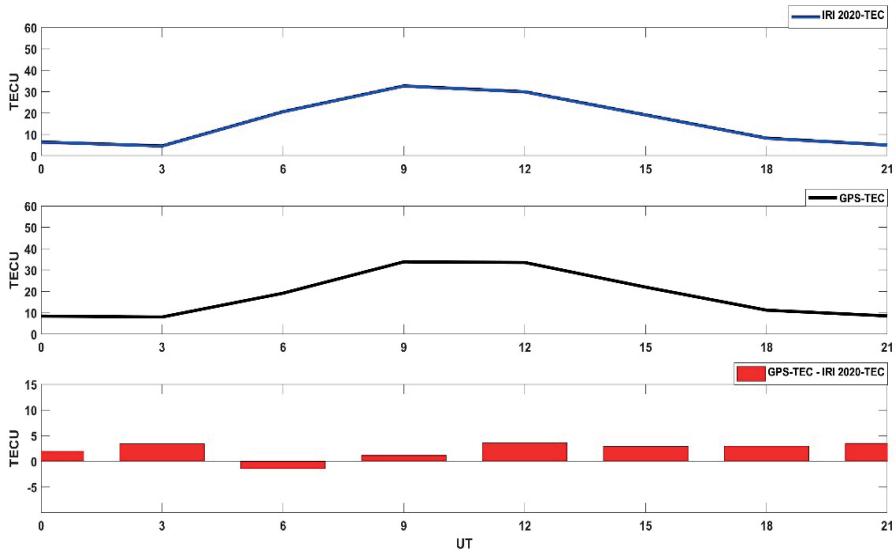

Figure 3. *Seasonal variation of IRI-2020 TEC and GPS TEC using average magnetic quiet days over KNYA station for December 2022 and January-February 2023*

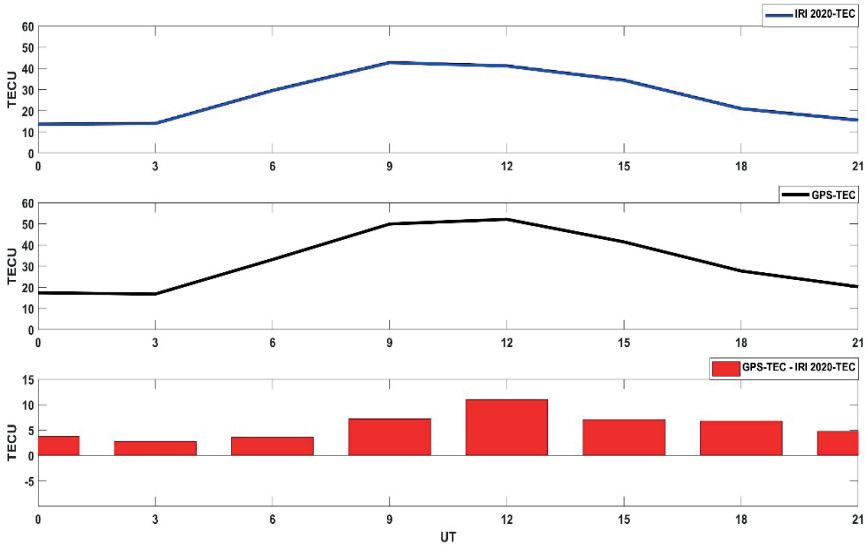

Figure 4. *Seasonal variation of IRI-2020 TEC and GPS TEC using average magnetic quiet days over KNYA station for March-April-May 2023*

Figure 5 illustrates the seasonal averaged TEC values belonging to the June-July-August period. It is seen that GPS and model-based TEC values are consistent and mostly less than 5 TECU. In Figure 6, the results corresponding

to September-October-November period are given. Figure 6 shows that differences are less than 5 TECU and mostly about 3 TECU levels. Although IRI-2020 TEC average values are slightly high at 6 and 9 UT, GPS TEC values are higher at other times.

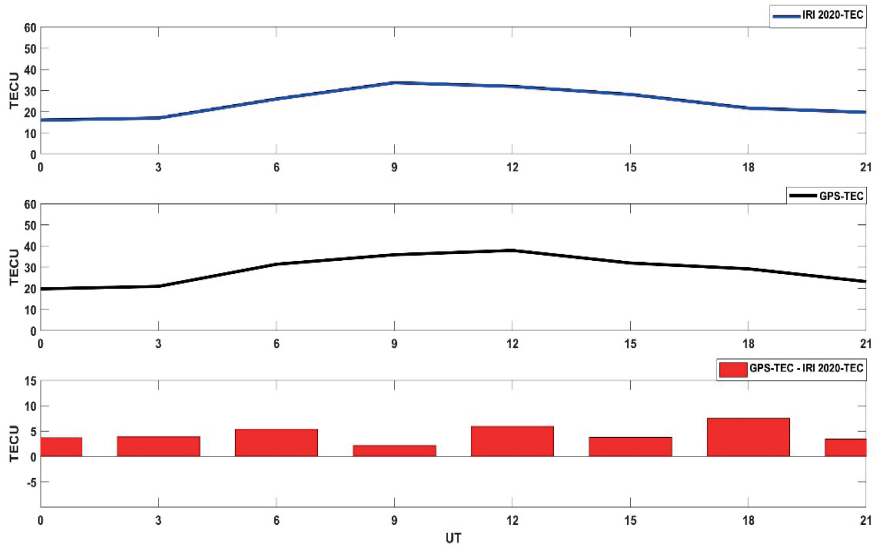

Figure 5. *Seasonal variation of IRI-2020 TEC and GPS TEC using average magnetic quiet days over KNYA station for June-July-August 2023*

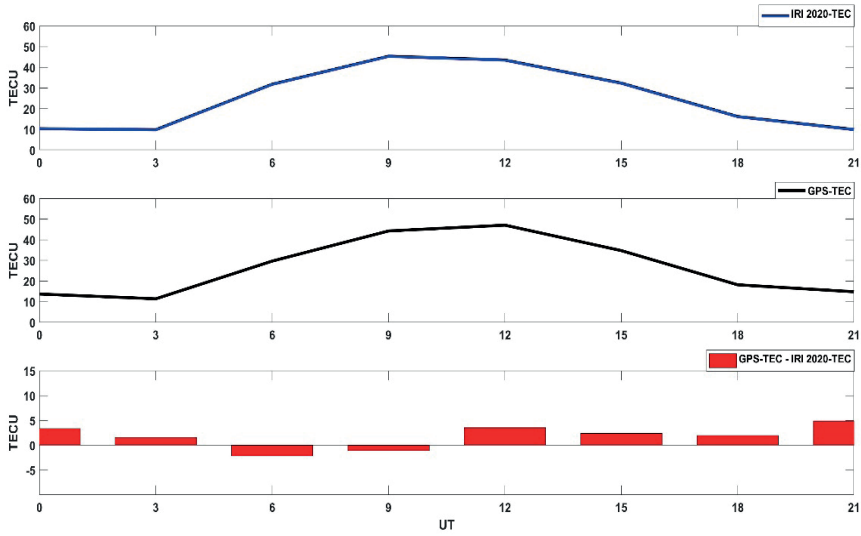

Figure 6. *Seasonal variation of IRI-2020 TEC and GPS TEC using average magnetic quiet days over KNYA station for September-October-November 2023*

The yearly variation of IRI-2020 TEC and GPS TEC for the quiet days from 1 December 2022 to 30 November 2023 are provided in Figure 7. It is seen that the results are consistent and show a similar trend. The averages of the discrepancies are generally below 4 TECU.

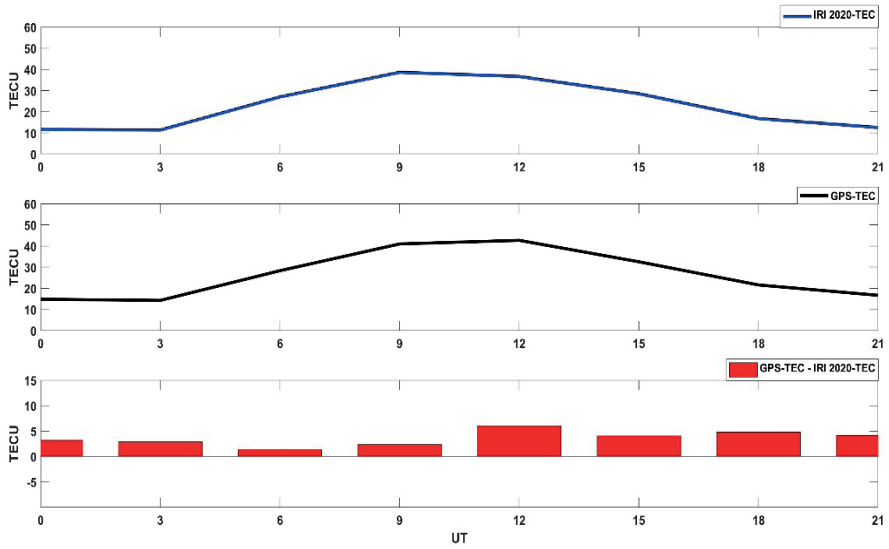

Figure 7. *Yearly variation of IRI-2020 TEC and GPS TEC using average magnetic quiet days over KNYA station from 1 December 2022 to 30 November 2023*

In order to further examine the differences some basic statistical values including absolute minimum, absolute maximum, absolute mean and range values were calculated for monthly basis and given in Table 2. Table 2 shows that absolute mean of differences are less than 5 TECU except March and October. The magnitude of the range values change according to the months. They are below 20 TECU in December, July, August and September. When the absolute minimum values are examined, it is seen that IRI-2020 and GPS can give the same TEC value. Besides the basic statistical values to evaluate the consistency and trend of the TEC values, the correlation coefficients between GPS TEC and IRI-2020 TEC were computed for diurnal, seasonal averaged and 1 year periods and given in Table 3. It is noticed that correlation coefficients are above %94 for all data sets. While it is %94.25 for diurnal, exceeds the %99 in the March-April-May period.

Table 2. *Basic statistical values corresponding to TEC differences on a monthly basis (December, 2022 to Novermber 2023)*

Statistical Value	Dec	Jan	Feb	Mar	Apr	May	Jun	July	Aug	Sep	Oct	Nov
Abs Min	0.00	0.05	0.00	0.00	0.00	0.00	0.00	0.00	0.00	0.00	0.09	0.00
Abs Max	12.36	23.88	23.06	39.30	20.47	20.47	20.47	14.02	9.46	13.36	20.81	23.07
Abs Mean	3.59	3.96	4.75	9.20	4.32	4.32	4.32	4.62	0.27	0.95	5.69	3.46
Range	19.85	32.00	30.95	55.23	28.98	28.98	28.98	19.00	13.56	19.16	20.72	34.59

Table 3. *Correlation coefficient between GPS TEC and IRI-2020 TEC*

Station	Period	Correlation Coefficients
KNYA	Diurnal	0.9425
	Dec 22-Feb 23	0.9889
	Mar 23-May23	0.9923
	June 23-Aug 23	0.9691
	Sep 23-Nov 23	0.9890
	1 Year	0.9918

4. CONCLUSIONS

This study evaluated the performance of the IRI-2020 model in terms of TEC prediction during quiet ionospheric conditions over a mid-latitude station. This is carried out by comparing model-based results with corresponding GPS TEC results. Besides the diurnal analysis including 7 consecutive days, seasonal, and yearly analyses have been performed. The December 2020 to November 2023 period was chosen for comparison. Diurnal results showed that IRI-2020 TEC mostly overestimated the GPS TEC. These are the periods when IRI-2020 TEC or GPS TEC values are larger, and when monthly and annual averages are taken into account, it has been observed that GPS TEC values are slightly higher. The absolute mean of differences between IRI-2020 and GPS TEC corresponding to 1 year period is 3.89 TECU. The empirical model-derived TEC and GPS TEC data are consistent and correlation coefficients range from ~0.97 to ~0.99 according to the different time periods.

ACKNOWLEDGEMENTS

We would like to thank the IRI Working group and Community Coordinated Modeling Center (CCMC) for IRI-2020 instant run access (https://kauai.ccmc.gsfc.nasa.gov/instantrun/iri/), Ionospheric Research Laboratory (IONOLAB) for the ionolabtecv1.39 software (http://www.ionolab.org/). We also thank the NASA/GSFC's OMNIWeb service for kp, Dst, and F10,7 indices (https://omniweb.gsfc.nasa.gov/), the General Directorate of Land Registry and Cadastre for providing CORS-TR daily observation data.

REFERENCES

Alcay, S., Oztan, G., Selvi, H.Z. Comparison of IRI_PLAS and IRI_2012 model predictions with GPS_TEC measurements in different latitude regions. Annals of Geophysics, 60 (5), G0549, 2017, https://doi.org/10.4401/ag-7311.

Alcay, S. Analysis of the TEC prediction performance of IRI-2016 model in the mid-latitude region, Geomagnetism and Aeronomy, 61, 600-618, 2021, https://doi.org/10.1134/S0016793221040149.

Arikan, F., Erol, C.B., and Arikan, O. Regularized estimation of vertical total electron content from Global Positioning System data, Journal of Geophysical Research, 108, A12, 1469, 2003, https://doi.org/10.1029/2002JA009605.

Arikan, F., Erol, C.B., and Arikan, O., Regularized estimation of vertical total electron content from GPS data for a desired time period, Radio Science, 39, no.RS6012, 2004, https://doi.org/10.1029/2004RS003061

Arikan, F.,Sezen, U., Gulyaeva T.L., Cilibas O. Online, automatic, ionospheric maps: IRI_PLAS-MAP, Advances in Space Research, 55 (8), 2106–2113, 2015, https://doi.org/10.1016/j.asr.2014.10.016.

Arikan, F., Sezen, U., Gulyaeva, T.L. Comparison of IRI-2016 F2 layer model parameters with ionosonde measurements. Journal of Geophyical Research 124 (10), 8092–8109, 2019. https://doi.org/10.1029/2019JA027048.

Bilitza, D. International reference ionosphere 2000. Radio Science, 36(2), 261-275, 2000. https://doi.org/10.1029/2000RS002432.

Bilitza, D., Altadill, D., Truhlik, V., Shubin, V., Galkin, I., Reinisch, B., Huang, X. International Reference Ionosphere 2016: From ionospheric climate to real-time weather predictions. Space Weather 15, 418–429, 2017, https://doi.org/10.1002/2016SW001593.

Bilitza, D., & Xiong, C. A solar activity correction term for the IRI topside electron density model. Advances in Space Research, 68(5), 2124-2137, 2021, https://doi.org/10.1016/j.asr.2020.11.012.

Bilitza, D., Pezzopane, M., Truhlik, V., Altadill, D., Reinisch, B. W., & Pignalberi, A. The International Reference Ionosphere model: A review and description of an ionospheric benchmark. Reviews of Geophysics, 60(4), e2022RG000792, 2022 https://doi.org/10.1029/2022RG000792.

Chen, J., Ren, X., Zhang, X., Zhang, J., & Huang, L. Assessment and validation of three ionospheric models (IRI-2016, NeQuick2, and IGS-GIM) from 2002 to 2018, Space Weather, 18, e2019SW002422, 2020, https://doi.org/10.1029/2019SW002422.

De Dieu Nibigira, J., Sivavaraprasad, G., & Ratnam, D. V. Performance analysis of IRI-2016 model TEC predictions over Northern and Southern Hemispheric IGS stations during descending phase of solar cycle 24, Acta Geophysica, 69(4), 1509–1527, 2021, https://doi.org/10.1007/s11600-021-00618-1.

Di Giovanni, G, Radicella, SM. An analytical model of the electron density profile in the ionosphere, Advances in Space Research, 10 (11), 27-30, 1990 https://doi.org/10.1016/0273-1177(90)90301-F.

Fagre, M., Zossi, B.S., Chum, J., Yiğit, E., Elias, A.G., Ionospheric high frequency wave propagation using different IRI hmF2 and foF2 models, Journal of Atmospheric and Solar-Terrestrial Physics, 196, 105141, 2019, https://doi.org/10.1016/j.jastp.2019.105141.

Friedrich, M., Pock, C., Torkar, K. FIRI-2018, an updated empirical model of the lower ionosphere, Journal of Geophysical Research, Space Physics, 123 (8), 6737–6751, 2018, https://doi.org/10.1029/2018JA025437.

Gulyaeva, T.L., & Bilitza, D. Towards ISO standard earth ionosphere and plasmasphere model. New developments in the standard model, 1-39, edited by R.J. Larsen, 1-39, 2012. NOVA, Hauppauge, New York.

He, R., Li, M., Zhang, Q., & Zhao, Q. A Comparison of a GNSS-GIM and the IRI-2020 model over China under different ionospheric conditions. Space Weather, 21, e2023SW003646, 2023, https://doi.org/10.1029/2023SW003646.

Inyurt, S., Yildirim, O., & Mekik, C. Comparison between IRI-2012 and GPS-TEC observations over the western Black Sea, Annals of Geophysics, 35, 4, 817-824, 2017, https://doi.org/10.5194/angeo-35-817-2017.

Jenan, R., Dammalage, T. L., & Panda, S. K. Ionospheric TEC response to severe geomagnetic storm and annular solar eclipse through GNSS based TEC observations and assessment of IRI-2016 model and global ionosphere maps over Sri Lankan equatorial and low latitude region. Astrophysics and Space Science, 367(2), 24, 2022, https://doi.org/10.1007/s10509-022-04051-8.

Liu, J., Jia, X., Zhu, Y., Xu, J., Fu, J., Zhang, R., & He, Y. Comparing GNSS TEC data from the African continent with IRI-2016, IRI-Plas, and NeQuick predictions. Advances in Space Research, 69(7), 2852-2864, 2022, https://doi.org/10.1016/j.asr.2022.01.008.

Luo, W., Liu, Z., & Li, M. A preliminary evaluation of the performance of multiple ionospheric models in low-and mid-latitude regions of China in 2010–2011. GPS solutions, 18, 297-308, 2014, https://doi.org/10.1007/s10291-013-0330-z.

Marew, H., Agmas, A., & Mersha, T. Performance evaluation for vertical TEC predictions over the East Africa and South America: IRI-2016 and IRI-2020 versions. Advances in Space Research, 73(1), 698-715, 2024, https://doi.org/10.1016/j.asr.2023.09.055.

Nayir, H., Arikan, F., Arikan, O., and Erol, C.B. Total electron content estimation with Reg-Est, Journal of Geophysical Research, Space Physics, 112, A11, 2007, https://doi.org/10.1029/2007JA012459.

Nigussie, M., Radicella, S. M., Damtie, B., Nava, B., Yizengaw, E., & Groves, K. Validation of the NeQuick 2 and IRI-2007 models in East-African equatorial region. Journal of Atmospheric and Solar-Terrestrial Physics, 102, 26-33, 2013, https://doi.org/10.1016/j.jastp.2013.04.016.

Pignalberi, A., Pietrella, M., Pezzopane, M. Towards a Real-Time Description of the Ionosphere: A Comparison between International Reference Ionosphere (IRI) and IRI Real-Time Assimilative Mapping (IRTAM) Models. Atmosphere, 12, 1003, 2021, https://doi.org/10.3390/atmos12081003.

Sezen, U., Arikan, F., Arikan, O., Ugurlu, O., Sadeghimorad, A. Online, automatic, near-real time estimation of GPS-TEC: IONOLAB-TEC. Space Weather 11, 297–305, 2013, https://doi.org/10.1002/swe.20054.

Tariq, M. A., Shah, M., Inyurt, S., Shah, M. A., & Liu, L. Comparison of TEC from IRI-2016 and GPS during the low solar activity over Turkey. Astrophysics and Space Science, 365, 1-13, 2020, https://doi.org/10.1007/s10509-020-03894-3.

Wang, J., Yu, Q., & Shi, Y. Comparison of observed hmF2 and the IRI-2020 model for six stations in East Asia during the declining phase of the solar cycle 24. Advances in Space Research, 2023, https://doi.org/10.1016/j.asr.2023.12.001.

Zakharenkova, I.E., Cherniak, I.V., Krankowski, A.,Shagimuratov, I.I. Vertical TEC representation by IRI_2012 and IRI Plas models for European mid-latitudes. Advances in Space Research, 55, 2070-2076, 2015. https://doi.org/10.1016/j.asr.2014.07.027.

CHAPTER 2

RESEARCH ON FIBER REINFORCED COMPOSITE MATERIALS AND PRODUCTION TECHNOLOGIES

Buket ERZEN[1]
Mukaddes KARATAŞ[2]
Ercan AYDOĞMUŞ[3]

1 Dr. Department of Chemical Engineering, Engineering Faculty, Fırat University, Elazığ, Türkiye, ORCID: 0000-0001-5098-7171, E-mail: bcetintas@firat.edu.tr
2 Dr. Department of Chemical Engineering, Engineering Faculty, Fırat University, Elazığ, Türkiye, ORCID: 0000-0001-5803-6821, E-mail: ercanaydogmus@firat.edu.tr
3 Dr. Department of Chemical Engineering, Engineering Faculty, Fırat University, Elazığ, Türkiye, ORCID: 0000-0002-1643-2487, Corresponding Author E-mail: ercanaydogmus@firat.edu.tr

History of Composite

'Materials formed by the combination of two or more macro-different components across an interface' is a brief definition of composite materials. Most of the constituent parts of the composite material retain their original characteristics [1].

The word composite is etymologically a word of French origin. Contrary to popular belief, the history of composite materials, which are widely used in many areas today, does not date back to World War II or several centuries back. Composite materials have been used for thousands of years and the first examples date back to ancient times. Since ancient times, people have tried to strengthen these fragile materials by adding fibers of animal or vegetable origin into them. The most common and oldest known example of this. Straw and straw mixed into the mud gave strength to this material and allowed human beings to build solid shelters.

Over time, human beings have become aware of the advantages of composite materials and have expanded their usage areas. The Mongols eliminated this problem by using animal tendons with different fiber directions in the flexible parts of the bow. At the same time, the Umayyads and Spartans combined natural fibers such as hemp with tree resins to produce war equipment such as helmets, armor, and shields. An ancient example of the use of composites can be given from Egypt. It reveals that fine glass fibers were made in Egypt in the 1600s [3, 4].

Industrial applications of fiber-reinforced synthetic resins date back to the mid-1950s. The substance known as "glass fiber reinforced polyester resin composite" is the most well-known category. Since the early 1960s, this material as "fiberglass" in our nation has been utilized in Turkey for the production of small sea boats, roof sheets, and liquid tanks.

The first domestically produced automobile was produced from this material. Synthetic resin main (matrix) materials reinforced with glass fibers are called "Glass Reinforced Plastic (GRP)". In the production of glass reinforced plastics, in addition to polyester, which is the most commonly, used material, thermosetting and thermoplastic resins are also used [4].

In an experimental study, they assessed the impact of hybridization between jute-reinforced composites and other textiles on the tensile, bending, in-plane shear, interlaminar shear, and bearing tests, as well as flexural modulus and similarly, an increase in the interlayer shear strength has been noted [5].

Aishe et al. studied the use of micro silica and granulated blast furnace slag comprising steel fiber and polypropylene fiber in ultra-high performance geopolymer concrete. The findings demonstrate that the mechanical properties

of samples containing steel fiber are enhanced when polypropylene fiber is present. Furthermore, the outcomes demonstrate that substituting steel fiber for polypropylene fiber lowers mechanical strength while boosting durability [6].

In another study conducted in the literature was to examine the modulus of elasticity, impact strength, and tensile strength of polypropylene-based nanocomposites reinforced with basalt fibers, nanoclay, and graphene nanosheets. The results showed that the addition of low-weight graphene nanosheets raised the tensile and impact strengths by 15% and 20%, while the inclusion of basalt increased the tensile strength (32%), modulus of elasticity (64%), and impact strength (18%). The experiment's mechanical property values are found to be relatively close to the information gleaned by attractiveness optimization [7].

Suzaki et al. investigated the physical properties of a fiber-reinforced CAD/CAM resin disc containing layers woven from multi-directional glass fibers and demonstrated that TRINIA showed significant anisotropy and that TRINIA could be used as a superior restorative material when orienting fiber network layers [8].

In their study, Furtos et al. created new wood fiber reinforced geopolymer composites with the addition of sand at room temperature through the combination of powdered fly ash, sand, and randomly reinforced wood fiber with alkaline activators such as sodium hydroxide and silicate. They concluded that it could be a promising green material [9].

Abbass et al. conducted a study to examine the impact of varying steel fiber sizes and lengths on the mechanical properties of concrete across three concrete strength values. The findings demonstrated that varying the amount and length of steel fibers in addition to raising the water/cement ratios significantly altered the mechanical characteristics of concrete, leading to increases in compressive strength of roughly 10-25% and 31-47%, respectively [10].

The specific properties of some natural fibers are suitable for producing commercial composite products. Among these, jute, flax, sisal, ramie, bamboo, hemp, abaca, coconut, and sisal have an important place. Such fibers are reinforced in polymer matrices [11].

Depending on the developments in the industry, traditional materials alone have become unable to meet the needs of developing technology. Accordingly, today, research and development activities on the production of composite materials and the properties of the obtained materials continue to increase. The need for lightweight and durable materials, especially in aviation, military application areas, automotive, and maritime industries,

constitutes an important driving force for this research. Because pure materials are insufficient, composite materials have been developed as a result of technological advancements, and their applications have grown throughout time. Fiber-reinforced composite materials offer excellent mechanical strength, flexibility, resistance to corrosion, and cost-effectiveness. Because of their properties, they are widely used around the world. Studies have shown that natural fibers and fillers have been successfully incorporated into composite materials with different production methods. It is seen that they can be used, have an improving effect on material properties, and reduce costs.

Composite Structures

Generally speaking, the materials are divided into three categories: organic, metal, and ceramic materials. There are benefits and drawbacks to these three material classes. A composite material is created by mixing two or more of these components at a macro level to combine their superior properties into a single material, depending on technological advancements. Composite materials are made to improve one or more of some of the properties of traditional materials, which are briefly explained below [12].

Three features are generally sought in composite materials:

- ✓ Being a mixed material that will meet the desired technical specifications
- ✓ Bringing together at least two materials with different chemical compositions separated by certain interfaces,
- ✓ It has properties that none of the components have or could have on their own.

Composite material consists of a matrix main phase and it consists of dispersed reinforcement elements.

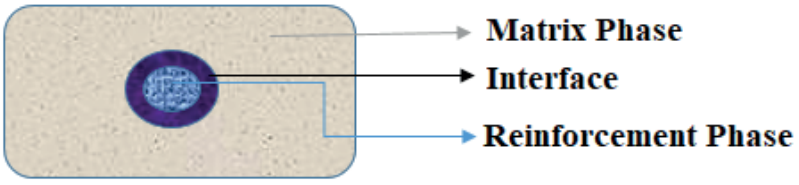

Figure 1. *Components of composite material schematically*

In a composite, reinforcement materials are embedded with the matrix. The reinforcement material's role is to increase strength and stiffness and to ensure that the matrix retains its shape and interfaces the load from carrying the maximum load, which can be transferred to the reinforcement materials through responsibility. High-performance materials sufficiently resist

compression or transverse load. Since they are not sensitive, they cannot form composites on their own. In this way, the matrix holds the fibers together and provides the necessary protection against environmental aggressions [13-16].

The advantages of production and use of composite materials

- ☆ High strength (fatigue and wear resistance, bending and tensile strength)
- ☆ Rigidity
- ☆ Lightness
- ☆ Resistance to corrosion and chemical effects
- ☆ Fracture toughness
- ☆ High-temperature resistance
- ☆ Easily shaped structure
- ☆ Aesthetic appearance

Some disadvantages of composite materials

- ☆ Production cost
- ☆ Damage assessment
- ☆ Manufacturing difficulty
- ☆ They are not recyclable
- ☆ Low elongation at break
- ☆ Fragile structures

Application Areas of Composites

- ☆ Space technology
- ☆ Maritime industry
- ☆ In the field of medicine (Manufacture of medical devices)
- ☆ Robotics
- ☆ Chemical industry
- ☆ Electrical-Electronic technology
- ☆ Musical instruments industry
- ☆ Automotive industry
- ☆ Defense Industry and Aviation Sector
- ☆ Food and Agriculture Sector

☆ It is used in many areas such as

Classification of Composites

Composite materials can be broadly categorized into two distinct categories [17].

☆ Classification based on matrices

☆ Classification based on reinforcement

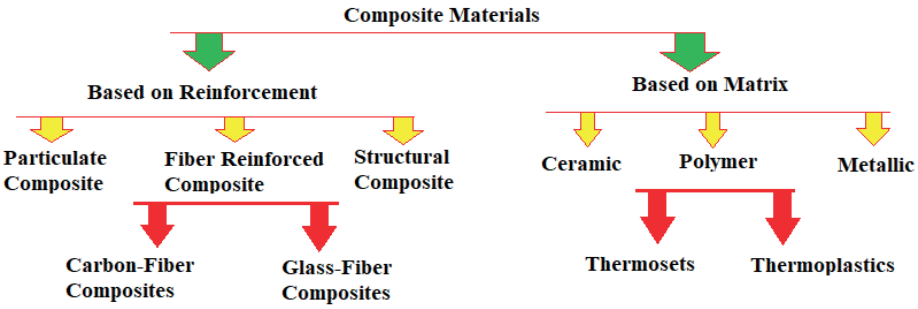

Figure 2. *Classification of composite materials*

Structural Composites

Structural composites are multilayer composite materials. These types of composites can be examined in 2 classes;

- Layered composites and
- Sandwich panels.

Particle Reinforced Composites

Particulate composites are made up of one material's particles scattered throughout a second material's matrix. Although particles can be any size or shape, they are typically irregularly shaped, spherical, ellipsoidal, or polyhedral. They can be cultivated in situ by a reaction like aging, added to a liquid matrix that solidifies, or crushed and then dispersed together using a powdered method [18].

Fiber Reinforced Composite Materials

They are composites formed by the combination of polymer matrix and fiber reinforcement. Reinforcement material choices range from synthetic fibers to organic fibers. The length and orientation of the fiber can be classified. Fiber reinforcement on the polymer matrix seriously improves the mechanical properties of the composite [19].

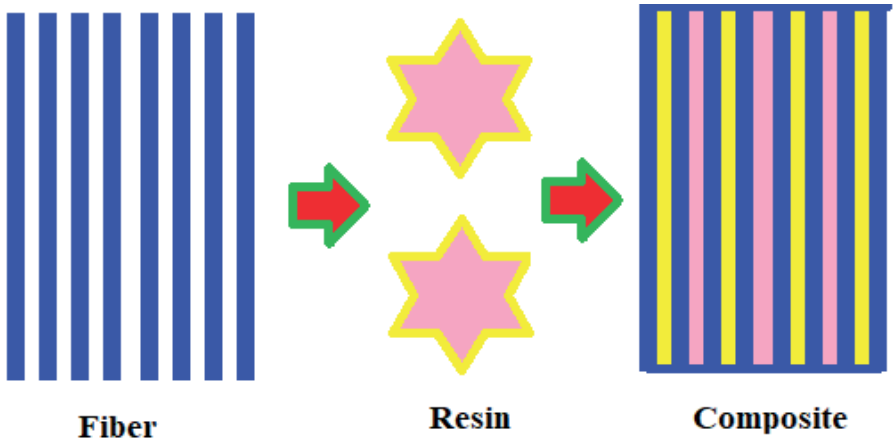

Figure 3. *Formation of fiber reinforced composite*

The most often utilized reinforcing materials in these composites, which play a significant role in the creation of contemporary composites, are glass, carbon, and aramid fibers [20].

When fibers with high elasticity are added into the soft and ductile matrix of fiber reinforced composites, tensile strength, fatigue strength, specific modulus, and specific strength properties are improved. The matrix material provides softness and toughness by transferring the force to the fibers, while the fibers absorb the applied load carries most of them. Unlike composites whose hardness is increased by precipitation, the strength of the composite is increased both at room and at elevated temperatures.

Chemical corrosion can also be resisted by fibers with high hardness, high elastic modulus, and low density. Fibers with very different dimensional and formal properties are used in composite reinforcement. For example, fibers such as glass fibers are prepared into bundles during production [21].

In fiber reinforced composite materials, the primary function of fibers is to increase strength and rigidity by carrying the load. According to ASTM, for a material to be called a fiber;

- Average length/width is at least 10 mm

- Largest cross-section at least 0.05 mm^2

- The largest width must meet the conditions of at least 0.25 mm.

Continuous fiber is also called roving or filament. The name wire is used for metal fibers. If the width/thickness ratio in the cross-section of a fiber is 4/1, it is called a sliver [22].

Fibers are divided into two types (natural and artificial)

Natural fibers (NFs) are a material found in nature that is easily obtained and readily available (Figure 4). They exhibit certain exceptional material qualities, including high strength, particular hardness, biodegradability, and low cost per unit volume. Reinforcements such as glass fiber, carbon fiber, sisal, and flax are used in composite materials. The use of natural fibers such as is increasing day by day. Increases in environmental pollution resulting in biodegradability, recycling due to its properties such as convertibility, and natural fiber reinforced composites are preferred. Although plant fibers are mostly used as natural fibers, silk fiber, which is an animal fiber, is also used in small amounts. In studies, generally, jute, hemp, kenaf, sisal, and wood fibers are the most important fibers used in composite materials due to their important mechanical properties. Also as an herbal fiber supplement; Cotton fiber and flax fiber are the most commonly used fibers in the textile industry [23, 24].

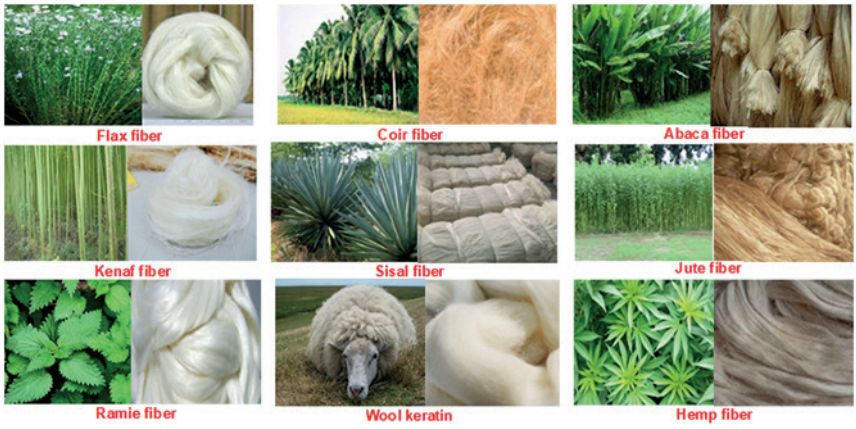

Figure 4. *Some examples of natural fiber types*

Synthetic fibers are artificial fibers generated by chemical synthesis; they are further divided into organic and inorganic categories according to their composition [25]. Their production is increasing day by day. Its low cost is seen as an advantage. As a result of the rapid increase in the world population and the resulting consumption needs, natural fibers began to fail to meet the needs and a trend toward artificial fibers began has started [26].

Mixed (hybrid) fibers: This sort of structure is present in the composite if it has two or more fiber types besides the matrix material. It is called a mixed (hybrid) composite. Although it varies depending on the fibers used as reinforcement in hybrid structured composites, higher strength properties can be achieved compared to single fiber composites [27]. The main fibers used in composite materials can be listed as follows:

✓ **Glass fibers**

In glass fiber production, various stones combine in liquid form at a temperature of approximately 1600 °C to form glass. This liquid passes through very thin barrels and forms glass fiber threads with diameters of 9 to 25 microns. These threads combine tightly to form fibers or loosely wicks. These are then coated with various chemicals to create the adhesion properties of the threads and increase their resistance to abrasion. The fiber shows good chemical resistance and easy processability. Tensile strength is excellent. However, they may deteriorate when exposed to long-term loads. Different types of glass fiber can be created depending on the types of stones used [28].

✓ **Boron fibers**

Boron fiber produced by chemical vapor deposition in monofilament reactors has high strength, and high modulus and ıt exhibits a wide range of unique combinations. On a thin tungsten wire substrate, elemental boron is deposited to achieve diameters of 142 microns and 102 microns. The resultant fiber has a tungsten core and is essentially amorphous boron. In resin matrix composites, the textured surface offers a great interface and does away with the necessity for sizing processes [29].

✓ **Silicon carbide fibers**

Titanium matrix is frequently utilized with these fibers. In jet engine parts, they are utilized in an alloy matrix consisting of titanium, aluminum, and vanadium. On the other hand, boron fibers are less dense than silicon carbide fibers. Low-density fibers are obtained by covering a carbon core with silicon carbide [30].

✓ **Alumina fibers**

Aluminum oxide (Al_2O_3) is the primary constituent of high-performance inorganic fiber known as alumina fiber. Its structure includes trace amounts of SiO_2, MgO, and other elements. Alumina fiber is widely utilized in aerospace, high-temperature insulation, and catalyst carrier areas because of its exceptional chemical stability, very low thermal conductivity, and remarkable heat resistance [31].

✓ **Aramid fibers**

Long-chain polymers called polyamides have six carbon atoms bound to one another by hydrogen atoms in their chemical structure. Because of their low compressive strength, they are used as hybrid composites with carbon fibers on control surfaces in airplane structures. There is no electrical conductivity in aramid fibers. Kevlar/epoxy composites have low moisture absorption qualities in addition to poor compressive strength [32].

✓ **Carbon fibers**

Carbon fibers are a type of synthetic carbon. Carbon fibers can be defined as materials with high modulus, high strength by weight, and high thermal conductivity. Additionally, carbon fibers have a coefficient of thermal expansion close to zero. Carbon fibers contain approximately 92% carbon. Their structure consists of an irregular arrangement from small two-dimensional graphitic domains to partially crystallized and disordered amorphous domains [33, 34].

Organic or Inorganic Reinforced Composites

In studies conducted in the literature, many organic and inorganic types of filler are reinforced into composites to produce economical and environmentally friendly materials. In particular, the use of waste polymers that are difficult to recycle improves some thermophysical properties of composites. Such fillers are preferred to produce composites with low density and low thermal conductivity coefficient [35-42].

For example, the use of industrial inorganic boron plant components in composites contributes to thermally stable materials. If it is desired to increase the density and porosity of the composite material, such fillers are preferred. However, using high amounts of such additives in the composite may lead to undesirable and negative effects. Properties of the composite such as pore distribution, surface morphology, matrix structure, and mechanical strength may be damaged [43-45].

The use of micro and nano fillers is becoming increasingly common in research in the literature. Nano-sized additives can provide high mechanical strength even if used in low amounts. In addition, conductive nano fillers are preferred to increase the thermal conductivity of composites depending on the intended use. It is known that functional nanocomposites have become especially widespread in the defense industry and electronic material production. In the future, semiconductor polymers will be used instead of metals [46-50].

In research, composites made with bioadditives and fillers can be used as an alternative to petrochemical raw materials. The use of environmentally friendly and renewable resources in the production of biocomposites is becoming increasingly common. With the decrease in fossil resources, the synthesis of bioraw materials instead of petrochemical raw materials is targeted in the future. Utilization of organic wastes in biocomposite production is also an important gain in economical biomaterial production. The use of petrochemical raw materials is also decreasing, especially with the use of fibrous plants in obtaining biocomposites. Many studies are available in the literature on the production of biocomposites by physical and chemical modification of biomass wastes and vegetable oils [51-59].

Basic Processes in Composite Production

- Impregnation
- Deposit
- Combining
- Hardening

Thermoset Composite Production Methods

- Hand deposit method
- Spray method
- Bag molding method
- Fiber wrapping
- Resin transfer molding method
- Pultrusion profile drawing process
- Structural reaction injection molding process
- Continuous plate method hand lay-up method

This method involves placing fibers/fabrics manually into a mold. The mold is formed as a result of resin impregnation with a roller or brush. It is the process of giving the shape. The mold surface is typically in contact with the outer surface of the part. The mold to be used can be a flat plate or it can be made of infinite edges and curves. First, the mold release agent puts the glass fiber part into the mold. It is applied to prevent sticking. Then colored gel coat, which is a resin, surface coating resin, adds color to the part. It is applied to the mold to give it. Then glass fiber and polyester resin are applied in accelerator layers and these layers spread the resin homogeneously and eliminate air pockets. It is pressed with rollers. Multilayer glass fiber and resin are deposited until the desired thickness is achieved. It is applied to fabrics in layers and depends on the properties of the fabric. Resin can be applied to multiple layers at the same time. Later resin impregnated fabrics at room temperature and atmospheric pressure to dry under different temperatures and pressures. The parts whose drying process is completed are removed from the mold, and operations such as cutting, deburring, and painting (Figure 5). They are then ready for use [60, 61].

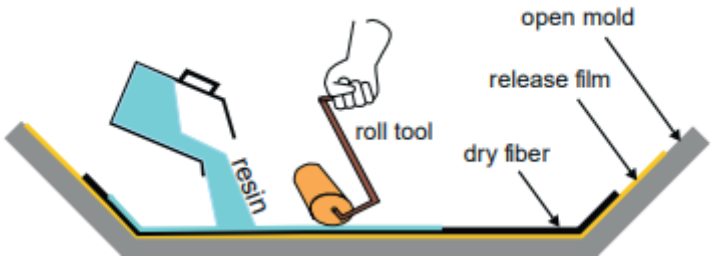

Figure 5. *Hand layup process*

Spraying Method

The spray method is the mechanized version of the hand lay-up method. In this method, cut fibers and resins are applied to the mold simultaneously. It is possible to produce more complicated shapes in the spraying method compared to the hand-laying method (Figure 6). With the manual rolling process, air bubbles that may occur after spraying are removed and the fibers are tightened [62].

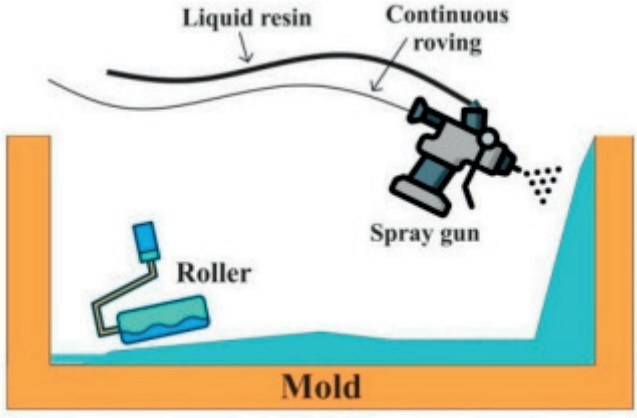

Figure 6. *Spraying method*

Autoclave Molding Method

Closed environments operating at high pressure and temperature are autoclave environments. By applying heat and pressure simultaneously, the laminates prepared before the process are consolidated, trapped air, if any, is removed and the thermosetting resin is cured (Figure 7). As a result of this process, it is possible to obtain high-quality products. It is a costly application [63].

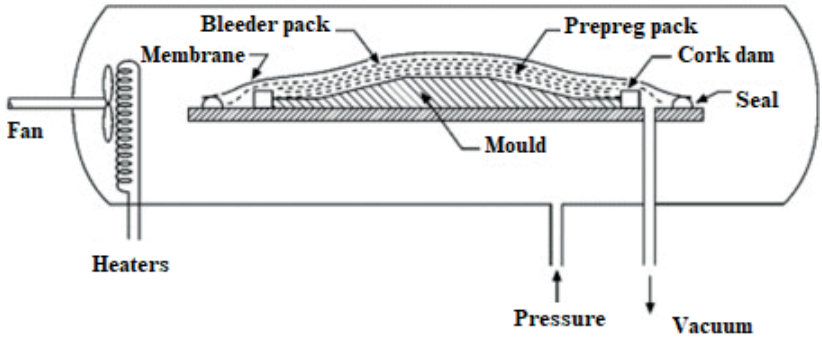

Figure 7. *Autoclave molding method*

Fiber Wrapping Method

In this method, continuous fibers pass through the resin and are coated on the part covered by the separator. This composite production technique is semi-automatic. With the fiber winding method, it is possible to produce PMK with a very high fiber ratio and high strength. Since it is a semi-automatic method, production can be done with fewer employees. It allows high fiber usage. Repetitive material production can be done. It is very difficult to produce complex shapes or very small parts (Figure 8). Although not as costly as autoclaving, it is a costly method [64,65].

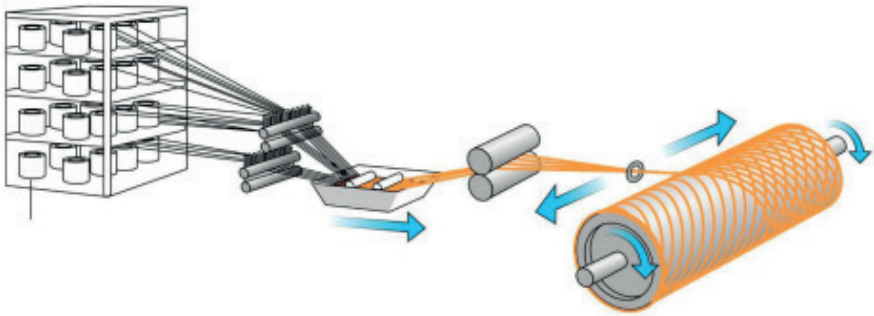

Figure 8. *Fiber wrapping method*

CONCLUSION

The most unique and promising materials of this century are composites. These days, composites reinforced with natural or synthetic fibers are becoming more and more common. The market is expanding and lightweight materials with high strength are becoming more and more necessary for specific applications. In addition to its exceptional strength, fiber-reinforced polymer composites exhibit remarkable qualities like weight

ratio, high durability, hardness, damping, and bending strength. They also offer resistance to fire, abrasion, corrosion, and impact. Because of these qualities, composite materials are being used in a wide range of industries, including the manufacturing, biomedical, automotive, and aerospace sectors. The components that make up composite materials and their manufacturing process have a major impact on their quality. This calls for an analysis of the production processes employed in the creation of composite materials as well as the functional characteristics, classifications, and classifications of the numerous fibers that are readily available throughout the world. The exceptional performance of fiber-reinforced composite materials in numerous application areas has made them a possible substitute for metals or alloys alone.

The scientific community is now interested in renewable resources to generate structural element materials in an environmentally responsible manner due to the depletion of oil supplies and changing climate. Numerous research studies on the evolution of composite materials have ushered in a new era by examining the feasibility of substituting non-biodegradable plastics most cost-effectively to reduce environmental risks.

Nevertheless, the poor mechanical and chemical stability of composites prevents them from being effectively used in end-use applications. The depth of potential for developing a polymer matrix composite that satisfies structural design requirements while being both economical and environmentally benign has been investigated in recent studies. Today's researchers can better concentrate on the new developments in composite materials by doing a thorough literature review on polymer matrix composites.

REFERENCES

[1] Rosato, D. V. (1997). Designing with reinforced composites: technology, performance, economics.

[2] Reingold, N., Park, J., & Rice, J. (1962). Materials research chronology, 1917-1957. Directorate of Materials and Processes, Aeronautical Systems Division, Wright Patterson Air Force Base.

[3] Hummel, R. E., (1997). Understanding Materials Science: History, Properties, Applications, Springer-Verlag, USA.

[4] Dolanay, S. S. (2023). A Historical Approach on the Opportunity to Acquire Technology Development Capability in Turkish Automobile Industry. Management, 11(3), 175-180.

[5] Allah, M. M. A., Hegazy, D. A., Alshahrani, H., Sebaey, T. A., & El-baky, M. A. A. (2023). Fiber metal laminates based on natural/synthesis fiber composite for vehicles industry: an experimental comparative study. Fibers and Polymers, 24(8), 2877-2889.

[6] Aisheh, Y. I. A., Atrushi, D. S., Akeed, M. H., Qaidi, S., &Tayeh, B. A. (2022). Influence of polypropylene and steel fibers on the mechanical properties of ultra-high-performance fiber-reinforced geopolymer concrete. Case Studies in Construction Materials, 17, e01234.

[7] Thongchom, C., Refahati, N., RoodgarSaffari, P., RoudgarSaffari, P., Niyaraki, M. N., Sirimontree, S., & Keawsawasvong, S. (2021). An experimental study on the effect of nanomaterials and fibers on the mechanical properties of polymer composites. Buildings, 12(1), 7.

[8] Suzaki, N., Yamaguchi, S., Hirose, N., Tanaka, R., Takahashi, Y., Imazato, S., & Hayashi, M. (2020). Evaluation of physical properties of fiber-reinforced composite resin. Dental Materials, 36(8), 987-996.

[9] Furtos, G., Silaghi-Dumitrescu, L., Pascuta, P., Sarosi, C., & Korniejenko, K. (2019). Mechanical properties of wood fiber reinforced geopolymer composites with sand addition. Journal of Natural Fibers.

[10] Abbass, W., Khan, M. I., & Mourad, S. (2018). Evaluation of mechanical properties of steel fiber reinforced concrete with different strengths of concrete. Construction and building materials, 168, 556-569.

[11] Rohit, K., & Dixit, S. (2016). A review-future aspect of natural fiber reinforced composite. Polymers from Renewable Resources, 7(2), 43-59.

[12] Wang, R. M., Zheng, S. R., & Zheng, Y. G. (2011). Polymer matrix composites and technology. Elsevier.

[13] Bulut, M. (2014).Composite material production in Turkey and general evaluation of the composite material sector. Master's Degree Graduation Project, Ankara, 47-70.

[14] Polat, B. (2019). Investigation of mechanical properties of glass-reinforced polymer matrix thermoplastic composites (Master's thesis, Iskenderun Technical University / Institute of Engineering and Science / Department of Mechanical Engineering).

[15] Thomas, S., Abraham, J., ManayanParambil, A., Krishnan, A., Maria, H. J., Ilschner, B., & McCullough, R. L. (2000). Composite materials. Ullmann's Encyclopedia of Industrial Chemistry, 1-44.

[16] Prasad, R. C. (2000). Composites, science, and technology. New Age International.

[17] Shehab, E., Meiirbekov, A., Amantayeva, A., & Tokbolat, S. (2022). Cost modelling for recycling fiber-reinforced composites: State-of-the-art and future research. Polymers, 15(1), 150.

[18] Gan, Y. X., Solomon, D., & Reinbolt, M. (2010). Friction stir processing of particle reinforced composite materials. Materials, 3(1), 329-350.

[19] Panthapulakkal, S., Raghunanan, L., Sain, M., KC, B., & Tjong, J. (2017). Natural fiber and hybrid fiber thermoplastic composites: advancements in lightweighting applications. In Green composites (39-72). Woodhead Publishing.

[20] Dixit, S., Goel, R., Dubey, A., Shivhare, P. R., &Bhalavi, T. (2017). Natural fibre reinforced polymer composite materials-a review. Polymers from renewable resources, 8(2), 71-78.

[21] Sur, G. (2008). Production of mixed reinforced aluminum matrix composites, examination of their mechanical properties and processability. Machine Training. Gazi University Institute of Science and Technology, Gazi University Ph. D.

[22] Zubair, N. (2017). Effects of Micro Cellulose Fibers Addition on Concrete Mechanical Properties Under Flexure and Uniaxial Tension.

[23] Ouarhim, W., Zari, N., &Bouhfid, R. (2019).Mechanical performance of natural fibers–based thermosetting composites. In Mechanical and physical testing of biocomposites, fibre-reinforced composites and hybrid composites (43-60). Woodhead Publishing.

[24] Akter, M., Uddin, M. H., & Tania, I. S. (2022).Biocomposites based on natural fibers and polymers: A review on properties and potential applications. Journal of Reinforced Plastics and Composites, 41(17-18), 705-742.

[25] Sathishkumar, T. P., Naveen, J. A., &Satheeshkumar, S. (2014). Hybrid fiber reinforced polymer composites–a review. Journal of Reinforced Plastics and Composites, 33(5), 454-471.

[26] Rajak, D. K., Pagar, D. D., Menezes, P. L., &Linul, E. (2019). Fiber-reinforced polymer composites: Manufacturing, properties, and applications. Polymers, 11(10), 1667.

[27] Velmurugan, R., & Manikandan, V. (2007). Mechanical properties of palmyra/

glass fiber hybrid composites. Composites Part A: applied science and manufacturing, 38(10), 2216-2226.

[28] Wallenberger, F. T., & Bingham, P. A. (2010). Fiberglass and glass technology. Energy-Friendly Compositions and Applications.

[29] Görgün, D. E., Kumartaşlı, S., Avinc, O., & Atar, N. (2021). Boron Fıbers And Theır Applıcatıons. Textıle Scıence And Economy, 56.

[30] DiCarlo, J. A., & Yun, H. M. (2005). Non-oxide (silicon carbide) fibers. In Handbook of ceramic composites (33-52). Boston, MA: Springer US.

[31] Li, J., Wu, W., Yang, H., Wang, X., Wang, X., Sun, C., & Hu, Z. (2019). Rigid silica xerogel/alumina fiber composites and their thermal insulation properties. Journal of Porous Materials, 26, 1177-1184.

[32] Chang, K. K. (2001). Aramid fibers, Composites, 21.

[33] Donnet, J. B., & Bansal, R. C. (1998).Carbon fibers. Crc Press.

[34] Park, S. J., & Kim, B. J. (2015). Carbon fibers and their composites. Springer Series in Materials Science, 210, 275-317.

[35] Karataş, M., & Aydoğmuş, E. (2023). Use of Inorganic Wastes as Fillers in Production of Polyester Composites and Evaluation of Properties of Obtained Composite. International Journal of Advanced Natural Sciences and Engineering Researches, 7(4), 20-24.

[36] Karataş, M., & Aydoğmuş, E. (2023). Physical and Chemical Properties of Organic Waste Reinforced Polyester Composites. International Journal of Advanced Natural Sciences and Engineering Researches, 7(4), 16-19.

[37] Aydoğmuş, E., Arslanoğlu, H., & Dağ, M. (2021). Production of waste polyethylene terephthalate reinforced biocomposite with RSM design and evaluation of thermophysical properties by ANN. Journal of Building Engineering, 44, 103337.

[38] Demirel, M. H., & Aydoğmuş, E. (2022). Waste Polyurethane Reinforced Polyester Composite, Production, and Characterization. Journal of the Turkish Chemical Society Section A: Chemistry, 9(2), 443-452.

[39] Aydoğmuş, E., Dağ, M., Yalçın, Z. G., & Arslanoğlu, H. (2022). Synthesis and characterization of EPS reinforced modified castor oil-based epoxy biocomposite. Journal of Building Engineering, 47, 103897.

[40] Aydoğmuş, E., Dağ, M., Yalçın, Z. G., & Arslanoğlu, H. (2022). Synthesis and characterization of waste polyethylene reinforced modified castor oil‐based polyester biocomposite. Journal of Applied Polymer Science, 139(27), e52526.

[41] Demirel, M. H., & Aydoğmuş, E. (2022). Production and characterization of waste mask reinforced polyester composite. İnönü Üniversitesi Sağlık Hizmetleri Meslek Yüksek Okulu Dergisi, 10(1), 41-49.

[42] Şahal, H., & Aydoğmuş, E. Production of SBS Reinforced Polyester Composite: Characterization of Physical and Chemical Properties. Journal of the Turkish

Chemical Society Section A: Chemistry, 10(3), 827-834.

[43] Orhan, R., Aydoğmuş, E., Topuz, S., & Arslanoğlu, H. (2021). Investigation of thermo-mechanical characteristics of borax reinforced polyester composites. Journal of Building Engineering, 42, 103051.

[44] Yilmaz, E., Aydoğmuş, E., & Demir, A. (2022). Life Cycle Assessment and Characterization of Tincal Ore Reinforced Polyester and Vinylester Composites. Journal of the Turkish Chemical Society Section B: Chemical Engineering, 5(2), 183-194.

[45] Dağ, M., Yanen, C., & Aydoğmuş, E. (2022). Effect of boron factory components on thermophysical properties of epoxy composite. European Journal of Science and Technology, 36, 151-154.

[46] Aydoğmuş, E., Aydın, M., & Arslanoğlu, H. (2022). Production and characterization of microsphere reinforced polyester composite: Modeling of thermal decomposition with ANN and optimization studies by RSM. Petroleum Science and Technology, 1-17.

[47] Şahal, H., Aydoğmuş, E., & Arslanoğlu, H. (2023). Investigation of thermophysical properties of synthesized SA and nano-alumina reinforced polyester composites. Petroleum Science and Technology, 41(23), 2173-2189.

[48] Yanen, C., & Aydoğmuş, E. (2021). Characterization of thermo-physical properties of nanoparticle reinforced the polyester nanocomposite. Dicle Üniversitesi Fen Bilimleri Enstitüsü Dergisi, 10(2), 121-132.

[49] Aydoğmuş, E., & Arslanoğlu, H. (2021). Kinetics of thermal decomposition of the polyester nanocomposites. Petroleum Science and Technology, 39(13-14), 484-500.

[50] Pekdemir, E., Aydoğmuş, E., & Arslanoğlu, H. (2023). Thermal decomposition kinetics of synthesized poly (n-isopropylacrylamide) and Fe_3O_4 coated nanocomposite: Evaluation of calculated activation energy by RSM. Petroleum Science and Technology, 1-18.

[51] Şahal, H., & Aydoğmuş, E. (2021). Production and characterization of palm oil based epoxy biocomposite by RSM design. Hittite Journal of Science and Engineering, 8(4), 287-297.

[52] Aydoğmuş, E. (2022). Biohybrid nanocomposite production and characterization by RSM investigation of thermal decomposition kinetics with ANN. Biomass Conversion and Biorefinery, 12(10), 4799-4816.

[53] Orhan, R., & Aydoğmuş, E. (2022). Production and characterization of waste corncob reinforced polyester composite. Avrupa Bilim ve Teknoloji Dergisi, (42), 176-179.

[54] Buran, A., Durğun, M. E., & Aydoğmuş, E. (2022). *Cornus alba* Reinforced Polyester-Epoxy Hybrid Composite Production and Characterization. Avrupa Bilim ve Teknoloji Dergisi, (43), 116-120.

[55] Karataş, M., & Aydoğmuş, E. (2023). Obtaining Pectin Reinforced Polyester

Composite and Investigation of Thermophysical Properties. Avrupa Bilim ve Teknoloji Dergisi, (48), 64-66.

[56] Orhan, R., & Aydoğmuş, E. (2022). Investigation of some thermophysical properties of *Asphodelus aestivus* reinforced polyester composite. Firat University Journal of Experimental and Computational Engineering, 1(3), 103-109.

[57] Buran, A., Durğun, M. E., Aydoğmuş, E., & Arslanoğlu, H. (2023). Determination of thermophysical properties of *Ficus elastica* leaves reinforced epoxy composite. Firat University Journal of Experimental and Computational Engineering, 2(1), 12-22.

[58] Şahal, H., & Aydoğmuş, E. (2023). Use of Sunflower Seed Shells as Filler in Polyester Resin and Characterization of Obtained Composite. In International Conference on Engineering, Natural and Social Sciences, 1, 233-236.

[59] Orhan, R., & Aydoğmuş, E. (2021). Synthesis and Characterization of Limonene-Based Sulfur Polymer. Avrupa Bilim ve Teknoloji Dergisi, (28), 1517-1520.

[60] Ersoy, M. S. (2005). Fiber reinforced polymeric composite material design (Master's thesis, Institute of Science and Technology).

[61] Uzay, Ç., & Geren, N. (2020). Advanced Technologies For Fiber Reinforced Polymer Composite Manufacturing: A Review Advanced Technologies for Fiber Reinforced Polymer Composite Production: Compilation. Journal of Engineering Sciences. Wallenberger.

[62] Mazumdar, S. K., & Manufacturing, K. C. (2002). Materials, product, and process engineering.

[63] Dhakal, H. N., & Ismail, S. O. (2021).Design, manufacturing processes and their effects on bio-composite properties. Sustainable Composites for Lightweight Applications, 121-177.

[64] Zeng, J. J., Duan, Z. J., Guo, Y. C., Xie, Z. H., & Li, L. J. (2020). Novel fiber-reinforced polymer cross wrapping strengthening technique: A comparative study. Advances in Structural Engineering, 23(5), 979-996.

[65] Doğan, A. F. (2022). Investigation of impact resistance of aramid fiber pipes produced by fabric winding method (Master's thesis, Necmettin Erbakan University Institute of Science and Technology).

CHAPTER 3

USABILITY AND CHARACTERIZATION OF INDUSTRIAL WASTES IN GEOPOLYMERS PRODUCTION[1]

Abdulkadir BAKIRDÖVEN[2]
Çiğdem SARICI ÖZDEMİR[3]

1 Çiğdem SARICI ÖZDEMİR https://orcid.org/0000-0003-2129-3044
Abdulkadir BAKIRDÖVEN https://orcid.org/0000-0003-0112-7778
İnönü Üniversitesi Fen Bilimleri Enstitüsü Yüksek Lisans Tezi
Tezin Adı: Endüstriyel Atıkların Geopolimerler Eldesinde Kullanılabilirliği Ve Karakterizasyonu
Öğrenci: Abdulkadir BAKIRDÖVEN Danışman: Prof. Dr. Çiğdem SARICI ÖZDEMİR
2 Öğr. Grv., Turgut Özal University, Yeşilyurt of Junior Technical College, Malatya, Turkey
3 Prof. Dr., Inonu University, Faculty of Engineering, Department of Chemical Engineering, Malatya, Turkey

1. INTRODUCTION

Today's technology is the most important building material. Knowing about its high mechanical strength and stability, it is known that there is more than 10 billion tons of concrete production. The carbon dioxide (CO_2) rate in the cement industry in the world contains 9% of the carbon dioxide formed as a result of all industrial production, so it is generally defined as the secret responsible for global warming[1].

Geopolymer is an environmentally friendly alternative to ordinary portland cement. Calcium silicate hydrate structures are used to provide matrix formation and strength in cement. The geopolymer, on the other hand, gets the necessary structural strength from alumino silicate polycondensation. CO_2 emissions caused by Portland cement are not found in the geopolymer production process. In addition, there is no need to rise to high temperatures during production. And most importantly, industrial wastes such as fly ash and slag are used as the main component thanks to the high rate of aluminosilicate they contain. In addition, metakaolin containing aluminosilicates, glass wastes, ashes of by-products of agricultural industries (such as coconut, rice husk, pulp, etc.), ferrocorm slag, red clay and concrete demolition waste are used as additives. Classical concrete is a non-combustible material with low thermal conductivity. For this reason, concrete surfaces show high strength under open fire, even if no additional precautions are taken. Geopolymer can withstand higher temperatures than standard concrete, namely Portlant cement, however it is more durable, cheaper and has lower energy requirements. In the 21st century, nuclear studies and the use of nuclear energy are rapidly developing to meet the increasing energy needs, however, the removal of radio-active nuclear waste has become a major problem. International Atomic Energy Agency (IAEA) announced that it is possible to protect from radioactive effects by solidification, burial, encapsulation and storage methods for the immobilization of nuclear waste. In the light of the studies, it is known that Na and K based geopolymer provides a better stabilization than Portland cement for the immobilization of nuclear and other hazardous wastes. Although geopolymer has a wide range of uses, there are also special-purpose productions such as fire resistant geopolymer facade paints, the use of geopolymer rock wool as insulation material, the use of geopolymer as fireproof composite panels, the encapsulation of nuclear and chemical wastes into geopolymer. [2-5]

In this study, it is aimed to obtain geopolymer from fly ash, which is a thermal power plant waste, from industrial wastes. Different concentrations of NaOH and different amounts of Na_2SiO_3 solutions were used as alkali activators. TiO_2 as an additive to determine the photocatalytic effect; red clay, apricot kernel shell in order to obtain a more binding structure; resin to

examine the effect of porosity on the geopolymer; zeolite, Al_2O_3, SiO_2 were used to investigate the catalyst effect and binding.

2. MATERIALS and METHODS

2.1. Materials

2.1.1. Fly ash

The fly ash used in this study was obtained from Afşin-Elbistan Thermal Power Plant in Kahramanmaraş in Turkey. Fly ash was ground and sieved under a 0.600 mm sieve. According to standards, $SiO_2 + Al_2O_3 + Fe_2O_3$ value is below 50% and CaO > 10%, it has been observed that it complies with Class C (high lime) fly ash class.

2.1.2. Apricot resin

Resin was used to increase the binding in the geopolymer. Resins collected from the trunk of apricot trees Akçadağ in Malatya in Turkey. After drying at room conditions, it was sieved under a 0.600 mm sieve.

2.1.3. Red Clay

In this study, a clay sample obtained from Battalgazi district of Malatya was used as a binder. After the red clay was reduced in size with suitable crushers and grinders before use, under 200 mesh was sieved using a modular sieve. The clay used in the production of geopolymer was used in two ways. The clay was evaluated in experimental studies without pretreatment and calcined at 1100 °C.

2.1.4. Apricot stone

In Akçadağ district of Malatya, the core shells of sun-dried apricots that have not been subjected to the heat treatment process were dried and sieved under a 0.600 mm sieve after they were reduced in size with a laboratory type mortar.

2.2.Methods

2.2.1. Geopolymer production

The production of geopolymer physically consists of two basic steps, which can be expressed as the preparation of alkaline solution, the addition of fly ash and additives.

2.2.1.1. Preparation of alkaline solution

Within the scope of this study, NaOH solutions varying in the range of 7-12 M were prepared in the first stage. 100 ml of the prepared solutions were used in each study. Na_2SiO_3 (sodium metasilicate) in powder form was added to the alkaline solution as a second variable. The amount of Na_2SiO_3

added varies between 8-25 g. The resulting mixture was mixed for 30 minutes in all experiments.

2.2.1.2.Addition of fly ash and additives

After the alkaline solution was prepared in the geopolymer production, fly ash amounts were added as indicated in Table 1. Then TiO_2, apricot resin, red clay, calcined red clay, zeolite, apricot stone, Al_2O_3 was added. The mixture obtained was mixed in a mechanical mixer for 1 hour and poured into molds. After the samples dried and were able to come out of the mold, they were taken out of their molds and stored under laboratory conditions.

Table1 *Sample kode and content*

Sample Kode	NaOH (M)	Na_2SiO_3 (g)	Fly ash (g)	Red Clay(g)	TiO_2 (g)	Zeolite (g)	Apricot stone (g)	Calsined red clay (g)	Al_2O_3 (g)	SiO_2 (g)
G-4	10M	8	100	-	15	-	-	-	-	-
G-35	10M	20	70	-	-	-	-	-	20	20
G-41	7M	25	70	-	20	-	-	-	-	-
G-42	10M	25	70	-	20	-	-	-	-	-
G-43	12M	25	70	-	20	-	-	-	-	-
G-46	10M	25	90	-	-	-	-	10	-	-
G-47	10M	25	80	-	-	-	-	20	-	-
G-48	10M	25	70	-	-	-	-	30	-	-
G-53	10M	25	70	30	-	-	-	-	-	-
G-54	10M	25	80	10	-	-	-	-	-	-
G-55	10M	25	30	-	-	-	25	-	-	-
G-59	10M	25	80	-	-	-	-	-	45	45
G-60	10M	25	70	-	-	20	-	-	-	-

2.2.2. Determination of density and amount of water absorption

The densities of the obtained samples were calculated with Equation.1

$$\rho = \frac{m}{v} \qquad (2.1)$$

Where ρ is geopolymer density ($g.cm^{-3}$). V is the volume occupied by geopolymer (cm^{-3}). m is the geopolymer amount (g).

In order to find the water absorption percentage, the geopolymer samples numbered 41, 42, 43 were kept in pure water and weighed daily or every other day. 7, 14 and 28 days were compared by taking into account.

$$Water\ absorption\ (\%) = \frac{W_s - W_d}{W_d} * 100 \quad (2.2)$$

Where W_s and W_d are sample weight after saturation and dry sample weight of geopolymers (g) respectively.

2.2.3. Adsorption experiments

Studies have been carried out to determine the adsorption properties of geopolymers obtained under different experimental conditions. In these studies, 0.5 grams of sample was mixed with 50 ml of 50 $mg.L^{-1}$ methylene blue solution at room temperature at 500 rpm for 1 hour. After the mixture was filtered, absorbance measurements were performed at 662 nm in a UV spectropotometer to determine the methylene blue concentration in the filtrate. The adsorption amounts of the samples obtained are as percentage;

$$Adsorption\ amount\ (\%) = \frac{C_0 - C_e}{C_0} * 100 \quad (2.3)$$

where C_0 and C_e are the initial and final liquid and phase concentrations of methylene blue ($mg.L^{-1}$), respectively.

2.2.4. Curing Process

In order to determine the effect of the curing process on the geopolymer production, samples 46, 47 and 48 were mixed in the specified ratios and then cured in an oven at two different temperatures, 50 and 70 °C at 12 hours.

2.2.5. Photocatalysis Studies

G-42 and G-48 geopolymers were used in photocatalysis studies. The reason for using these two geopolymers is that the G-42 geopolymer contain TiO_2, while the G-48 geopolymer does not contain TiO_2 photocatalyst. In order to understand the photocatalytic effect more clearly, the experiment was carried out in two ways, between 12:00-15:00 hours, which are the hours when the sunlight is indirect in the laboratory environment and the sunlight is perpendicular in the open area. For both experiments, 5 grams of samples were taken and 50 $mg.L^{-1}$ 500 mL methylene blue solution was added on it, and samples were taken at 3, 5, 15, 20, 30, 45, 60, 90, 120, 150, 180 minutes durations and at 662 nm UV spectrophotometer. Absorbance measurements were made in .

3. RESULT AND DİSCUSSİON

3.1. FTIR Analysis

In Figure.1a, the effect of NaOH molarity on obtaining geopolymer was investigated. In example G-41, where the molarity is used as 7 M, the peaks obtained around 2000-2500 cm^{-1} are vibrations caused by the structures

due to the interaction between the Na-CO groups. Thus, more distinct groups emerged in the samples no. G-42 and G-43[6-7]. FTIR graphs of geopolymers obtained by adding different additives are given in Figure.1b. When the figure is examined, it belongs to physically bound H-O-H groups in the structure around 1600 cm^{-1}. The peak observed in sample 59 at around 800-1100 cm^{-1} belongs to Al-O-Si groups in the structure. Sample 55 belongs to the geopolymer in which apricot kernels are used as additive material. It is observed that the apricot kernel closes some functional groups in the structure and reduces their intensity. Chemically bound water appears around 3000 cm^{-1} in the G-35 sample[8].Two clay samples were used as binder in the production of geopolymer. It is the clay which is subjected to the activation process at 1100°C, which is specified as calcined from the clay samples. The other clay sample is the clay sample used as it is found in nature. FTIR analyzes of geopolymers obtained from these additives are given in Fig.1c. When the figure is examined, Si-O-Si groups and H-O-H groups in the structure are seen in different intensities[9-10].

3.2. XRD Analysis

XRD diffractograms of the samples prepared by changing the NaOH concentration are given in Fig.2a When the figure is examined, it is seen that the concentration change does not affect the quartz and mullite peaks, which are our main phases. The crystallinity belonging to these structures appeared at the same degrees. In the geopolymer gelation region, the amorphous structure draws attention. Especially in the sample no. G-41, in which 7 M NaOH solution is used, the amorphous character is more evident. This situation was also observed in the differentiation in the FTIR graphs of this sample. The efficiency of the ambient pH while obtaining the geopolymer is seen more clearly in this case. The pH will decrease with increasing NaOH concentration. It is evident in both FTIR and XRD graphs that there is not much change with the use of 12 M NaOH. Thus, it is possible to say that the concentration change does not have an effect on the gel structure after 10 M [11-13]. XRD diffractograms of geopolymers obtained by using different additives are given in Fig.2b. When the figure is examined, it is seen that the crystallinity is almost absent in the sample no. G-59 and it is not in amorphous character. This is due to Al_2O_3 and SiO_2 in the structure. With the addition of these chemicals, peak overlaps probably occurred and very little crystallinity was observed because the peaks extinguished each other. The same situation emerged in the sample no. G-55, in which apricot kernels were added. The addition of zeolite in the sample no. G-60 made the structures of quarz and mullite a little more obvious[14]. XRD diffractograms of samples G-46, G-47, G-48, G-53 and G-54, in which red clay is used as an additive, are given in Fig.2c. When the diffractograms are examined, the geopolymer gelation in the structure is observed in the range of 20-35 °. While the crystal structures

belonging to Al and Si groups in the structure are observed as kaolinite around 20^0,

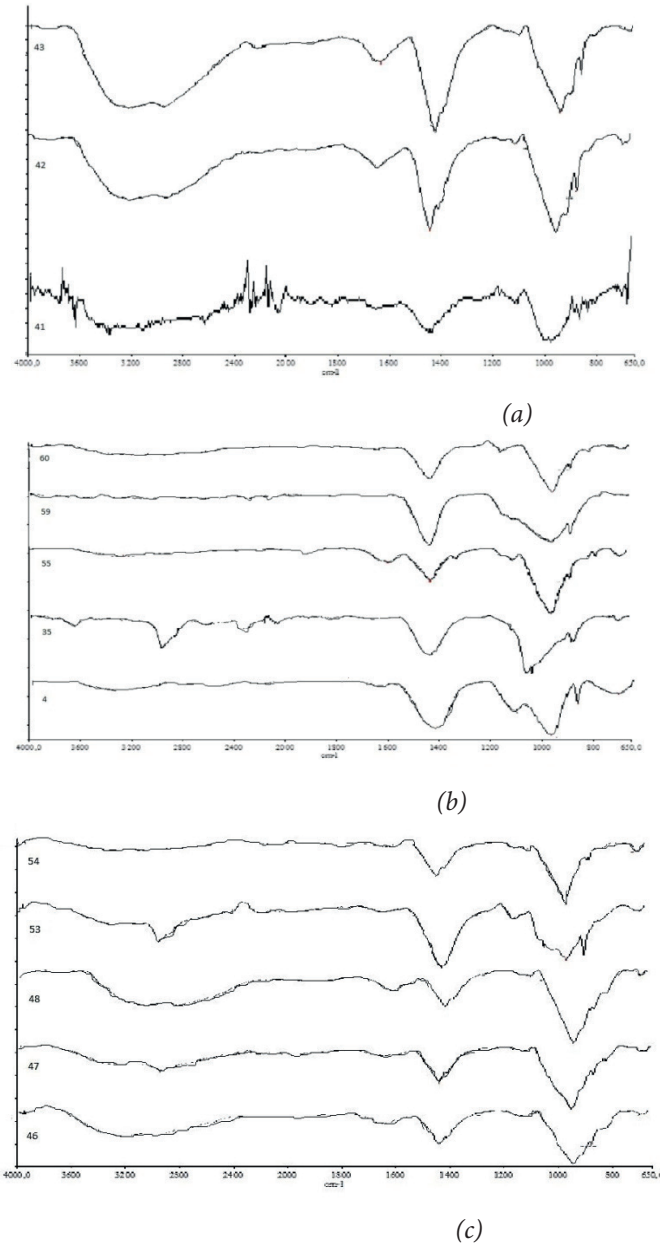

Figure. 1 *FTIR spectra of samples.*

quartz structures around 25 and 30° are observed, while around 45°

they belong to illite groups. Compared to the XRD diffractograms of other samples, more crystalline structures emerge and most of them belong to clay.

When the XRD diffractograms of the generally obtained geopolymers are examined, it is seen that the structures in Table 2 are observed. Geopolymer gel formations, quartz, calcium silicate structures, illite, mullite are among the observed crystal peaks[11-16].

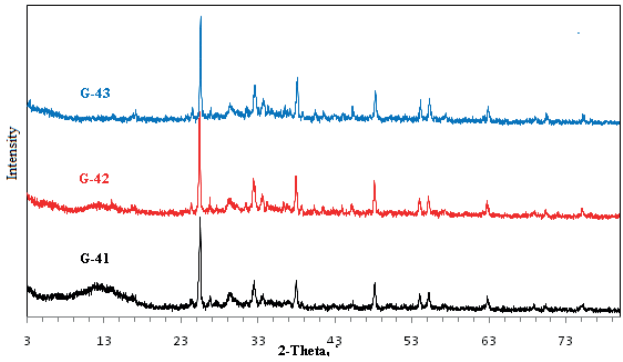

(a)

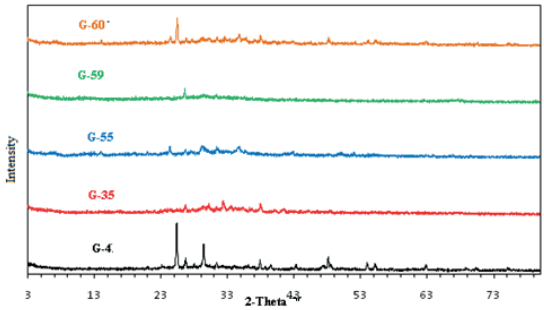

(b)

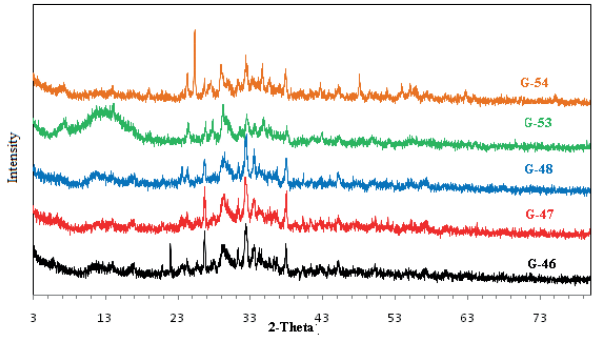

(c)

Figure 2 *XRD spectra of samples*

Table. 2 *Summary display of amorphous and crystalline structures determined in the samples obtained*

Structure	2Θ		
Geopolimer JEL	20-35		
Zeolit	6.5-13	41-42	60.5-62
Gypsum (alçı taşı)	13-15	20-25	
Quarz	20-28	49.5-50.5	
C-S-H(Kalsiyum Silikat Hidrat)	28-30		
Mullite	15-18	35-40	
Ettringite	42.5-44.5		
CaO	32-38		
Opal	22-23		
Hematit	33-36		
Anataz(TiO_2)	24.5-25.5	42.5-44	67.5-69.5
Rutil(TiO_2)	26-27		

3.3. SEM Analysis

SEM images of the samples in which the variation of NaOH molarity is examined are given in Figure 3. When the figure is examined, it is determined that mesoporous structures are formed and microporosity is not observed depending on the changes in the reaction with the increase in molarity. Unreacted fly ash reveals irregular structuring.

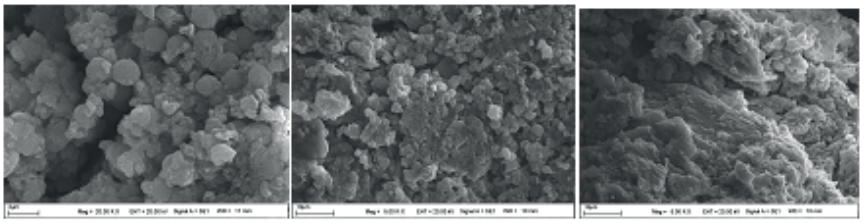

Figure.3 *SEM image of samples (a) G-41 (b) G-42 (c) G-43.*

When the SEM images of some samples obtained by the addition of additives are examined (Figure 4), the different structuring in the sample no. G-55, in which apricot kernels are used, is evident. These structures were determined as acicular nanoparticles. The variation of Al_2O_3 and SiO_2 in the structure is seen in the example G-59. Cage formations are observed with agglomeration in certain regions. In the sample no. G-60 obtained from

bentonite, the mesoporous structure attracts more attention. The secondary structures formed are indicative of incomplete reactions.

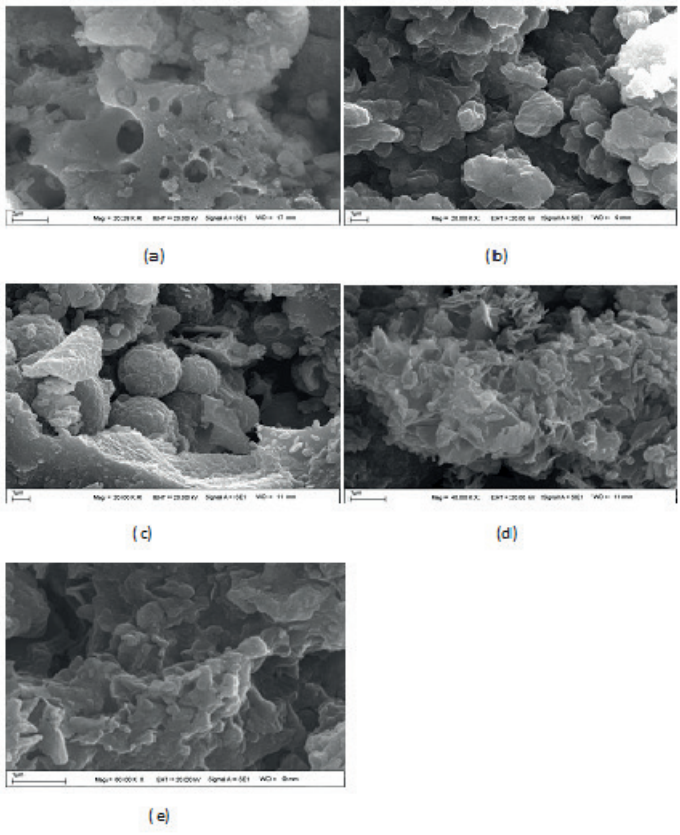

Figure.4 *SEM image of samples (a) G-4 (b) G-35 (c)G-55 (d) G-59 (e) G-60*

In the samples where red clay is used, the crystal structure development manifests itself as agglomeration (Figure 5). It can be said that these structures are formed due to the swelling of clay as a result of its reaction with water. More microporosity is remarkable in calcined samples.

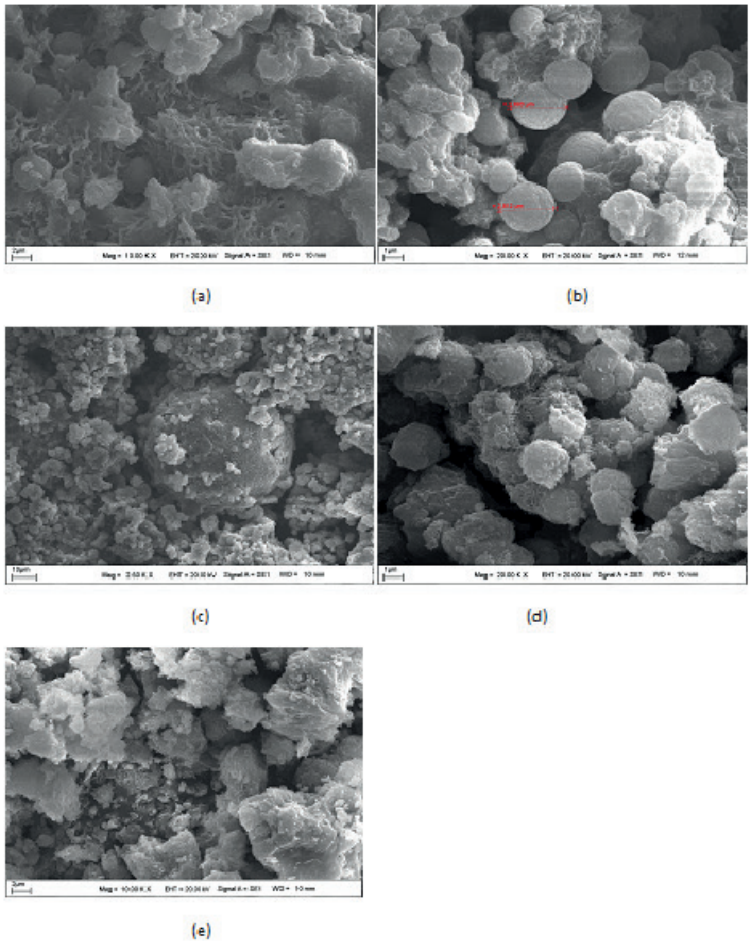

Figure. 5 *SEM image of samples (a) G-46 (b) G-47 (c) G-48 (d) G-53 (e) G-54.*

3.4. Adsorption experiments

Studies were carried out on the adsorption of methylene blue dyestuff in order to examine the surface properties of the obtained geopolymers and to determine the adsorbent character of the structure (Figure 6). When the samples in which the amount of NaOH changes are examined, it is seen that the amount of adsorption decreases with increasing amount of NaOH. The reason for this is that NaOH molecules in high concentration fill the pores and as a result, the adsorption area decreases. At the same time, it is seen that the porosity decreases with concentration with secondary structures formed from SEM images. When the adsorption capacities of the samples to which additives are added are examined, the TiO_2 difference is clearly seen due to the

photocatalytic effect. At the same time, it is seen that the adsorption efficiency decreased due to the decrease in the porosity of the increasing Al_2O_3 and SiO_2 amount when the samples 59 and 35 are compared. It is determined by the high yield in which the apricot kernel shell plays an active role. When the effect of red clay on the adsorption capacity is examined, it is seen that the yield increases with the increase in the amount of calcined clay. It is understood from these results that the porosity of the clay becomes more pronounced with activation.

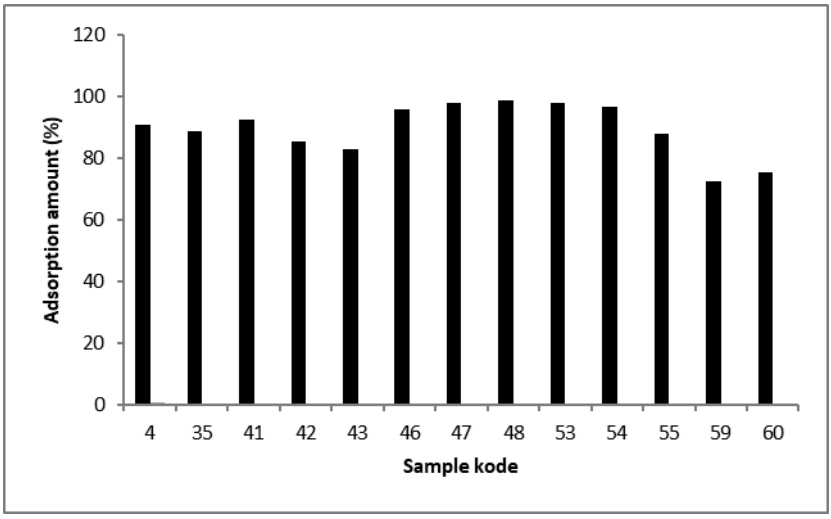

Figure. 6 *The amount of dye adsorbed by the samples obtained.*

3.5. Density and Water Absorption

When the densities of the samples are examined, changes are observed depending on the amount of fly ash, base concentration and the amount and properties of the additive material (Table 3). But in general, the density of the samples varies around 1.5 $g.cm^{-3}$. The changes in densities are due to the differentiation of the network structures in the geopolymer formation depending on the structure of the material used. The water absorption amounts of the samples in which the variation of the NaOH concentration from the obtained geopolymers were examined are given in Figure.7. When the figures are examined, it is seen that the changes in the water absorption capacity were observed rapidly in the early days, and it became stable as time passed. A lower absorption capacity was determined at higher concentration [17].

Table 3 *Densities of sample*

Sample	Density g/cm^3
G-4	1.256
G-35	1.433
G-41	1.593
G-42	1.652
G-43	1.657
G-46	1.646
G-47	1.595
G-48	1.616
G-53	1.476
G-54	1.553
G-55	1.160
G-59	1.567
G-60	1.628

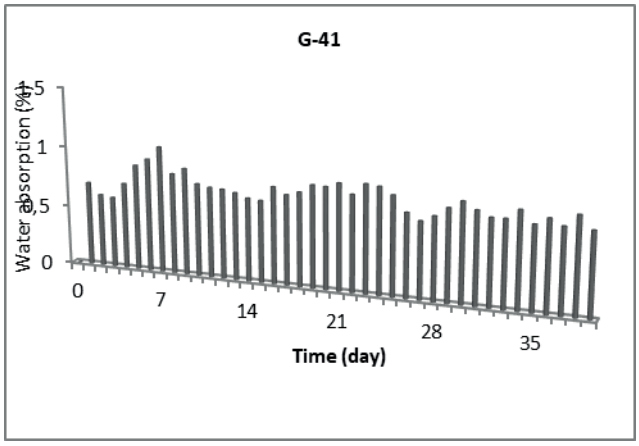

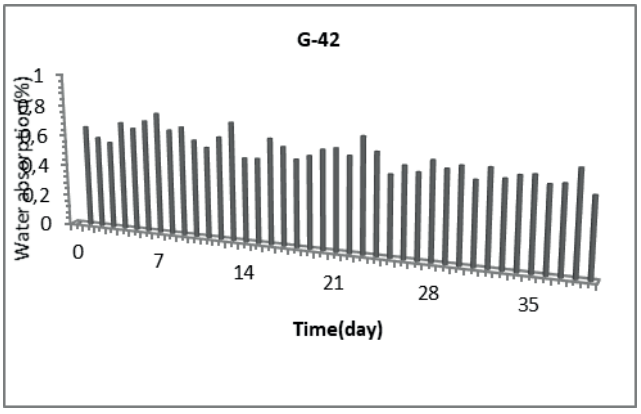

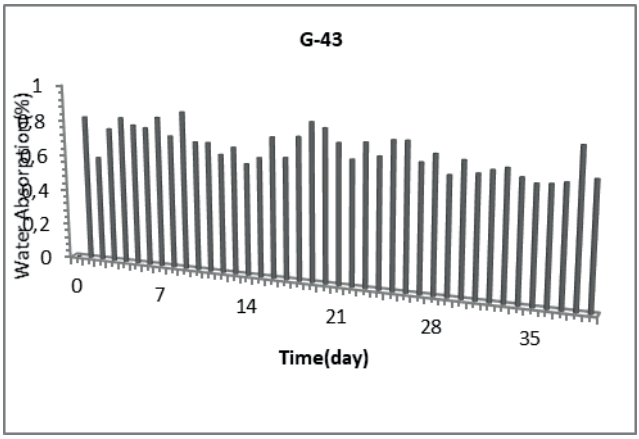

Figure.*7. 7, 14, 28 and 35 days of water absorption*

3.6. Curing Process

The changes as a result of the curing process of the samples G-46, G-47 and G-48 obtained by using different amounts of calcined clay and fly ash are given in Figure.8. When the figure is examined, the sample weights vary depending on the amount of water removed from the samples with the changing curing temperature. When the curing results are examined, it is seen that the samples start to reach a constant mass after the 14th day. While there is a rapid loss of mass until the 7th day, there is a slowdown in mass loss afterward. When the drying kinetics of the samples with temperature were examined, it was determined that the average mass loss after the treatment at room temperature was around 2.2%. While this mass loss was around 5.6% in the processes at 50 °C, it was calculated around 11.9% in curing at 70 °C .

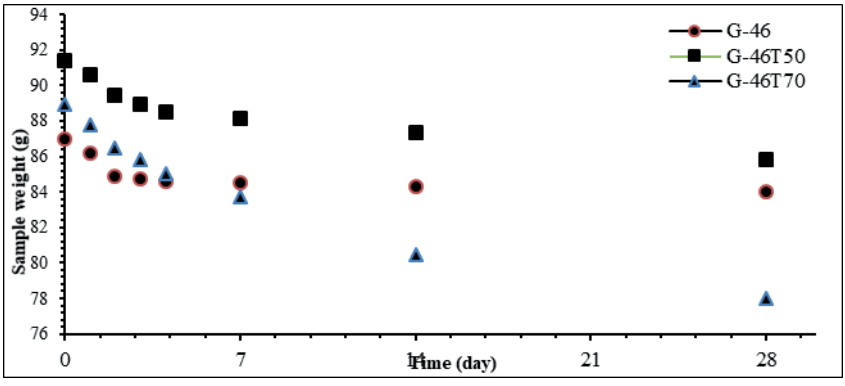

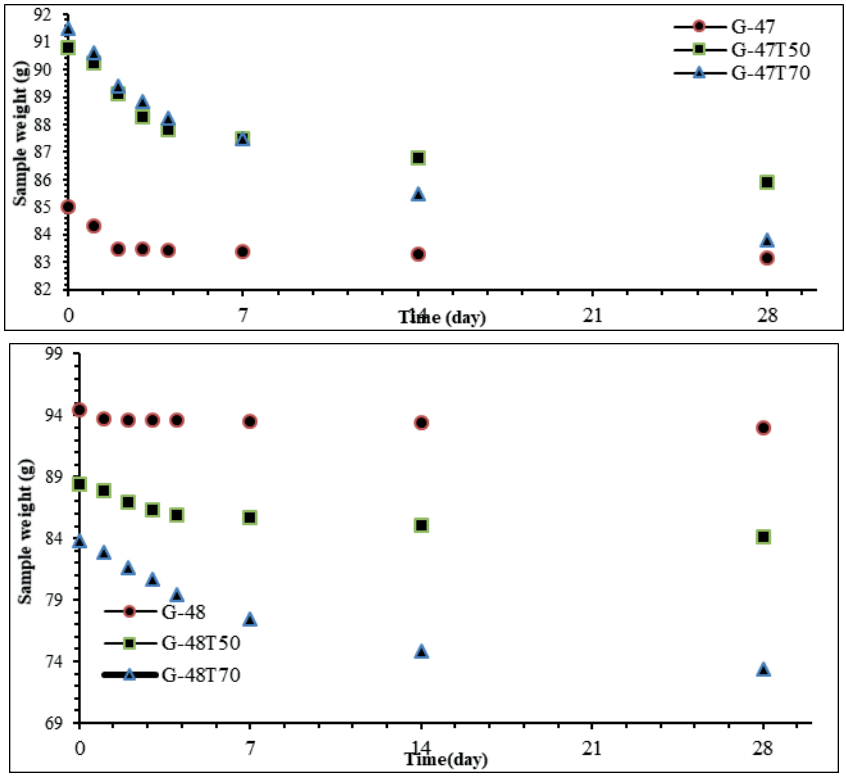

Figure. 8 *Change after curing*

3.7. Photocatalysis Studies

The sample no G-48, which was synthesized using fly ash and clay, and the sample no G-42, which was synthesized by adding TiO_2 additive, were used in the photocatalysis studies. This study was carried out in order to test the self-cleaning properties of the obtained geopolymers as a building material. Experiments in the study were carried out in a laboratory environment and daylight. Experiments were carried out in daylight between 12:00 and 15:00, when the sunlight came vertically outdoors in July. When Figure.9 is examined, it is seen that the amount of dye removal in the G-48 sample, which does not contain titanium dioxide in the laboratory environment, increased over time and stabilized at around 78 %. In the G-42 sample containing titanium dioxide in the same environment, this value was slightly higher, but was calculated as 80 %. As a result of the experimental studies carried out in the outdoor environment to determine the direct effect of sunlight, it is seen that the dye removal in the G-42 sample is up to 90 %. This shows that the TiO_2 photocatalyst in the sample becomes active with sunlight and breaks down the dye molecules in the environment. The dye molecules have undergone oxidation as a result of the UV excitation of titanium dioxide in sunlight[18-21].

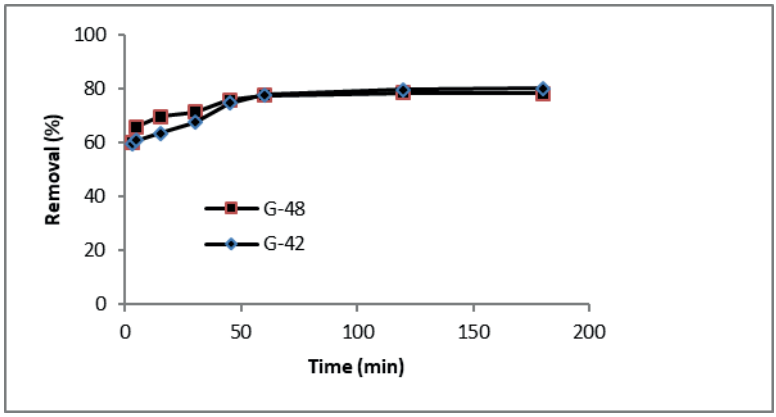

(a)

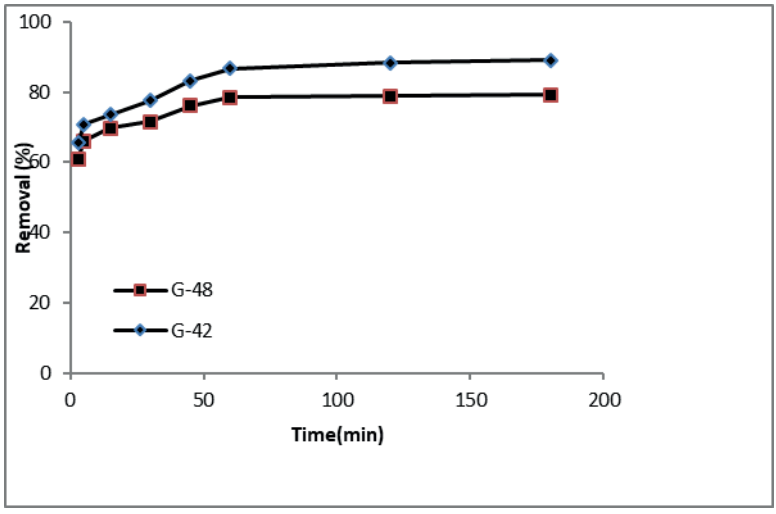

(b)

Figure. 9 *Photocatalysis effect (a) Laboratory environment (b) Direct sunlight environment*

4. Conclusion

In this study, it was aimed to obtain geopolymer using fly ash. Many additives were used in the study. The effect of the concentration and the amount of additives used on the geopolymer production was investigated. FTIR, XRD and SEM methods were used in characterization studies. Adsorption methods were used to determine the surface properties.

- Physically and chemically bound H-O-H groups, Si-O-Si, Si-O-Al functional groups

and Ti-O groups were determined in the geopolymer samples obtained after FTIR analysis. After XRD analysis, amorphous structures were observed,

and geopolymer gelation was observed in most samples. With SEM images, information about the pore structures was obtained and it was determined that there were mostly mesoporous structures.

- The increase in the amount of NaOH strengthened the structure up to 10 M. Afterwards, no effect was observed and it is thought that it weakens the structure due to the dissolution of the free sodium hydroxide in the structure in the liquid environment.

- After the adsorption of the methylene blue dyestuff, over 80% removal was obtained in 60 minutes. After the water absorption experiments, changes were determined depending on the pore structure of the sample, and it was found that more absorption occurred in the samples with more porosity.

- The titanium dioxide used in the preparation of the geopolymer caused the paint to break down with the photocatalyst effect. The geopolymer obtained in this way can also be used for special purposes such as the spontaneous disappearance of unwanted pollutants in the environment by sunlight.

Acknowledgements

This work was supported by Inönü University Scientific Research Coordination Unit.Project Number: FYL-2020-1987. This study is derived from master's thesis.

REFERENCES

[1] Zannerni G M, Fattah K P, Al-Tamimi A K, (2020).Ambient-cured geopolymer concrete with single alkali activator. Sustainable Materials and Technologies 23: 00131

[2] Tiffo E., Mbah J B B, Belibi P D B, Djobo J N Y, Elimbi A, (2020) Physical and mechanical properties of unheated and heated kaolin based-geopolymers with partial replacement of aluminium hydroxide. Materials Chemistry and Physics 239:122103.

[3] Top S, Vapur H, Altiner M, Kaya D, Ekicibil A (2020) Properties of fly ash-based lightweight geopolymer concrete prepared using pumice and expanded perlite as aggregates. Journal of Molecular Structure 1202: 127236.

[4] Cai J, Tan J, Li X (2020) Thermoelectric behaviors of fly ash and metakaolin based geopolymer. Construction and Building Materials 237: 117757.

[5] Zhang H Y, Qiu G H, Kodur V, Yuan ZS (2020) Spalling behavior of metakaolin-fly ash based geopolymer concrete under elevated temperature exposure. Cement and Concrete Composites 106:103483.

[6] Iftikhar S, Rashid K, Haq U, Zafar I, Alqahtani K, Khan I. (2020) Synthesis and characterization of sustainable geopolymer green clay bricks: An alternative to burnt clay brick. Construction and Building Materials 259:119659.

[7] Maiti M, Sarkar M, Maiti S, Malik MA, Xu S (2020) Modification of geopolymer with size controlled TiO_2 nanoparticle for enhanced durability and catalytic dye degradation under UV light. Journal of Cleaner Production 255:120183.

[8] Kaze C R, Alomayri T, Hasan A, Tome S, Lecomte-Nana G L, Nemaleu J G D. (2020) Reaction kinetics and rheological behaviour of meta-halloysite based geopolymer cured at room temperature: Effect of thermal activation on physicochemical and microstructural properties. Applied Clay Science 196 :105773.

[9] Zulkifly K, Cheng-Yong H, Yun-Ming L, Abdullah MMAB, Shee-Ween O, Khalid MSB (2020). Effect of phosphate addition on room-temperature-cured fly ash-metakaolin blend geopolymers. Construction and Building Materials 270: 121486.

[10] Jamil N H, Abdullah M M A B, Pa F C, Mohamad H, Ibrahim W M A W, Chaiprapa J (2020). Influences of SiO_2, Al_2O_3, CaO and MgO in phase transformation of sintered kaolin-ground granulated blast furnace slag geopolymer. Journal of Materials Research and Technology 9(6): 14922-14932.

[11] Cong P, Mei L. (2021) Using silica fume for improvement of fly ash/slag based geopolymer activated with calcium carbide residue and gypsum. Construction and Building Materials 275 :122171.

[12] Guo X, Xiong G. (2021) Resistance of fiber-reinforced fly ash-steel slag based geopolymer mortar to sulfate attack and drying-wetting cycles. Construction

and Building Materials 269:121326.

[13] Fu C, Ye H, Zhu K, Fang D, Zhou J (2020) Alkali cation effects on chloride binding of alkali-activated fly ash and metakaolin geopolymers. Cement and Concrete Composites 114: 103721.

[14] Freire A L, Moura-Nickel C D, Scaratti G, De Rossi A, Araújo M H (2020) Geopolymers produced with fly ash and rice husk ash applied to CO_2 capture. Journal of Cleaner Production 273:122917.

[15] Fuad Kabir Moni S M, Ikeora O , Pritzel C , Görtz B , Trettin R (2020) Preparation and properties of fly ash-based geopolymer concrete with alkaline waste water obtained from foundry sand regeneration process Journal of Material Cycles and Waste Management 22: 1434-1443.

[16] Sastry K G K, Sahitya P, Ravitheja A (2021) Influence of nano TiO_2 on strength and durability properties of geopolymer concrete. Materials Today: Proceedings 45:1017-1025.

[17] Nana A, Ngoune J, Kaze R C, Boubakar L, Tchounang S K, Tchakoute H K, Kamseu E, Leonelli C (2019) Room-temperature alkaline activation of feldspathic solid solutions: Development of high strength geopolymers, Construction and Building Materials 195:258-268.

[18] Chen D, Cheng Y, Zhou N, Chen P, Wang Y, Li K, Huo S, Cheng P, Peng P, Zhang R, Wang L, Liu H, Liu Y, Rua R (2020) Photocatalytic degradation of organic pollutants using TiO_2-based photocatalysts: A review. Journal of Cleaner Production 268 :121725.

[19] Zulfiqar M, Sufian S, Bahadar A, Lashari N, Rabat N E, Manso N. (2021) Surface-fluorination of TiO_2 photocatalysts for remediation of water pollution: A review Journal of Cleaner Production 317: 128354.

[20] Niu L, Zhao X, Tang Z, Lv H, Wu F, Wang X, Zhao T, Wang J, Wu A, Giesy J P. (2021) Difference in performance and mechanism for methylene blue when TiO_2 nanoparticles are converted to nanotubes Journal of Cleaner Production 297:126498.

[21] Kartal Ö E, Özdemir G D T (2012) Decolourization of C.I. Reactive Orange 16 via photocatalysis involving TiO_2/UV and TiO_2/UV/ oxidant systems. Desalination and Water Treatment 48: 199-206.

CHAPTER 4

DEVELOPMENT TRENDS FOR URBAN TRANSPORTATION AND URBANISATION FOR ISTANBUL

Yunus Emre Ayözen[1]

1 T.C. ULAŞTIRMA ALTYAPI BAKANLIĞI, *ayozenyunusemre@gmail.com*

Introduction

In this context, the use of multimodal transportation systems for Istanbul was reviewed. It was seen that there is a high imbalance towards the use of highway transportation. Especially, the marine and the railroad lines are underutilized and have not developed properly over the years. Due to extensive use of highway transportation, inter- and intra-city traffic experiences extensive congestions, delays, time and monetary losses. One of the bottlenecks of this congestion is at the Bosphorus Straight where there are two long span bridges.

Recently, one of the bridges on the strait, Fatih Sultan Mehmet (FSM) Bridge, has undergone rehabilitation, thus offering reduced traffic capacity. This reduced capacity is taken partially by the other long span bridge (Bogazici Bridge) and partially by the marine transportation lines. In this paper, the traffic flow data before and after the FSM Bridge maintenance are presented along with the marine line data, especially for the redistribution of the traffic during the rehabilitation work at the FSM Bridge. It was concluded that with a well-developed and designed strategy, the marine lines can provide a more balanced modal distribution and more efficient transportation for the city of Istanbul. Table 1 shows population improvement and Table 2 shows residential and economical values in Asian-Europan sides as yearly based.

Table 1. *Asian-Europan Sides Population Distribution In Istanbul By Years (Kiziltas, 2015)*

Istanbul	**1970**	**1980**	**1990**	**2000**
Europan Side	76%	69%	66%	64%
Asian Side	24%	31%	34%	36%

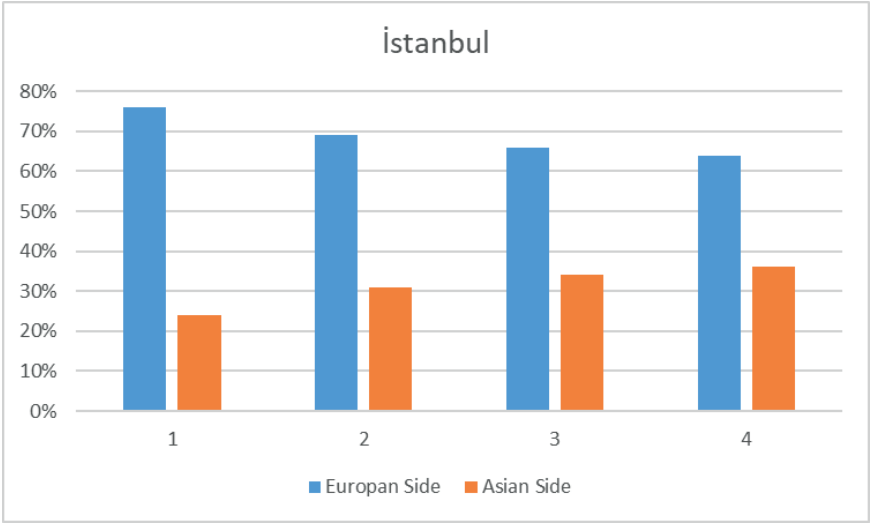

Figure 1. *Side Distributions*

Table 2. *Europan-Asian Sides Residential, Population and Carownership Values In Istanbul By Years (Kiziltas, 2015)*

Istanbul	**1970**	**1980**	**2000**
Population	3.500.000	4.800.000	12.900.000
Number Of Private Cars	60.000	200.000	1.800.000
Private Car Per Person	0,017	0,042	0,140
Residential Ratio Of Europan Side	80%	77%	71%
Residential Ratio Of Asian Side	20%	23%	29%

When Istanbul is considered, we can assume a level of 20% for marine transportation to be suitable for Istanbul's inter-modal distribution based on the presence of natural inner water lines. However, because of the high personal car ownership, lack of effective transportation demand-supply management, smart line decisions, effective investment strategies, existing contribution of marine transportation to overall transportation can be seen to be far from this 'ideal figure' for Istanbul. Table 4 shows the modal distribution in Istanbul in yearly based.

Istanbul contains a huge volume as population and employment that incorporates continuously positive and negative affects which comes from the position of being regional and international center. All of these affects reflect directly to Istanbulites too. As it has known Istanbul as a city that continuously and higly amount of allow immigrants which has an active population that is more than official population. Likewise the city has been expanded an area that is from Gebze in east to Çorlu in west that has continued to carry the role of the center of attraction on transportation of adjacent cities. It has been shared yearly based population increases for given years in Istanbul below on Table 3.

	2009-2010	**2010-2011**	**2011-2012**	**2012-2013**	**2013-2014**	**2014-2015**
Increase(People)	340.527	368.555	230.500	305.727	216.551	280.416
Increase(‰)	26,0	27,4	16,8	21,8	15,2	19,3

Table 3. Yearly Population Increase and Rate Of Increase Of Istanbul Source TUIK 2015

Below on Table 4 is illustrated cultivated area amounts of Istanbul and rates to national wide that has seen the relevant city is industrialized and centralized on advanced levels.

	CultivationArea	Vegetable Gardens Area	Orchard Area	Ornament Plant Area	FallowingArea	Total Area
Istanbul	65.546	3.079	2.709	33	166	71.533
Turkey	15.737.705	808.507	3.283.848	4.597	4.113.976	23.948.633
Istanbul / Turkey	0,4	0,4	0,08	0,7	0,004	0,3

Table 4. Cultivated Areas In Istanbul (Hectare) Source. TUIK 2015

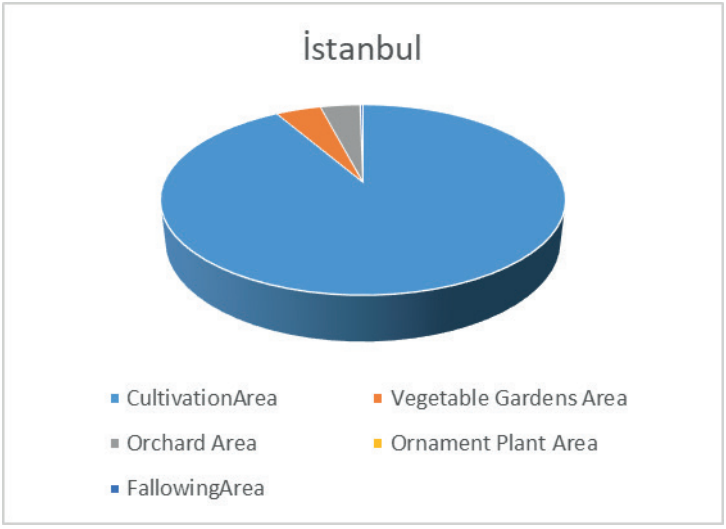

Figure 2. *Istanbul Land Use*

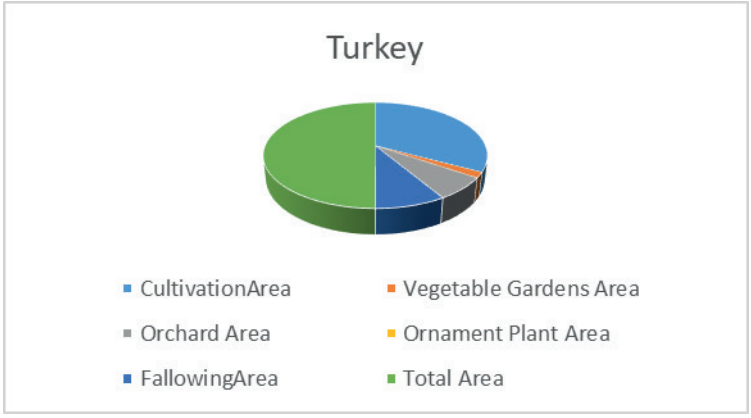

Figure 3. *Turkey Land Use*

28% of GDP (Gross Domestic Product), 37% of national industrial manufacture, 63% of national service production and 43% of national tax revenue are provided by Istanbul. Approximately half of foreign trade in Turkey has been met from Istanbul. Below on Table 5 is given that the import and export values for Istanbul and Turkey.

Data	**Exportation**(Million $)			**Importation**(Million $)		
	2004	**2015**	**2016-June**	2004	**2015**	**2016-June**
Turkey	63.167	143.850	71.668	97.540	207.206	99.651
Istanbul	36.834	77.016	39.097	60.817	117.781	58.401
Istanbul/Turkey	58%	54%	55%	62%	57%	59%

Table 5.Yearly Based Importation and Exportation Values For Istanbul and Turkey

Below on Table 6 is shared the tourism sector values for Istanbul.

Year	**Turkey**	**Istanbul**
2010	28.632.204	6.960.980
2011	31.456.076	8.057.879
2012	31.782.832	9.381.670
2013	34.910.098	10.474.867
2014	36.837.900	11.842.983
2015	36.244.632	12.414.677
2016	(January-June) 10.740.226	(January-June) 4.441.458
	-	(January-July) 5.366.144

Table 6. Yearly Based Foreign Tourist Numbers For Istanbul and Turkey

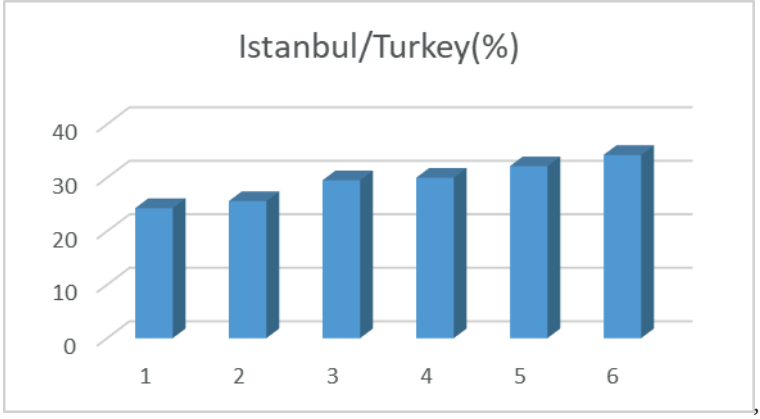

Figure 4. *Istanbul/Turkey Portion*

As it is seen on Table 5 and Table 6, it has been understood that the Istanbul has a substantially share by employment and other economical datas in national wide because of this, the transportation system necessities of the urban have been realised by meeting these measures which contains interurban and intraurban passenger and freight transport amounts of a city that has a position of regional center. It has seen that Istanbul has met 55% of export and 59% of import of Turkey by Table 3 that is established which

is the consumption of Istanbul is partially higher than the manufacturing of Istanbul from these two values. Similarly, it is inferred that the export and import shares of Istanbul has been partially decreased year by year from Table 3. It has been read by Table 4 that a big increase has been recorded on foreign tourist numbers both for Istanbul and Turkey for the years of 2010-2016 and can be read that approximately half of total increase amount has been provided by Istanbul. Also on this context, foreign tourist rate of Istanbul to Turkey has been reached by 25's% to 33's% in a short period as six years.

Transportation Investment Trends and Infrastrcuture Of Istanbul

By all these tables, it can be read that the central position of Istanbul for Turkey and region has been enhanced continuously. Below on Table 7 is given sectoral distribution of consolidated investments of Istanbul in 2016. It can be seen clearly by the table that approximately half of the investment costs are reserved for transportation projects. Rather big part of transportation investments are realized by Istanbul Metropolitan Municipality (IBB).

Sectors	Investment Rates %
Transportation	49
Environment	35
Culture/Tourism	3
Health/SocialServ.	7
Disaster	6
Total	**100**

Table 7. Sectoral Distribution Of Consolidated Investments In 2016

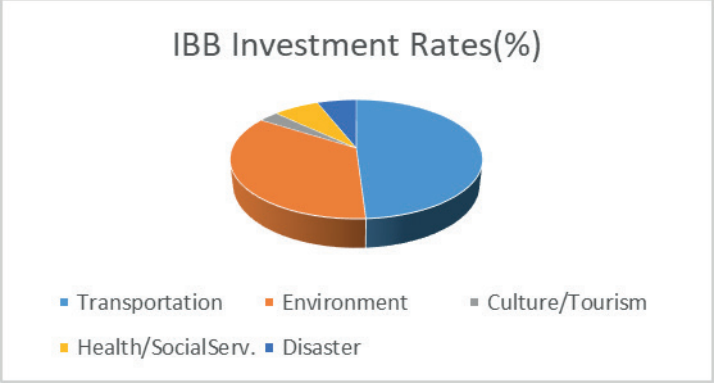

Figure 5. *Sectoral Distribution OF Istanbul*

Below on Figure 6 is illustrated that the distribution of expropriated area according to the objectives in Istanbul in 2016.

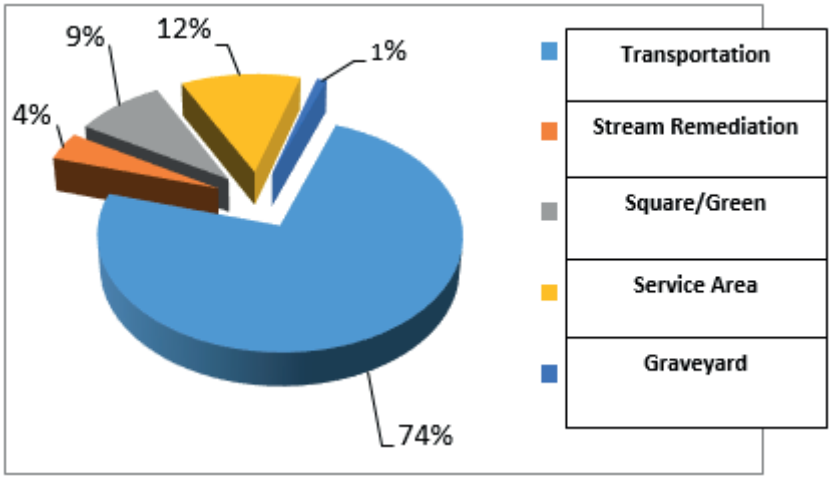

Figure 6. Distribution Of Expropriated Area According To The Objectives In Istanbul In 2016

It has seen at Figure 1 that the share of the transportation on expropriated area in 2016 in Istanbul is 74%. A percentage so much higher reveals the care degree and investment costs level of transportation by municipality. The majors of these investments are Marmaray suburbline (Gebze-Halkalı) rehabilitation works, Eurasia Tunnel (rubber tyred) that is going to start to operate in December 2016, 3rd Bosphorus Bridge which started to operate in August 2016, Üsküdar-Ümraniye-Çekmeköy-Sancaktepe subway line, Kartal-Pendik-Tavşantepe subway line and 3rd Istanbul Airport etc. Each of these are projects that will affects remarkably to Istanbul transportation system and national transportation policies. At reducing the traffic congestion to tolorable levels in Istanbul, urban railway sytems especially subway lines have a vital role. In addition to this, a city is in fact in the center of the sea and surrounds the sea as Istanbul has a modal distribution that contains only 1-2% seaway modal share. Whereas this rate can be operated at 20% levels in Istanbul. Before, the seaway transportation implementations were experienced between the locations which are on the same continental side as paralel to coast but the expected efficiency could not get. At this point, existing city line ferry fleet types become insufficient (the size of the ferry is bigger than the necessary) and this case intercepts the true direction of the demand.

Modal Distribution Of Investment Costs and Transportation System

49% of planned investment costs have been reserved for transportation that the railway system share in transportation investment costs is 48.3% in 2016. Below on Table 8 has been given the modal distribution of transportation costs of Istanbul Grand Municipality (IBB) in 2004-2016 years period. It has seen on the tables too that railway systems have a considerable rate which has

been tried to break the unbalanced high share of highway transportation mode and making high scaled investments to urban railway systems has been seen as the solution of reducing to the tolerable levels of Istanbul urban traffic.

Unit		**CCompleted Amount** (Thousand TL)	**Continuing Amount** (Thousand TL)	**Total Amount** (Thousand TL)	**%**
Highway*		11.583.748	680.313	12.264.061	**27,7**
Railway		17.956.045	3.435.610	21.391.655	**48,3**
Seaway		912.365	-	912.365	**2**
Airway		1.378	-	1.378	**0,01**
Maintenance, Repair, Traffic Services		8.962.680	737.468	9.700.148	**21,9**
Total	Thousand TL	**39.416.216**	**4.853.391**	**44.269.607**	**100**
	%	**89**	**11**	**100**	

Table 8. Modal Distribution Of Transportation Costs In 2004-2016 Years Period
**Highway: included tunnel, road-intersection, park and vehicle*

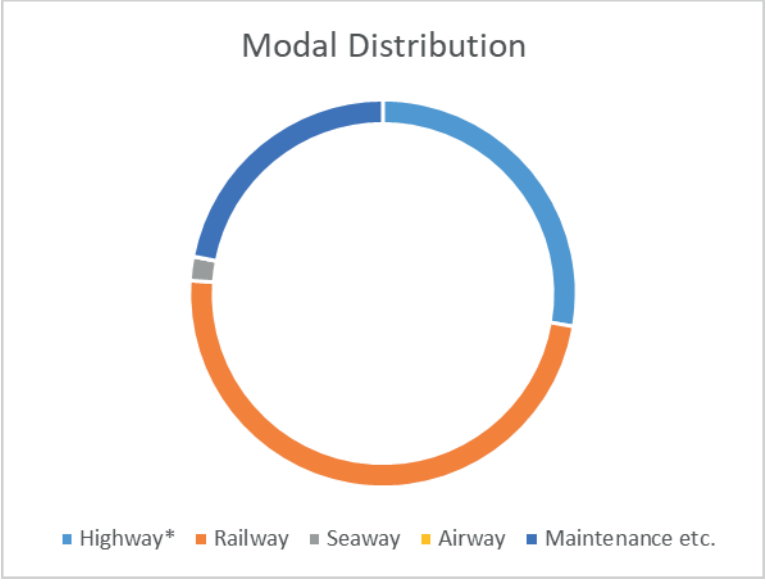

Figure 7. *Modal Distribution*

The continuous increase in transportation totally and each transportation modes that the amount increase of railway system is very high and the share in investments of this mode has been increasing too. Below on Table 9 is illustrated the proportional distribution of mass transport modes in Istanbul in 2004-2015 years period. It has seen that 10% decrease has been recorded in urban highway transportation mode and this rate has transeferred to railway systems by the table.

Transportation Mode	Modal Share (%)			2004-2015 Change
	2004	2011	2015	
Highway	87,7	83,5	77,8	-9,9
Railway	8,6	13,2	17,4	8,8
Seaway	3,7	3,3	4,8	1,1
TOTAL	100	100	100	-

Table 9. Modal Share Of Mass Transport

Railway system length of Istanbul is 145.45 km on existing case that either a considerable km increase in uban railway system will be provided or the important nodes of the urban will be connected to each other when Çekmeköy-Sancaktepe subway line, Marmaray Gebze-Halkalı connection (full capacitied Marmaray), Mecidiyeköy-Mahmutbey subway line, Kabataş-Mecidiyeköy subway line and Bakırköy-İDO (Kirazlı) subway line is completed. Kartal-Pendik-Tavşantepe subway line has started to operate in 10th October 2016 that will provide railway system connection to Sabiha Gökçen Airport. So this means to continuous railway connection (respectively: Atatürk Airport Heavy Rail System, Marmaray, Kadıköy-Kartal-Pendik subway) between to airport of Istanbul (Sabiha Gökçen and Atatürk) on the south axis. Railway system length and transported passenger numbers that are on the responsibility of Istanbul Grand Municipality (IBB) for 2015 are illustrated on Table 10. It has seen that a geometrically increase has been recorded both on constructed length km and transported passenger number by the table too. The increase on transported passenger is higher than the increase on the increase of constructed railway length km that is related to integration enhance and the route speciality of new lines.

Data	**Length** (Km)	**Passenger** (Passenger/Day)
2004	45,1	402.000
2015	128,65	2.089.057
Increase Amount	83,55	1.687.057
Increase Rate (%)	185	419

Table 10. Railway System Length and Transported Passengers In The Responsibility Of Istanbul Grand Municipality

Below on Table 11 is illustrated the distribution of existing railway systems of Istanbul. A general consideration has been done as before 2004 and after 2004 for constructed lines on the table. It is remarkable that hgh share of the railway system investments is subway lines after 2004. Kadıköy-Kartal has the speciality that is the first subway line in Anatolian side of Istanbul.

Than Marmaray has started to operate and Ayrılıkçeşme-Üsküdar section of Marmaray has enhanced the railway system km of Anatolian side. In 2016, firstly Kartal-Pendik-Tavşantepe subway line has been started to operate and the opening of Üsküdar-Ümraniye subway line will follow this. In generally, the most part of the passenger number is transported by subway line between urban railway lines which is understood that a big amount of passenger is transported by Kabataş-Bağcılar light railway train (LRT).

In this context, the railway system investments are given detailed on Table 10 that urban railway length km will be increase highly by completing of the railway constructions (initially subway constructions) in 2016-2018 years period.

Railway System Mode	Route Name	Length Before 2004 (km)	Length After 2004 (km)	Transported Passenger (Passenger/ Day)
Subway	Taksim – 4.Levent	8,5	-	542.366
	4.Levent – AOS – Darüşşafaka -Hacıosman	-	8,12	
	Sanayi - Seyrantepe	-	1,67	
	Şişhane – Taksim	-	1,65	
	Yenikapı-Şişhane-Aksaray LRTS	-	3,55	
	Kadıköy-Kartal	-	21,7	308.290
	Kirazlı –Başakşehir Olimpiyat Köyü		15,9	104.269
	Levent Hisarüstü Mini Metro – Seyrantepe Bağlantısı*		3,3	27.882
Light Railwy Tram (LRT)	Aksaray – Havaalanı	20,3	-	472.377
	Esenler – Kirazlı	-	5,8	
	Yenikapı – Aksaray LRTS Bağlantısı		0,7	
Tramway	Tünel – Taksim Nostaljik Tramvay	1,6	-	1.957
	Kadıköy – Moda Nostaljik Tramvay	2,6	-	2.005
	Eminönü – Zeytinburnu	11,2	-	410.431
	Kabataş – Eminönü	-	2,9	
	Zeytinburnu – Güngören – Bağcılar	-	5,2	
	Edirnekapı – Sultançiftliği	-	12,8	158.437
	Edirnekapı –Topkapı	-	2,5	
Funicular	Taksim - Kabataş	-	0,64	38.149
	Tünel – Karaköy	0,6	-	14.403
Cableway	Eyüp - Piyerloti	-	0,42	6.945
	Taksim – Maçka	0,3	-	1.546
Suburb	MARMARAY**		13,5	209.983

Table 11. Existing Case Railway System Lines In Istanbul

Constructor Body	Route Name	Railway System Mode	Length (Km)	Capasity (hour/ direction)	Complete Estimation Date
İBB (IGM)	Mecidiyeköy-Mahmutbey	Subway	18	70.000	2018
	Kabataş -Mecidiyeköy-	Subway	6,5		
	Kartal -Kaynarca Arası	Subway	4,5	70.000	2016
	Üsküdar-Altunizade-Ümraniye - Çekmeköy-Sancaktepe	Subway	20	50.000	2016
	Ataköy - Basın Ekspres - İkitelli	Subway	13,00	45.000	-
	Dudullu - Kayışdağı - İçerenköy - Bostancı	Subway	14,30	45.000	2019
	Total		**76,3**	-	-
The Ministry Of Transport, Maritime Affairs and Commnication	Marmaray	Suburb	63,5	75.000	-
	Bakırköy (İDO) - Kirazlı	Subway	9	70.000	2018
	Sabiha Gökçen Havalimanı – Kaynarca Merkez	Subway	7,4	70.000	2018
	Total		**79,9**	-	-
Sum Total			**156,2**	-	-

Table 12. Urban Railway System Lines On Construction Phase In Istanbul

Conclusions

A rapidly and effective establishment period has been realized on high speed railway (HSR) transportation modes, intraurban-inter urban and interregional projects railway system prjects particularly Marmaray have been realized, the load on the highway transportation mode has been transferred to railway and airway transportation modes comparatively by existing transportation investments. On this context, human focused approach, considering the environmental factors and improving a sustainable understanding will be very signicifant on the investment period.

According to 2023 Strategy Action Plan, the target of being one of the biggest ten economy of the world which was specified by Turkish Republic Government can be realized by establishing a transportation system that functional, efficient, powered by smart investment perspective, focused to supporting of social justice, canalized the consumption culture and habits on the right way, accessed on highly level of safety, education, health and basic socio-economic instruments.

It is an open issue that the economical progress goals of Turkey can be ensured with existance of functional transportation systems. However economic progress as reason and result of social and cultural progress necessitate an integrated approach. Transportation and urbanization are either reason or result of economic, social, technic, cultural and political developments and phases.

Accordingly the problems of transportation system particularly traffic safety necessitates a range of solutions that contain technological advancements (smart transportation systems), the providing of intermodal integration and balanced modal split, management of consumption culture, featuring of environmentalist and sustainable approaches. Sustainable approach is not only a better choice, but also obligation for awareness of the people about consuption culture.

The basic focus of transportation is people. The parameters of the service for people are safety, comfort, punctuality, accessability and cost. These parameters provides a cross check possibility of the people oriented level of a given system (Gercek et al, 2008).

REFERENCES

[1] Kiziltas, M, C, 2015, İstanbul Özelinde Türel Dağılım, Boğaz Geçişleri ve Servis Araçlarının Yönlendirilmesi (Modal Distribution, Bosphorus Accesses and Routing Of Service Vehicles On Istanbul Scale), Transit 2015, 8.Uluslararası Ulaşım Teknolojileri Sempozyumu ve Fuarı, 17-19 Aralık 2015, Istanbul

[2] T.C. 10.Kalkınma Planı Ulaştırma ve Trafik Güvenliği Ö.İ.K. Raporu (Turkey Republic 10th Development Plan), 2012, Ankara

[3] Ilicali, Mustafa (2013), 'Akıllı Ulaşım Sistemlerinin Güvenli ve Düzenli Bir Trafik İçin Önemi - 2' (Importance Of Intelligent Transportation Systems For A Safety and Steady Traffic – 2), http://www.tasimadunyasi.com/akilli-ulasim-sistemlerinin-guvenli-ve-duzenlibir-trafik-icin-onemi-2-makale,258.html (24.04.2014)

[4] Lobb, B., Harré N., Terry, N., 2003, 'An Evaluation of Four Types of Railway Pedestrian Crossing Safety Intervention'

[5] Kiziltas, M, C, 2015, İstanbul' da Kent içi Raylı Sistem Yatırımları ve Sistem Entegrasyonu Çerçevesinde Değerlendirilmesi (Urban Railway Systems of Istanbul and An Evulation On The Context Of System Integration), 6.Karayolu Trafik Güvenliği Sempozyumu ve Sergisi, 12-14 Kasım 2015, Ankara

[6] Ilıcalı, M., Camkesen, N., Tanoğlu, S., 2011, 'Kentiçi Trafik denetlemelerinde Elektronik Denetleme Sistemlerinin (EDS) kullanılması' (Usage Of Electronical Supervision Systems On Urban Traffic Controls)

[7] Kiziltas, M, C, 2015, Yüksek Hızlı Demiryolları ve Yapısal Değerlendirmesi-3 (High Speed Railways and Structural Evaluation), Ulaştırma Dünyası Gazetesi

[8] Gercek, H., and O. Demir. 2008. Urban Mobility in Istanbul. Blue Plan Workshop on Urban Mobility in Istanbul, Developments and Prospects, Istanbul

[9] Kiziltas, M, C, 2015, 'Yüksek Hızlı Demiryolu Politikaları-5' (High Speed Railway Policies-5) http://www.ulastirmadunyasi.com/?p=824

[10] Kiziltas, M, C, 2015, 'İstanbul' da Deniz Ulaşımı-2' (Marine Transportation In Istanbul-2) http://www.ulastirmadunyasi.com/?p=9

[11] Quinet, E., 2000. Evaluation methodologies of transportation projects in France. Transport Policy 7 (1), 27–35.

[12] Rothengatter, W., 2000. Evaluation of infrastructure investments in Germany. Transport Policy 7 (1), 17–27.

[13] Kızıltaş, M, Ç, 2014, High Speed Railways and European Union-U.S.A. Transportation Policies, Newspaper of Transportation World

[14] Mackie, P., Preston, J., 1998. Twenty-one sources of error and bias in transport project appraisal. Transport Policy 5 (1), 1–8.

CHAPTER 5

MAMMALIAN CELL FACTORIES FOR THE PRODUCTION OF BIOPHARMACEUTICAL PROTEINS

Sema KARABUDAK[1]

1 Araş. Gör. Dr. Sema KARABUDAK
(1) Ankara Yıldırım Beyazıt Üniversitesi Tıp Fakültesi Tıbbi Genetik ABD
(2) Ankara Yıldırım Beyazıt Üniversitesi Merkez Araştırma Laboratuvarı Uygulama ve Araştırma Merkezi, ORCID ID: 0000-0002-3646-0442
(3) Yıldırım Beyazıt Üniversitesi Yenimahalle Eğitim ve Araştırma Hastanesi

Biopharmaceutical Proteins

In 1978, using genetic engineering techniques, researchers succeeded in cloning the genes for the human insulin hormone into *E.coli* cells (Chang, Rey, Bochner, Heyneker, & Gray, 1987). This advancement resulted in the introduction of human insulin as the first biotechnology product receiving approval from the US Food and Drug Administration (FDA) in 1982 (Reichert & Paquette, 2003). Following this development, Protropin®, an FDA-approved human growth hormone was launched. After these initial products, many other therapeutic proteins entered the market (Goodman, 2009). The Biopharmaceutical Proteins market, valued at USD 265.16 billion in 2023, is expected to reach USD 461.86 billion in 2029, with a growth of 8.25% (Maximize Market Research Pvt Ltd., n.d., 2023).

Biopharmaceutical proteins comprise a diverse array of products, including vaccines, hormones, enzymes, antibodies, coagulation factors, cytokines and recombinant proteins (M. Butler & Meneses-Acosta, 2012; Ebrahimi & Samanta, 2023; O'Flaherty et al., 2020). Biopharmaceutical proteins are used in the treatment of various diseases such as diabetes, cancer, hemophilia, rheumatoid arthritis, growth hormone deficiency, and multiple sclerosis (Jorge Angel Ascacio-Martínez & Hugo Alberto Barrera-Saldaña, 2012; Ogihara, Mizoi, & Ishii-Watabe, 2023).

Peptides and other low molecular weight proteins are typically produced by chemical synthesis techniques, whereas larger, more intricate proteins containing extensive amino acid sequences are often synthesized by recombinant DNA technology (Tariq, Akash, Rehman, & shuqing, 2015). This method enables the synthesis of therapeutic proteins, which are now widely available as reasonably priced pharmaceuticals for treating a variety of diseases, by modifying DNA molecules and introducing them into host expression systems (Karvar, 2014).

Expression systems consist of a transfected DNA vector and a host cell that cooperate in transcription and translation processes, resulting in the production of recombinant protein from the introduced gene sequence (O'Flaherty et al., 2020). Various platforms, including bacteria, yeast, plant, and mammalian cells can be used in the production of pharmaceutical proteins by recombinant DNA technology. Yeast and bacterial expression systems are generally superior in terms of growth rate and maximum cell density of the host cell, and final protein therapeutic concentration. However, the similarity of therapeutic proteins to those produced in the human body is an important consideration, and therefore mammalian cell-based expression systems are more preferred. Notably, approximately 70% of commercially available therapeutic proteins are reported to be produced using mammalian expression systems (Walsh & Walsh, 2022).

Mammalian Expression Systems

The structural quality of biotherapeutic molecules principally defines their therapeutic efficacy and safety level. The choice of the correct expression system plays an extremely important role in biopharmaceutical product development. The expression system includes a host cell that expresses recombinant proteins via the vector including the recombinant gene. This process involves the conversion of DNA sequence information to a specific amino acid chain that determines the characteristics of proteins (O'Flaherty et al., 2020).

Mammalian cell lines enable the production of complex proteins with proper folding and also post-translational modifications (PTMs; particularly glycosylation) that closely resemble those in human proteins. Mammalian cell expression systems can produce proteins with sialyl glycoforms closely resembling the glycoproteins naturally produced by humans. In contrast, bacterial expression systems like *E. coli* lack the machinery for glycosylation, and yeast expression systems tend to produce hypermannose-type glycosylation. These features of mammalian expression systems are crucial for the therapeutic protein product to accurately represent its biological function (Durocher & Butler, 2009; Gray, 2001; Zhu, Mollet, Hubert, Kyung, & Zhang, 2017).

Additionally, in contrast to prokaryotic bacterial expression systems, eukaryotic mammalian expression systems enable the produced proteins to be secreted out of the cell in a natural form, eliminating the need for cell lysis during protein extraction (Dumont, Euwart, Mei, Estes, & Kshirsagar, 2016; Verma, Boleti, & George, 1998).

In mammalian protein production, quality control mechanisms of endoplasmic reticulum (ER) result in selective inhibition to the movement into secretory pathway only for those that are not properly folded or misassembled and/or un assembled. If proteins do not fold as they should, ER stress is provoked with the activation of Endoplasmic-reticulum-associated protein degradation to target them for ubiquitination and further degradation by proteasomes. This guarantees that only correctly folded proteins move through the secretory pathway preserving quality of secreted proteins in biopharmaceutical production (Gray, 2001; Krshnan, van de Weijer, & Carvalho, 2022).

Due to the conservation of transcription, mRNA processing, and translation signals in higher eukaryotic cells, mammalian systems provide a stable platform for efficient gene expression. Cloned DNA including genomic and cDNA clones from mammalian cells can be easily expressed in these systems (Kaufman, 2000).

Transient and stable expression approaches can be used in the context of protein synthesis in mammalian cells.Transient expression involves the temporary insertion of foreign genes into host cells, leading to short-term protein production without permanent integration into the host genome. This strategy is advantageous in generating small quantities of protein for early biochemical characterization allowing quick investigation of several protein variations.

Stable expression ensures permanent integration of foreign genes into the host genome, ensuring continuous and consistent protein synthesis in the long term. When targeting large amounts of protein production, a stable expression strategy is generally preferred (Dalton & Barton, 2014; Gray, 2001). Reduced plasmid DNA requirements, the establishment of a sustainable source of recombinant cells, and scalability of production quantities are the main advantages of stable expression. However, the primary drawback of this approach is the extended duration required for gene transfer and protein production (Hacker & Balasubramanian, 2016). In addition, recent studies have attempted to develop new transient expression systems that aim to facilitate high-level recombinant protein production on a larger scale (Meissner et al., 2001).

Host Cell

A wide variety of mammalian host cell lines are employed in the production of heterologous proteins because they have the capability to perform post-translational modifications such as glycosylation, sulfation, carboxylation, hydroxylation, phosphorylation, acylation and amidation (Gray, 2001; Walsh & Jefferis, 2006).

In choosing a host cell for pharmaceutical protein production, the focus revolves around specific criteria. The preferred cell lines should exhibit continuous growth, support suspension growth in bioreactors, present a minimal risk of adventitious infection by potentially pathogenic viruses, and maintain genetic stability. These considerations collectively ensure the selection of a host cell that aligns with the requirements for consistent quality, safety, and performance in pharmaceutical protein manufacturing (Gray, 2001).

The most often preferred mammalian cell lines for producing recombinant therapeutic proteins are chinese hamster ovary (CHO) cells, human embryonic kidney 293 cells (HEK293), baby hamster kidney (BHK21) cells, and murine myeloma cells (NS0 and Sp2/0), with CHO being the most frequently preferred in both scientific research and commercial production processes (Dumont et al., 2016; Estes & Melville, 2014; Khan, 2013).

Table 1: Examples of Biopharmaceutical Proteins Produced in CHO Cell Line (Alldread et al., 2014)

Year	Product	Importance	Company
1987	Tissue plasminogen activator (Activase1)	First mammalian product	Genentech
1989	Epoeitin (Epogen1/ Procrit1)	First mammalian produced blockbuster	Amgen; Johnson & Johnson
1992	Factor VIII (Recombinate)	High molecular weight protein (over 200 kDa)	Baxter
1997	CD20MAb (Rituxan1)	First monoclonal antibody product in CHO cell line	Genentech; Biogen Idec
2002	Adalimumab (Humira1)	First fully human monoclonal antibody	Abbott

Mammalian cell lines can be classified as mammalian cell lines of human origin (e.g., HEK293, HT1080, and HeLa) and non-human origin (e.g., CHO, BHK21, NS0, and Sp2/0). The production of certain non-human type glycan structures (i.e. N-glycolylneuraminic acid (NGNA), and galactose-α1,3-galactose (α-gal)) in non-human cell lines is a disadvantage for these cell lines. Glycosylation form variations are crucial in determining the quality of the therapeutic product. (Brooks, 2004; Michael Butler & Spearman, 2014). Moreover, the presence of non-human glycan structures in therapeutic proteins poses challenges because the human immune system can induce antibody production in reaction to these foreign structures (Ghaderi, Taylor, Padler-Karavani, Diaz, & Varki, 2010).

Selecting mammalian cell lines with human origin offers an important advantage in terms of the quality of the therapeutic protein product especially in terms of PTMs such as glycosylation. (Fliedl, Grillari, & Grillari-Voglauer, 2015). Because of their low growth rates and specific media requirements, some human cell lines are not appropriate for the industrial production of proteins. Nonetheless, a number of human cell lines, including HT1080 and HEK293, have been effectively used for this purpose (Fliedl et al., 2015).

Mammalian Expression Vectors

The construction of the expression vector is a critical step in establishing a cell factory that generates the required recombinant protein. Mammalian vectors, which act as carriers during the introduction of foreign genes into mammalian cells, are essential tools in biotechnology for producing therapeutic recombinant proteins. These vectors contain core components with different functions. Core components are selected according to the host cell type, desired application, and experimental goals.

Mammalian vectors used for gene expression can be divided into two types namely viral vectors and plasmid vectors. In viral vectors, gene transfer is achieved by the virus carrying the desired recombinant gene generally infecting the target cell and transferring its genetic material to the host cell. This process is called transduction. Plasmid vectors enable the genetic material contained in plasmid DNA to be transferred directly to host cells and this process is called transfection. (Khan, 2013; Savvas C. Makrides, 2003; O'Flaherty et al., 2020).

- **Viral Vectors**

Viral vectors are commonly employed to deliver foreign genetic material into the host cells. Most of the viruses that replicate in mammalian cells cause host cell death and lysis. In certain cell types, such as primary cultures and epithelial cells, where the transfer efficiency of non-viral techniques may be poor, viral vectors may be a more effective alternative (Kurian, Watson, & Wyllie, 2000).

Adenoviruses are medium-sized DNA viruses that are commonly utilized as expression vectors transferring genes that are required for heterologous protein expression in mammalian cells. Adenoviral vectors provides transient expression serving as important tools for gene transfer research as well as potential medical applications (Graham & Prevec, 1995; Kurian et al., 2000).

Retroviruses are a class of RNA viruses. These viruses are used as gene transferring tools because of their capacity to incorporate their genetic information into the DNA of host cells, resulting in stable expression.

Baculoviruses are DNA viruses that are extensively utilized for protein synthesis, particularly in insect cells. When mammalian promoters are present, baculoviruses have been shown to transfer genes into mammalian cells. Although it is generally considered a transient system, stable cell lines can be created using specific strategies, such as by incorporating antibiotic resistance genes (Mansouri & Berger, 2018).

- **Plasmid Vectors**

Plasmids are extrachromosomal genetic elements capable of independent replication from the host cell chromosome. Plasmids are consisted of double-stranded DNA fragments arranged in circular structures. These plasmid structures can be can be passed on between generations. Researchers often use a variety of plasmid vectors for gene expression in non-viral gene transfer applications in mammalian cells. Plasmid vectors allow certain genes to be transferred into the host cell and subsequently expressed for research and therapeutic purposes (Gill, Pringle, & Hyde, 2009; Khan, 2013). Plasmid vectors are flexible instruments with an almost limitless capacity for inserting

DNA segments. They may accommodate inserts of different sizes, including large fragments of genomic DNA. Plasmids, which are relatively simple to build, enable the manipulation of multiple regulatory elements required for gene transfer and expression (Gill et al., 2009; Lufino, Edser, & Wade-Martins, 2008).

Components of Mammalian Expression Vectors

A promoter is a DNA segment that plays crucial role in initiating transcription of the gene of interest placed in the vector. Mammalian expression vectors generally include a constitutive or inducible promoter region. To ensure effective and robust gene expression in the host cells, promoters with high transcriptional activity are frequently used in expression vectors (S. C. Makrides, 1999; Wang & Guo, 2020).

Inducible promoters initiate gene expression in response to the presence of a specific stimulus or inducer molecule. These types of promoters are used as a method of regulating and controlling gene expression in applications such as gene therapy or protein production in mammalian cells (Rossi & Blau, 1998; Weber et al., 2004). Constitutive promoters offer continuous expression of a gene at a relatively constant rate without being influenced by external factors. Human Ubiquitin C promoter (UBC), simian virus 40 early promoter (SV40), human elongation factor 1α promoter (EF1A) and, cytomegalovirus immediate-early promoter (CMV) are examples of constitutive promoters utilized in mammalian cells (Qin et al., 2010).

The multiple cloning site, located downstream of the promoter sequence, is a short segment of DNA that contains common restriction sites that allow the insertion of genes to be expressed (Carter & Shieh, 2015a).

It is known that mammalian cells can express cDNA segments that lack introns. Studies have revealed that insertion of introns increases gene expression by 10-20 fold (Buchman & Berg, 1988). Because placing introns at the 3' end of the transcription unit causes aberrant splicing, it is recommended to place introns at the 5' end of the open reading frame (Wise, Orkin, & Collins, 1989).

By directly interacting with their promoters, enhancer DNA sequences play a crucial function in promoting transcription initiation. Enhancers, which are positioned far from their target promoters, often include particular DNA patterns that serve as binding regions for transcription factors and cofactors. The relationship between enhancers and their target promoters is critical in gene expression control (Blackwood & Kadonaga, 1998).

In most eukaryotic cells, including mammalian cells, a poly(A) tail is added to the 3' end of most nascent mRNA molecules. This process, called polyadenylation, plays a crucial role in mRNA stability, efficient translation, and nuclear export. Mammalian expression vectors commonly include poly(A) signal sequences taken from bovine growth hormone, the early transcription unit of SV40, and mouse β-globin. (Savvas C. Makrides, 2003).

In mammalian expression vectors, continuous transcription from an upstream promoter may interfere with the downstream promoter activity. The addition of a termination signal at the 3' end of the coding sequence provides proper transcriptional termination, enabling each transcriptional unit within the vector to operate independently and correctly.

In higher eukaryotes, CC(A/G)CC**AUG**G sequences have been defined as Kozak sequences with AUG as the start codon. When generating recombinant expression constructs in mammalian cells, the addition of the Kozak consensus sequence helps increasing the efficiency of translation initiation. This is a design strategy to ensure that the inserted gene is translated correctly and expressed more effectively in the cell. Within Kozak sequence, the purines A or G at position -3 and the nucleotide G at position +4 are the most important nucleotides that enhance translation initiation (Dröge, 2006; Zucchelli, Patrucco, Persichetti, Gustincich, & Cotella, 2016).

Certain DNA elements, such as insulators, can protect transgenes from positional cloning effects, as exemplified by the use of MAR/S-MAR (matrix attachment region/scaffold/matrix association region). MARs help create an open chromatin domain that supports transcription, potentially anchoring chromatin to the nuclear matrix. They increase reporter expression and stability by minimizing silencing effects. Another strategy involves using UCOEs (ubiquitous chromatin unwinding elements) from flanking housekeeping genes, maintaining a transcription-friendly chromatin conformation. The incorporation of MARs and UCOEs into mammalian expression vector design is gaining traction to increase efficiency and shorten development timelines (Alldread et al., 2014).

Selectable marker sequences are routinely inserted into expression vectors for the purpose of choosing and identifying mammalian cell clones that have stably integrated the genes to be produced. Antibiotic resistance, fluorescent proteins, reporter genes, and metabolic selection markers are the most popular selection mechanisms used in mammalian cells (Gray, 2001; O'Flaherty et al., 2020).

Mammalian cell lines employ their secretory system to deliver naturally occurring proteins including hormones and enzymes into the extracellular

environment (Bachhav, de Rossi, Llanos, & Segatori, 2023). Following synthesis, the protein undergoes its initial modification in the endoplasmic reticulum (ER). It is then delivered to the Golgi to undergo further modifications. After these steps, secretory vesicles carry the proteins to the cell's plasma membrane (Viotti, 2016).

The production of therapeutic recombinant proteins in secretable form has become an essential technique in mammalian cell line engineering (Zucchelli et al., 2016). A signal peptide (SP) sequence is inserted into the N-terminus of the target protein to guide its translocation into the endoplasmic reticulum lumen. These sequences are typically 5-30 amino acids in length. Once the peptide chain enters the ER lumen, the signal peptidase enzyme removes the SP from the target protein (Stern, Olsen, Trösse, Ravneberg, & Pryme, 2007).Because different SPs have significant effects on protein secretion, the selection of the appropriate signal peptide is crucial when aiming to maximize recombinant protein production in mammalian cells. Many studies have shown that the use of different signal peptides increases protein production efficiency (Haryadi et al., 2015; Knappskog et al., 2007).

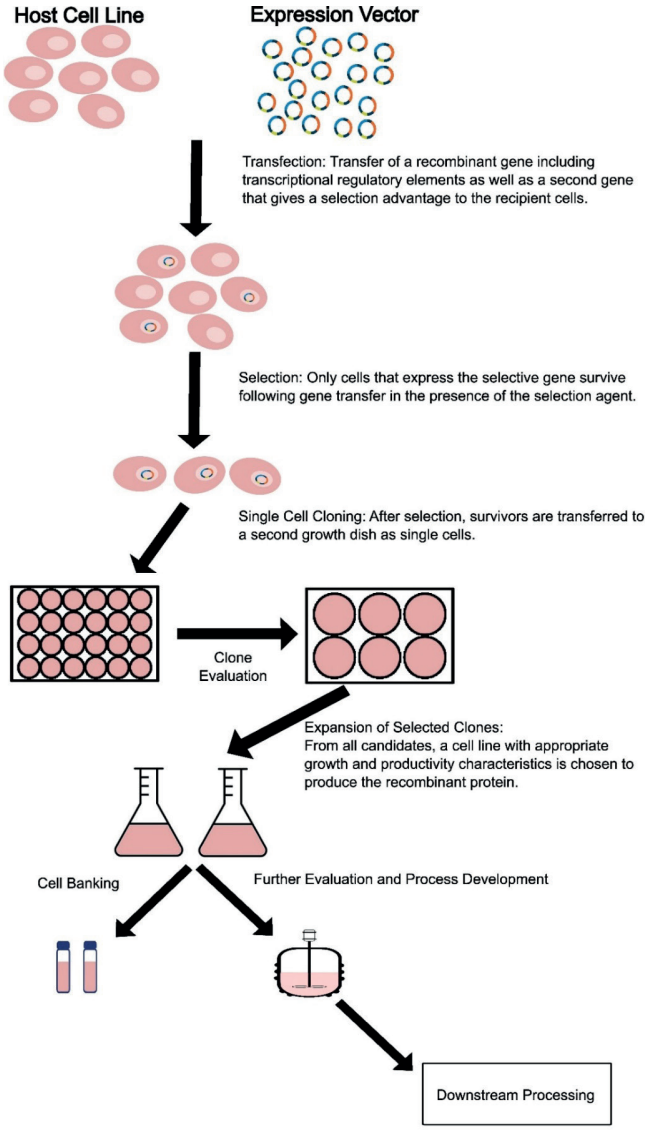

Figure 1: Depiction of the main steps in the development of a recombinant mammalian cell expression system (adopted from (Gray, 2001; Wurm, 2004))

Introduction of Foreign Genetic Material into Mammalian Cells

- **Biological Methods**

In the virus-mediated transfection method, also known as transduction, the genes to be expressed are transported to the host cell via viral vectors. Different types of viruses are used for this purpose, such as lentiviruses, adenoviruses and retroviruses. Virus-mediated transfection is highly efficient (Kim & Eberwine, 2010).

- **Chemical Methods**

The calcium phosphate transfection method entails the combination of DNA with a buffer containing calcium chloride and phosphate to form precipitate. If insoluble calcium phosphate-DNA precipitate is applied to cells, it attaches to the cell surface and enters into a cytoplasm through endocytosis (Dudek, Ghosh, & Greenberg, 2001).

Positive charges present in cationic polymers can bind nucleic acids through electrostatic interactions. This binding leads to the formation of small nanoparticles. Nucleic acid delivery with cationic polymers is based on the fact that positive charges interact with negatively charged cell membranes, allowing polymer-nucleic acid complexes to enter the cell (Cai et al., 2023).

Liposomes can spontaneously interact with DNA and then provide gene transfer in mammalian cells by fusion with the cell membrane. In the lipofection method, the similar structure of the host cells membrane consisting of double-layered phospholipids and liposomes, facilitates gene transfer (Carter & Shieh, 2015b; Felgner et al., 1987).

- **Physical Methods**

Electroporation is one of the physical techniques that researchers frequently apply to transfer recombinant genes into mammalian cells. During electroporation, generating an intense electric field for short periods leads to temporary pores in the plasma membrane that allow foreign genetic materials to access cells(Sokołowska & Błachnio-Zabielska, 2019).

The technique of microinjection involves the direct transfer of foreign nucleic acids to the cytoplasm or nucleus of host cells using a small glass needle or micropipette. This method is currently being utilized in recombinant cell line generation among other applications (Chenuet, Derouazi, Hacker, & Wurm, 2009; Dean, 2013).

Selection of Positive Clones

In the context of mammalian cell line development for a target therapeutic protein of interest, selection involves applying selective pressure to isolate and maintain cells that successfully incorporate the recombinant genes into their genome and express these genes (Gray, 2001).

Antibiotic selection, one of the most common methods, is based on inserting antibiotic resistance genes into expression vectors and ensuring the survival of only clones that successfully integrate and express foreign genes in the antibiotic-containing medium (O'Flaherty et al., 2020).

Fluorescent protein genes such as Green Fluorescent Protein (GFP) are fused with the transgene and provide the visualization and classification of clones based on fluorescence intensity (Kume, Hashiyama, Suda, & Ozawa, 1999).

Combined with genes of interest, reporter genes are inserted into mammalian cells (Zhang, Liu, He, Gong, & Yang, 2006). Reporter genes, encode proteins such as luciferase and exert tractable phenotypic properties enabling the identification of clones expressing the desired recombinant genes (Alam & Cook, 2003). Glutamine synthetase (GS) and dihydrofolate reductase (DHFR) systems are commonly preferred metabolite selection strategies. The GS system involves insertion of the GS gene into cells that lack endogenous GS activity, allowing growth in a glutamine-free medium. The DHFR system uses DHFR-deficient cells, allowing survival and proliferation in a hypoxanthine- and thymidine-deficient environment when only the transfected DHFR gene is expressed (Budge et al., 2021).

Clone Evaluation, Expansion of Positive Clones and Cell Banking

In therapeutic protein-producing cell line development, the process of post-selection is vital for acquiring high-producing cell lines. Transfer of the survivors using a single clone technique following the selection ensures that clonal populations are generated. Clonal expansion facilitates the study of individual clones to determine the best producer colony. The respective cell line, showing the favorable growth and productivity properties is then developed further for cultivation and analysis highlighting the characteristic selection of a robust and very effective platform for therapeutic protein manufacturing (Wurm, 2004).

In the field of commercial therapeutic protein production, it is very important to establish a cell source storage system using cryopreservation to ensure consistent product manufacturing. The master cell bank and working cell bank system guarantee a stable supply of the therapeutic protein over a long period. This procedure allows not only for the long-term preservation of the producer cell line but also provides proactive safety and quality testing, therefore ensuring reliability and security in the biotherapeutic protein supply. This strategy corresponds to the industry that requires a constant high quality where in its commercial stage of therapeutic protein manufacturing (Kshirsagar & Ryll, 2018).

Process Design

The cultivation of mammalian cells poses unique challenges attributed to their inherent characteristics. Mammalian cells are known for their relatively slow growth rates affecting the overall efficiency of cell culture processes. Furthermore, productivity may be comparatively low. Another critical factor contributing to the challenges in mammalian cell cultivation is their vulnerability to shear stress. Unlike bacterial cells, mammalian cells lack a rigid cell wall, rendering them highly sensitive to mechanical forces generated during agitation or mixing in bioreactors. The susceptibility to shear stress necessitates careful optimization of culture conditions and the

use of specialized equipment to ensure the well-being and productivity of mammalian cells in industrial processes (Kretzmer & Schügerl, 1991; Pörtner, 2015).

Adherent cell cultures and suspension cultures are used to produce recombinant protein in mammalian cells with the suspension cultures are the more common (Wurm, 2004). Adherent cells require a surface to attach to for growth and multiplication. Various bioreactor designs used for adherent cell cultures include microcarriers, plate stacks, hollow fibers, rolled membranes, and roller bottles. Microcarriers, such as those in fluidized or packed-bed mode, provide a large surface area for cell attachment within a culture vessel. Plate stacks involve stacking traditional culture plates in batch mode. Hollow fiber bioreactors, using bundled fibers encased in a cartridge, facilitate cell growth on the outer surface while fresh medium circulates through the lumina. Rolled membranes, a less common strategy, involve introducing a long-rolled membrane within a traditional roller bottle, providing a continuous surface for cell attachment. Adherent cells are commonly cultured in roller bottles that function as suitable solutions, both for cell production and also medium collection. Specifically, their efficiency is attributed to the better medium usage; increased surface area of the culture; and effective gas transfer making them suitable for biopharmaceutical applications (Simón, 2015).

Although there are numerous alternative production strategies, large-scale manufacturing with adherent cells might be difficult since they require a great amount of surface to proliferate. Compared to the adhered cultures, the suspension culture method offers a well-mixed and homogenous environment for process parameter measurement and quantitative modeling of growth parameters. If appropriate methods and the medium composition are used, physical challenges such as cell damage by agitation or oxygen delivery can be efficiently managed. As such, industrially relevant cell lines that include the Chinese hamster ovary (CHO), baby hamster kidney (BHK) and hybridoma cells can be modified to grow in the suspension cultures enabling them for large scale production (Werner, Walz, Noé, & Konrad, 1992).

Bioreactors required for the growth of mammalian cells must provide an environment arranged to ensure mass and energy transfer according to protein synthesis requirements. The selection of equipment, raw materials and process control parameters must be made carefully. The design of the bioreactor should allow for process scale-up (Alldread et al., 2014).

Stirred-tank bioreactors use an impeller for the stirring of the culture medium. Design considerations include impeller dynamics, tank dimension ratio and gas flow rates, and sample locations for pH-dissolved oxygen probes in baffles to establish temperature control. As the field of industrial mammalian cell culture continues to develop at a rapid pace, efforts are

focused on optimizing large stirred-tank bioreactors for improved compliance with specific features associated with commonly used mammalian cell lines. This constant evolution highlights the need for designing bioreactors to maximize protein synthesis from proliferating and metabolic mammalian cell cultures while also promoting scalability in industrial lifecycles (Alldread et al., 2014). Stainless steel stirred tank reactors are most commonly used in the biopharmaceutical manufacturing industry, especially for processes on the largest scales (Kuystermans & Al-Rubeai, 2011).

Airlift bioreactors employ gas injection at the base to oxygenate and agitate cultures, featuring distinct gas-containing (riser) and liquid-containing (downcomer) zones created by internal baffles. They offer advantages like low energy costs, minimal shear, no internal moving parts, high reliability for sterilization, and efficient O2 absorption. Design factors for large-scale airlift fermenters include aspect ratio, gas flow rate, feed points, pH and dissolved oxygen probes, base design, and temperature control (Alldread et al., 2014; Kuystermans & Al-Rubeai, 2011).

The wave-based bioreactor is one of the several single-use systems that work on principle as rocking or waving motion within a plastic bag or chamber which contains cell culture and creates gentle, oscillating waves. This motion creates the homogeneity of cells and nutrients without any typical impellers or stirrers. In the realm of biopharmaceutical protein production, wave-based bioreactors have some distinct advantages to offer like convenience in operation along with scalability and also minimal chances of contamination as the entire apparatus is disposable. The rocking motion ensures an efficient mixing and also enhances the oxygenation, which together promote cell growth and protein expression. Wave-based bioreactors have become a very popular choice in the field of industrial bioprocessing (Alldread et al., 2014; Rodrigues, Costa, Henriques, Azeredo, & Oliveira, 2012).

Cell culture medium is an important factor affecting recombinant protein production in mammalian cells. Mammalian cell culture media are more complex compared to the simply defined media used for bacterial and yeast growth. Such complexity comprises the supply of numerous nutrients, growth factors, and other substances that are required for normal mammal cellular development and metabolism. Although some cell lines can be adapted to a wide range of environments and supplements, this becomes quite critical in normal cells and stem cells. Critical steps in producing recombinant proteins include selecting and fine-tuning cell culture media and supplements (Gray, 2001; Price, 2017).

Natural and synthetic media types are used in mammalian cells (Arora, 2013). Natural media rely on the presence of natural biological materials such as serum.However, the complexity and uncertain content of these media

make the reproducibility of the results poor (Morgan, Morton, & Parker, 1950). On the other hand, synthetic media with defined components provides an efficient path for research and development (O'Flaherty et al., 2020). The medium used in the process is selected according to cost and the selected cell type. In addition, whether the applied method is adherent or suspended culture and the presence of an affinity tag for the purification steps also affect the choice of medium (Dalton & Barton, 2014).

Downstream Processing

Mammalian cell factories are grown in a complex cell culture solution to secrete therapeutic proteins, which are biological molecules secreted by these cell factories. The next step is to separate and purify desired products while preserving a suitable level of product recovery and quality (Singh et al., 2013). To remove producer cells, contaminants,and cellular debris from the culture medium, centrifugation is often used as the primary step (Westoby, Rogers, Haverstock, Romero, & Pieracci, 2011). In addition, filtration and sedimentation processes are also used as unit operation steps in mammalian cell processes (M. Butler & Meneses-Acosta, 2012).

Chromatography plays a crucial role in the separation and purification processes for recombinant protein production, leveraging its high resolution. This technology capitalizes on the distinctive physical and chemical characteristics of biomolecules to achieve effective separation. An important stage of purifying monoclonal antibodies is the protein A affinity chromatography which provides efficient selectivity, flow rates, and relatively low-cost binding capacity. It efficiently eliminates contaminants including host cell proteins and DNA to provide a purified highly stable protein product (Liu, Ma, Winter, & Bayer, 2010).

REFERENCES

Alam, J., & Cook, J. L. (2003). Reporter genes for monitoring gene expression in mammalian cells. In *New Comprehensive Biochemistry* (Vol. 38, pp. 291–308). Elsevier. https://doi.org/10.1016/S0167-7306(03)38018-4

Alldread, R. M., Birch, J. R., Metcalfe, H. K., Farid, S., Racher, A. J., Young, R. J., & Khan, M. (2014). Large Scale Suspension Culture of Mammalian Cells. In *Industrial Scale Suspension Culture of Living Cells* (pp. 410–462). https://doi.org/10.1002/9783527683321.ch12

Arora, M. (2013). Cell Culture Media: A Review. *Materials and Methods*, *3*. Retrieved from https://api.semanticscholar.org/CorpusID:83604958

Bachhav, B., de Rossi, J., Llanos, C. D., & Segatori, L. (2023). Cell factory engineering: Challenges and opportunities for synthetic biology applications. *Biotechnology and Bioengineering*, *120*(9), 2441–2459. https://doi.org/10.1002/bit.28365

Blackwood, E. M., & Kadonaga, J. T. (1998). Going the Distance: A Current View of Enhancer Action. *Science*, *281*(5373), 60–63. https://doi.org/10.1126/science.281.5373.60

Brooks, S. A. (2004). Appropriate glycosylation of recombinant proteins for human use. *Molecular Biotechnology*, *28*(3), 241–255. https://doi.org/10.1385/MB:28:3:241

Buchman, A. R., & Berg, P. (1988). Comparison of intron-dependent and intron-independent gene expression. *Molecular and Cellular Biology*, *8*(10), 4395–4405. https://doi.org/10.1128/mcb.8.10.4395-4405.1988

Budge, J. D., Roobol, J., Singh, G., Mozzanino, T., Knight, T. J., Povey, J., … Smales, C. M. (2021). A proline metabolism selection system and its application to the engineering of lipid biosynthesis in Chinese hamster ovary cells. *Metabolic Engineering Communications*, *13*, e00179. https://doi.org/10.1016/j.mec.2021.e00179

Butler, M., & Meneses-Acosta, A. (2012). Recent advances in technology supporting biopharmaceutical production from mammalian cells. *Applied Microbiology and Biotechnology*, *96*(4), 885–894. https://doi.org/10.1007/s00253-012-4451-z

Butler, Michael, & Spearman, M. (2014). The choice of mammalian cell host and possibilities for glycosylation engineering. *Chemical Biotechnology • Pharmaceutical Biotechnology*, *30*, 107–112. https://doi.org/10.1016/j.copbio.2014.06.010

Cai, X., Dou, R., Guo, C., Tang, J., Li, X., Chen, J., & Zhang, J. (2023). Cationic Polymers as Transfection Reagents for Nucleic Acid Delivery. *Pharmaceutics*, *15*(5). https://doi.org/10.3390/pharmaceutics15051502

Carter, M., & Shieh, J. (2015a). Chapter 10—Molecular Cloning and Recombinant DNA Technology. In M. Carter & J. Shieh (Eds.), *Guide to Research Techniques in Neuroscience (Second Edition)* (pp. 219–237). San Diego: Academic Press. https://doi.org/10.1016/B978-0-12-800511-8.00010-1

Carter, M., & Shieh, J. (2015b). Chapter 11—Gene Delivery Strategies. In M. Carter & J. Shieh (Eds.), *Guide to Research Techniques in Neuroscience (Second Edition)* (pp. 239–252). San Diego: Academic Press. https://doi.org/10.1016/B978-0-12-800511-8.00011-3

Chang, C. N., Rey, M., Bochner, B., Heyneker, H., & Gray, G. (1987). High-level secretion of human growth hormone by Escherichia coli. *Gene*, *55*(2–3), 189–196. https://doi.org/10.1016/0378-1119(87)90279-4

Chenuet, S., Derouazi, M., Hacker, D., & Wurm, F. (2009). DNA delivery by microinjection for the generation of recombinant mammalian cell lines. *Methods in Molecular Biology (Clifton, N.J.)*, *518*, 99–112. https://doi.org/10.1007/978-1-59745-202-1_8

Dalton, A. C., & Barton, W. A. (2014). Over-expression of secreted proteins from mammalian cell lines. *Protein Science*, *23*(5), 517–525. https://doi.org/10.1002/pro.2439

Dean, D. A. (2013). Microinjection. In S. Maloy & K. Hughes (Eds.), *Brenner's Encyclopedia of Genetics (Second Edition)* (pp. 409–410). San Diego: Academic Press. https://doi.org/10.1016/B978-0-12-374984-0.00945-1

Dröge, A. (2006). Recombinant Protein Production in Mammalian Cell Culture. In *Encyclopedic Reference of Genomics and Proteomics in Molecular Medicine* (pp. 1616–1620). Berlin, Heidelberg: Springer Berlin Heidelberg. https://doi.org/10.1007/3-540-29623-9_3640

Dudek, H., Ghosh, A., & Greenberg, M. E. (2001). Calcium phosphate transfection of DNA into neurons in primary culture. *Current Protocols in Neuroscience*, *Chapter 3*, Unit 3.11. https://doi.org/10.1002/0471142301.ns0311s03

Dumont, J., Euwart, D., Mei, B., Estes, S., & Kshirsagar, R. (2016). Human cell lines for biopharmaceutical manufacturing: History, status, and future perspectives. *Critical Reviews in Biotechnology*, *36*(6), 1110–1122. https://doi.org/10.3109/07388551.2015.1084266

Durocher, Y., & Butler, M. (2009). Expression systems for therapeutic glycoprotein production. *Current Opinion in Biotechnology*, *20*, 700–707. https://doi.org/10.1016/j.copbio.2009.10.008

Ebrahimi, S. B., & Samanta, D. (2023). Engineering protein-based therapeutics through structural and chemical design. *Nature Communications*, *14*(1), 2411. https://doi.org/10.1038/s41467-023-38039-x

Estes, S., & Melville, M. (2014). Mammalian cell line developments in speed and efficiency. *Advances in Biochemical Engineering/Biotechnology*, *139*, 11–33. https://doi.org/10.1007/10_2013_260

Felgner, P. L., Gadek, T. R., Holm, M., Roman, R., Chan, H. W., Wenz, M., … Danielsen, M. (1987). Lipofection: A highly efficient, lipid-mediated DNA-transfection procedure. *Proceedings of the National Academy of Sciences of the United States of America*, *84*(21), 7413–7417. https://doi.org/10.1073/pnas.84.21.7413

Fliedl, L., Grillari, J., & Grillari-Voglauer, R. (2015). Human cell lines for the production of recombinant proteins: On the horizon. *European Congress of Biotechnology - ECB 16*, *32*(6), 673–679. https://doi.org/10.1016/j.nbt.2014.11.005

Ghaderi, D., Taylor, R. E., Padler-Karavani, V., Diaz, S., & Varki, A. (2010). Implications of the presence of N-glycolylneuraminic acid in recombinant therapeutic glycoproteins. *Nature Biotechnology*, *28*(8), 863–867. https://doi.org/10.1038/nbt.1651

Gill, D. R., Pringle, I. A., & Hyde, S. C. (2009). Progress and Prospects: The design and production of plasmid vectors. *Gene Therapy*, *16*(2), 165–171. https://doi.org/10.1038/gt.2008.183

Goodman, M. (2009). Market watch: Sales of biologics to show robust growth through to 2013. *Nature Reviews. Drug Discovery*, *8*(11), 837. https://doi.org/10.1038/nrd3040

Graham, F. L., & Prevec, L. (1995). Methods for construction of adenovirus vectors. *Molecular Biotechnology*, *3*(3), 207–220. https://doi.org/10.1007/BF02789331

Gray, D. (2001). Overview of protein expression by mammalian cells. *Curr Protoc Protein Sci*, *Chapter 5*(1), Unit5.9. https://doi.org/10.1002/0471140864.ps0509s10

Hacker, D. L., & Balasubramanian, S. (2016). Recombinant protein production from stable mammalian cell lines and pools. *New Constructs and Expression of Proteins • Sequences and Topology*, *38*, 129–136. https://doi.org/10.1016/j.sbi.2016.06.005

Haryadi, R., Ho, S., Kok, Y. J., Pu, H. X., Zheng, L., Pereira, N. A., … Song, Z. (2015). Optimization of heavy chain and light chain signal peptides for high level expression of therapeutic antibodies in CHO cells. *PloS One*, *10*(2), e0116878. https://doi.org/10.1371/journal.pone.0116878

Jorge Angel Ascacio-Martínez & Hugo Alberto Barrera-Saldaña. (2012). Genetic Engineering and Biotechnology of Growth Hormones. In Hugo A. Barrera-Saldaña (Ed.), *Genetic Engineering* (p. Ch. 7). Rijeka: IntechOpen. https://doi.org/10.5772/38978

KARVAR, S. (2014). The role of ABC transporters in anticancer drug transport. *TURKISH JOURNAL OF BIOLOGY*, *38*, 800–805. https://doi.org/10.3906/biy-1407-3

Kaufman, R. J. (2000). Overview of vector design for mammalian gene expression. *Molecular Biotechnology*, *16*(2), 151–160. https://doi.org/10.1385/MB:16:2:151

Khan, K. H. (2013). Gene expression in Mammalian cells and its applications. *Advanced Pharmaceutical Bulletin*, *3*(2), 257–263. https://doi.org/10.5681/apb.2013.042

Kim, T. K., & Eberwine, J. H. (2010). Mammalian cell transfection: The present and the future. *Analytical and Bioanalytical Chemistry*, *397*(8), 3173–3178. https://doi.org/10.1007/s00216-010-3821-6

Knappskog, S., Ravneberg, H., Gjerdrum, C., Trösse, C., Stern, B., & Pryme, I. F. (2007).

The level of synthesis and secretion of Gaussia princeps luciferase in transfected CHO cells is heavily dependent on the choice of signal peptide. *Journal of Biotechnology*, *128*(4), 705–715. https://doi.org/10.1016/j.jbiotec.2006.11.026

Kretzmer, G., & Schügerl, K. (1991). Response of mammalian cells to shear stress. *Applied Microbiology and Biotechnology*, *34*(5), 613–616. https://doi.org/10.1007/BF00167909

Krshnan, L., van de Weijer, M. L., & Carvalho, P. (2022). Endoplasmic Reticulum-Associated Protein Degradation. *Cold Spring Harbor Perspectives in Biology*, *14*(12). https://doi.org/10.1101/cshperspect.a041247

Kshirsagar, R., & Ryll, T. (2018). Innovation in Cell Banking, Expansion, and Production Culture. In B. Kiss, U. Gottschalk, & M. Pohlscheidt (Eds.), *New Bioprocessing Strategies: Development and Manufacturing of Recombinant Antibodies and Proteins* (pp. 51–74). Cham: Springer International Publishing. https://doi.org/10.1007/10_2016_56

Kume, A., Hashiyama, M., Suda, T., & Ozawa, K. (1999). Green fluorescent protein as a selectable marker of retrovirally transduced hematopoietic progenitors. *Stem Cells (Dayton, Ohio)*, *17*(4), 226–232. https://doi.org/10.1002/stem.170226

Kurian, K. M., Watson, C. J., & Wyllie, A. H. (2000). Retroviral vectors. *Molecular Pathology : MP*, *53*(4), 173–176. https://doi.org/10.1136/mp.53.4.173

Kuystermans, D., & Al-Rubeai, M. (2011). *Bioreactor Systems for Producing Antibody from Mammalian Cells*. https://doi.org/10.1007/978-94-007-1257-7_2

Liu, H. F., Ma, J., Winter, C., & Bayer, R. (2010). Recovery and purification process development for monoclonal antibody production. *mAbs*, *2*(5), 480–499. https://doi.org/10.4161/mabs.2.5.12645

Lufino, M. M., Edser, P. A., & Wade-Martins, R. (2008). Advances in High-capacity Extrachromosomal Vector Technology: Episomal Maintenance, Vector Delivery, and Transgene Expression. *Molecular Therapy*, *16*(9), 1525–1538. https://doi.org/10.1038/mt.2008.156

Makrides, S. C. (1999). Components of vectors for gene transfer and expression in mammalian cells. *Protein Expression and Purification*, *17*(2), 183–202. https://doi.org/10.1006/prep.1999.1137

Makrides, Savvas C. (2003). Vectors for gene expression in mammalian cells. In *New Comprehensive Biochemistry* (Vol. 38, pp. 9–26). Elsevier. https://doi.org/10.1016/S0167-7306(03)38002-0

Mansouri, M., & Berger, P. (2018). Baculovirus for gene delivery to mammalian cells: Past, present and future. *Plasmid*, *98*, 1–7. https://doi.org/10.1016/j.plasmid.2018.05.002

Maximize Market Research Pvt Ltd. (n.d.). *Global Protein Drugs Market Report*. Retrieved from https://www.maximizemarketresearch.com/market-report/global-protein-drugs-market/82226/

Meissner, P., Pick, H., Kulangara, A., Chatellard, P., Friedrich, K., & Wurm, F. M.

(2001). Transient gene expression: Recombinant protein production with suspension-adapted HEK293-EBNA cells. *Biotechnology and Bioengineering*, *75*(2), 197–203. https://doi.org/10.1002/bit.1179

Morgan, J. F., Morton, H. J., & Parker, R. C. (1950). Nutrition of Animal Cells in Tissue Culture. I. Initial Studies on a Synthetic Medium.,. *Proceedings of the Society for Experimental Biology and Medicine*, *73*(1), 1–8. https://doi.org/10.3181/00379727-73-17557

O'Flaherty, R., Bergin, A., Flampouri, E., Mota, L. M., Obaidi, I., Quigley, A., … Butler, M. (2020). Mammalian cell culture for production of recombinant proteins: A review of the critical steps in their biomanufacturing. *Biotechnology Advances*, *43*, 107552. https://doi.org/10.1016/j.biotechadv.2020.107552

Ogihara, T., Mizoi, K., & Ishii-Watabe, A. (2023). Pharmacokinetics of Biopharmaceuticals: Their Critical Role in Molecular Design. *Biomedicines*, *11*(5). https://doi.org/10.3390/biomedicines11051456

Pörtner, R. (2015). *Bioreactors for Mammalian Cells*. Retrieved from https://api.semanticscholar.org/CorpusID:61441784

Price, P. J. (2017). Best practices for media selection for mammalian cells. *In Vitro Cellular & Developmental Biology - Animal*, *53*(8), 673–681. https://doi.org/10.1007/s11626-017-0186-6

Qin, J. Y., Zhang, L., Clift, K. L., Hulur, I., Xiang, A. P., Ren, B.-Z., & Lahn, B. T. (2010). Systematic comparison of constitutive promoters and the doxycycline-inducible promoter. *PloS One*, *5*(5), e10611. https://doi.org/10.1371/journal.pone.0010611

Reichert, J. M., & Paquette, C. (2003). Therapeutic recombinant proteins: Trends in US approvals 1982 to 2002. *Current Opinion in Molecular Therapeutics*, *5*(2), 139—147.

Rodrigues, M. E., Costa, A. R., Henriques, M., Azeredo, J., & Oliveira, R. (2012). Wave characterization for mammalian cell culture: Residence time distribution. *New Biotechnology*, *29*(3), 402–408. https://doi.org/10.1016/j.nbt.2011.10.006

Rossi, F. M., & Blau, H. M. (1998). Recent advances in inducible gene expression systems. *Current Opinion in Biotechnology*, *9*(5), 451–456. https://doi.org/10.1016/s0958-1669(98)80028-1

Simón, M. (2015). Bioreactor design for adherent cell culture: The bolt-on bioreactor project, part 2-process automation. *BioProcess International*, *13*.

Singh, N., Pizzelli, K., Romero, J. K., Chrostowski, J., Evangelist, G., Hamzik, J., … Cheng, K. S. (2013). Clarification of recombinant proteins from high cell density mammalian cell culture systems using new improved depth filters. *Biotechnology and Bioengineering*, *110*(7), 1964–1972. https://doi.org/10.1002/bit.24848

Sokołowska, E., & Błachnio-Zabielska, A. U. (2019). A Critical Review of Electroporation as A Plasmid Delivery System in Mouse Skeletal Muscle. *International Journal of Molecular Sciences*, *20*(11). https://doi.org/10.3390/ijms20112776

Stern, B., Olsen, L., Trösse, C., Ravneberg, H., & Pryme, I. (2007). Improving mammalian cell factories: The selection of signal peptide has a major impact on recombinant protein synthesis and secretion in mammalian cells. *Trends Cell Mol. Biol.*, *2*, 1–17.

Tariq, M., Akash, M. S. H., Rehman, K., & shuqing, chen. (2015). Development of therapeutic proteins: Advances and challenges. *Turkish Journal of Biology*, *39*. https://doi.org/10.3906/biy-1411-8

Verma, R., Boleti, E., & George, A. J. T. (1998). Antibody engineering: Comparison of bacterial, yeast, insect and mammalian expression systems. *Journal of Immunological Methods*, *216*(1), 165–181. https://doi.org/10.1016/S0022-1759(98)00077-5

Viotti, C. (2016). ER to Golgi-Dependent Protein Secretion: The Conventional Pathway. *Methods in Molecular Biology (Clifton, N.J.)*, *1459*, 3–29. https://doi.org/10.1007/978-1-4939-3804-9_1

Walsh, G., & Jefferis, R. (2006). Post-translational modifications in the context of therapeutic proteins. *Nature Biotechnology*, *24*(10), 1241–1252. https://doi.org/10.1038/nbt1252

Walsh, G., & Walsh, E. (2022). Biopharmaceutical benchmarks 2022. *Nature Biotechnology*, *40*(12), 1722–1760. https://doi.org/10.1038/s41587-022-01582-x

Wang, T.-Y., & Guo, X. (2020). Expression vector cassette engineering for recombinant therapeutic production in mammalian cell systems. *Applied Microbiology and Biotechnology*, *104*(13), 5673–5688. https://doi.org/10.1007/s00253-020-10640-w

Weber, W., Rimann, M., Spielmann, M., Keller, B., Baba, M. D.-E., Aubel, D., … Fussenegger, M. (2004). Gas-inducible transgene expression in mammalian cells and mice. *Nature Biotechnology*, *22*(11), 1440–1444. https://doi.org/10.1038/nbt1021

Werner, R. G., Walz, F., Noé, W., & Konrad, A. (1992). Safety and economic aspects of continuous mammalian cell culture. *Continuous Bioprocesses for Proteins and Fine Chemicals*, *22*(1), 51–68. https://doi.org/10.1016/0168-1656(92)90132-S

Westoby, M., Rogers, J. K., Haverstock, R., Romero, J., & Pieracci, J. (2011). Modeling industrial centrifugation of mammalian cell culture using a capillary based scale-down system. *Biotechnology and Bioengineering*, *108*(5), 989–998. https://doi.org/10.1002/bit.23051

Wise, R. J., Orkin, S. H., & Collins, T. (1989). Aberrant expression of platelet-derived growth factor A-chain cDNAs due to cryptic splicing of RNA transcripts in COS-1 cells. *Nucleic Acids Research*, *17*(16), 6591–6601. https://doi.org/10.1093/nar/17.16.6591

Wurm, F. M. (2004). Production of recombinant protein therapeutics in cultivated mammalian cells. *Nature Biotechnology*, *22*(11), 1393–1398. https://doi.org/10.1038/nbt1026

Zhang, S., Liu, W., He, P., Gong, F., & Yang, D. (2006). Establishment of stable high expression cell line with green fluorescent protein and resistance genes. *Journal of Huazhong University of Science and Technology. Medical Sciences = Hua Zhong Ke Ji Da Xue Xue Bao. Yi Xue Ying De Wen Ban = Huazhong Keji Daxue Xuebao. Yixue Yingdewen Ban*, *26*(3), 298–300. https://doi.org/10.1007/BF02829556

Zhu, M., Mollet, M., Hubert, R., Kyung, Y., & Zhang, G. (2017). *Industrial Production of Therapeutic Proteins: Cell Lines, Cell Culture, and Purification*. https://doi.org/10.1007/978-3-319-52287-6_29

Zucchelli, S., Patrucco, L., Persichetti, F., Gustincich, S., & Cotella, D. (2016). Engineering Translation in Mammalian Cell Factories to Increase Protein Yield: The Unexpected Use of Long Non-Coding SINEUP RNAs. *Computational and Structural Biotechnology Journal*, *14*, 404–410. https://doi.org/10.1016/j.csbj.2016.10.004

CHAPTER 6

SUSTAINABLE MODULAR BUILDING BRICK OR PANEL ELEMENT MADE OF WASTE CONCRETE AND HEAT INSULATING MATERIALS

Furkan Birdal[1], Hasan Dilbas[2]
Erkam Köseömür[3], Emre Şahin[4],
Mustafa Kerem Soyal[5]

1 Ph.D., Asst. Prof., Kırşehir Ahi Evran University, Faculty of Engineering and Architecture, Department of Civil Engineering, Kırşehir, TÜRKİYE, ORCID: 0000-0002-2243-418X, f.birdal@ahievran.edu.tr
2 Ph.D., Asst. Prof., Van Yuzuncu Yil University, Faculty of Engineering, Department of Civil Engineering, Van, TÜRKİYE, ORCID:0000-0002-3780-8818, hasandilbas@yyu.edu.tr
3 M.Sc. candidate, Kırşehir Ahi Evran University, Faculty of Engineering and Architecture, Department of Civil Engineering, Kırşehir, TÜRKİYE, ORCID: 0009-0000-7888-1221, erkam_koseomur3@hotmail.com
4 M.Sc. candidate, Kırşehir Ahi Evran University, Faculty of Engineering and Architecture, Department of Civil Engineering, Kırşehir, TÜRKİYE, ORCID: 0009-0006-5985-2103, emresahinresmi@gmail.com
5 M.Sc. candidate, Kırşehir Ahi Evran University, Faculty of Engineering and Architecture, Department of Civil Engineering, Kırşehir, TÜRKİYE, ORCID: 0009-0005-6113-0380, keremsoyal@gmail.com

1. Introduction

The aim of the book chapter covers the methodology of developing and producing innovative modular building construction brick or panel systems using concrete wastes resulting from urban transformation studies and natural disasters. These systems are also designed to be sustainable, heat efficient, environmentally friendly, and resistant to earthquakes or other natural disasters. As the problem definition titles in the area; environmental impact of waste concrete, damages occurred in structures caused by natural disasters, non-modular building designs, heat efficiency problems, long building construction time and sustainability. In the selection of these topics, the interaction between the construction sector and the developments in the fields of environment, energy and climate has been taken into consideration. The design details, general assembly procedure of the modular building brick or panel elements that will solve the problem definitions listed above have been developed. In addition, many existing methods in the literature in this field were examined and comparisons were made with a proposed method. As a result of the study, all the details for solutions of the problems are presented in this chapter as a method. It is aimed that these developed panel elements can be used in the construction of residential, commercial, and industrial structures. The motivations of the book chapter are given listed below:

- Reuse of concrete wastes resulting from urban transformation works and natural disasters.
- Innovative building systems made of sustainable materials, environmentally friendly, high thermal efficiency, resistant to earthquakes and other natural disasters.
- Modular, practically applicable, cost-optimal structural designs.

In the book chapter, the solutions are investigated to the questions given below.

- How to design a sustainable modular structural panel element?
- How to design a sustainable modular structural panel element in case of low environmental impact and carbon emission?
- How to design a sustainable modular structural panel element in case of high disaster resistant?
- How to design a sustainable modular structural panel element in case of short construction time and cost?
- How to design a sustainable modular structural panel element in case of high heat efficient?

1.1. **Problem Definitions**

Problems related to environmental impact, sustainability, modularity, and energy have been identified in the construction sector. As a result of urban transformation works and natural disasters, millions of tons of building demolition waste are generated. These wastes cause serious environmental burden. It is very important to evaluate these wastes, develop new environmentally friendly technologies and bring the waste into the economy. However, the use of recycled aggregate concrete in real engineering applications and building construction is quite limited. Modularity in buildings is a current research area. However, most of the buildings built in the construction sector do not have this feature. The ability to dismantle a building and move it to another location is an innovative approach. After disasters, modular structures are preferred because they enable rapid building production. Therefore, modularity emerges as a sought-after feature in the construction industry today. The heat conduction coefficient of the concrete material used in the building construction industry today is high. In reinforced concrete designs, this coefficient increases even more with the reinforcement placed in the section. Therefore, reinforced concrete is a material that requires additional application for thermal insulation. However, heat efficiency problems may arise in prefabricated designs used in the industry. Thermal efficiency is a parameter directly proportional to energy consumption. The concept of sustainability is an effective parameter in the construction industry, as in every field. It is important that the materials to be used are sustainable (recyclable) in order to build a building that causes the least harm to the environment. Sustainable designs are not only environmentally friendly but also produce economical solutions in the long term.

A literature review has been made for these problems. Structural systems produced from given in the suggestion section have provided solutions to 7 main problems in the construction sector (Fig. 1). These problem titles are Fig. 1 has also been defined. Each problem title for this solution methodology produced was compared in detail with the literature studies and examined. The advantages and disadvantages of the approach and the aspects that are open to improvement are presented.

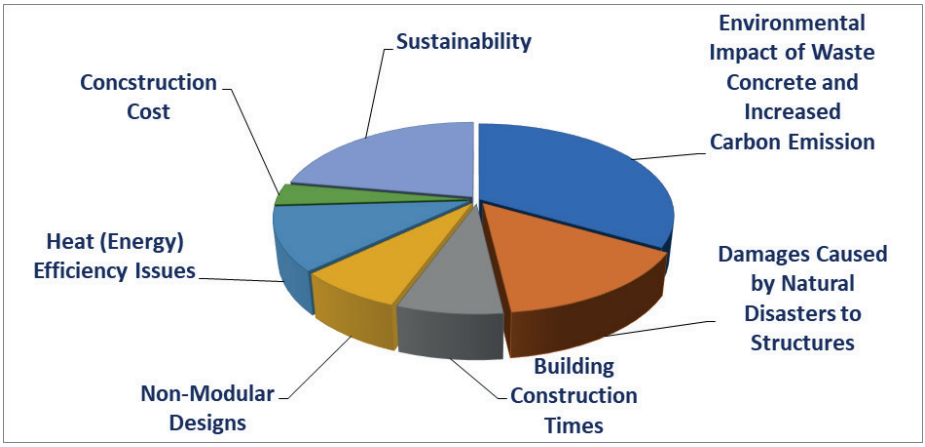

Fig.1 *Problem Definitions*

1.1.1. **Environmental Impact of Waste Concrete and Increased Carbon Emission (A-1)**

Concrete consumption is increasing considerably today. Today, the most common systems used in building construction are reinforced concrete bearing systems. This situation increases the concrete production and consumption rapidly. In this context, concrete consumption is expected to exceed 18 billion tons per year in 2050 [1,2]. The increase in concrete consumption also increases cement production. Therefore, the demand for cement is expected to increase by 200% in 2050 compared to 2010. While producing cement, carbon dioxide is emitted to nature [1]. Although there are solutions in the literature in which different materials are used as binders instead of cement in concrete and even geopolymer concrete approaches, it has been seen that these solutions have not become widespread yet [2]. The most important contribution to this problem in the field of environment is the method of using high performance sustainable materials obtained from the recycling of waste concrete resulting from urban transformation and natural disasters in the construction of new structures and minimizing the percentage of concrete in the bearing modular concrete panel section [3].

1.1.2. **Damages Caused by Natural Disasters to Structures (A-2)**

Earthquakes, flood, fires, high wind effects can damage our structures. Our building designs must have sufficient resistance against all these natural disasters. In order to solve this problem in designs, modular panel steel connection details for earthquake, modular adjustable height and impermeable composite section for flood resistant design, fire resistant composite section for fire resistant design, domed modular roof and curvilinear aerodynamic wall systems consisting of panels for wind resistant design should be detailed [4].

1.1.3. **Building Construction Times (A-3) and Non-Modular Designs (A-4)**

Construction time is an important parameter in the cost analysis of a building. As the construction period of the building increases, the costs increase. However, after natural disasters, the need for rapid construction of residential, commercial, and industrial buildings may arise in locations affected by disasters. In this context, minimizing building construction times will increase the benefit/cost ratio. Modularity in buildings is a current research area [5]. Practical application without a crane will provide a great advantage in terms of construction time.

1.1.4. **Heat (Energy) Efficiency Issues (A-5)**

Heat efficiency is a parameter directly proportional to energy consumption. Panel sections should consist of sustainable and environmentally friendly building materials with high heat and energy efficiency. The heat efficiency of high-performance concrete, which is recommended to be used in panel sections, produced from waste concrete and with polymer additives, is higher than normal concrete [6]. In panel elements, 80% of the cross-section should consist of natural material. As a building material, pumice has a very good thermal insulation capacity as well as its sustainability feature.

1.1.5. **Construction Cost (A-6) and Sustainability (A-7)**

The increase in building construction time, additional applications for energy efficiency, detailed workmanship, equipment used, non-sustainable building materials, non-modular designs can negatively affect the cost of the building. In engineering, producing statically safe, aesthetic, and economical building solutions is an optimization problem. The parameters of using waste concrete in panel sections, practical application and minimum labor requirement, modularity, and high section energy efficiency without requiring additional applications will make a positive contribution in terms of construction costs. In addition, considering the life cycle analyzes of the structures, the parameters listed above will provide an economic gain in the long run. The concept of sustainability is an effective parameter in the construction industry, as it is in every field. It is important that the materials to be used are sustainable (recyclable) for the construction of a building that causes the least damage to the environment. Sustainable designs produce long-term economic solutions as well as being environmentally friendly. Panel systems and structures made of sustainable materials; stands out with its environmentalist, innovative and modular features. The proposed approach makes a significant contribution to UN Sustainable Development Goals [7].

2. Literature Review

The solution titles of the problems detailed in sections A-1, A-2, A-3, A-4, A-5, A-6, A-7 of the most up-to-date articles within the scope of the topic selected from the literature are given comparatively in Table 1. As can be seen from Table 1, the need to develop a method for all these defined problems in the literature has been identified. However, modularity has been described as a panel wall in most of these studies in the literature. Therefore, the solution we propose details a structural unit element, such as a brick. These unit elements can be applied practically with the help of technical personnel. Although some of the systems given in Table 1 provide installation modularity, their disassembly after construction is limited.

When the first reference article given in Table 1 is examined, it is stated that prefabricated concrete-steel modular panels are not within the scope of waste recycling, are only resistant to earthquake effects, have advantages in terms of building construction time, are designed to be heat efficient and reduce the building cost. However, no evaluation has been made regarding whether the design consists of sustainable materials [8]. In the second reference article, bamboo material that exists in nature was used. Therefore, this design has a sustainability aspect. However, there is no evaluation in the study regarding resistance to natural disasters, recycling of waste, and full modularity [9]. In the third reference article, solutions to many of the problem definitions are detailed with prefabricated and modular designed sandwich panels. However, only the recycling of waste and resistance to all natural disasters have been addressed to a limited extent [10].

In the fourth reference article, it is stated that the use of bamboo material reduces carbon emissions and high energy efficient panel systems are obtained. However, there is no evaluation in terms of cost in the article [11]. In the fifth reference article, a building design method for carbon neutral cities where low carbon emissions are at the forefront with wood-based panel systems is detailed [12]. In the last reviewed reference article, the horizontal load carrying capacities of modular panels consisting of concrete plates and detailed combination with steel elements were examined experimentally and analytically [13].

Table 1 *Comparative analysis of the most recent articles in the literature*

Reference	Existing Method	Year	A-1	A-2	A-3 A-4	A-5	A-6 A-7
1- Dynamic Performance Analysis by Laboratory Tests of a Sustainable Prefabricated Composite Structural Wall System [8]	Precast Concrete Steel Panel-Infilled Steel Frame	2022	N/A	P/A	+/+	+	+/-
2- Bamboo Reinforced Prefabricated Wall Panels For Low-Cost Housing [9]	Prefabricated Bamboo Reinforced Wall	2016	N/A	N/A	-/ P/A	+	+/+
3- Mechanical and Thermal Properties of Composite Precast Concrete Sandwich Panels: A Review [10]	Precast Concrete Sandwich Panel	2022	+	P/A	+/+	+	+/+
4- Thermal and energy performance of a steel-bamboo composite wall structure [11]	Lightweight Steel-Bamboo Wall Structure	2017	P/A	P/A	+/+	+	+/ N/A
5- Low carbon construction systems using prefabricated engineered solid wood panels for urban infill to significantly reduce greenhouse gas emissions [12]	Cross-Laminated Timber	2012	+	P/A	+/+	+	+/+
6- Construction Solutions and Materials to Optimize the Energy Performances of EPS-RC Precast Bearing Walls [14]	Expanded Polystyrene-Reinforced Concrete Precast Bearing Walls	2022	+	N/A	+/+	+	N/A / +
7- Mechanical performance of sustainable modular prefabricated composite shear panels under cyclic loading [13]	Modular Prefabrication Composite Shear Panel	2021	N/A	P/A	N/A/ +	N/A	N/A / N/A

N/A: Not Available P/A: Partially Available
+: This topic is discussed in the article. -: This topic isn't discussed in the article.
A-1: Environmental Impact of Waste Concrete and Increased Carbon Emission
A-2: Damages Caused by Natural Disasters to Structures
A-3/4: Building Construction Times and Non-Modular Designs
A-5: Heat (Energy) Efficiency Issues
A-6/7: Construction Cost and Sustainability

3. Suggestions

Within the scope of our book chapter, after examining many current research articles and related article, an approach to the problem titles identified in sustainable modular building design is detailed.

3.1. Engineered Cementitious Composites (ECC) Surface Layer

The unit element's shell should be designed to resist external influences and should consist mainly of engineered composite (ECC). ECC with fiber

content is a useful material with high energy absorption behavior. The crack formation of ECC can be controlled due to fiber inclusion and the mechanical performance of ECC is depended on the used components while design of ECC. However, the usage of ECC in the design of building elements is limited [15]. There are two different components in ECC content, binder medium and filler medium. Cement type with mineral additives in the binding medium and low carbon emission in its production should be selected. ECC filling medium may consist of small waste concrete with a diameter of less than 2 mm, ground pumice powder with a diameter of less than 0.063 mm, ground limestone-based stone flour with a diameter of less than 0.063 mm.

Polycarboxylate ether based hyper plasticizer can be used for ECC workability and has a high performance in workability [16]. For internal curing, superabsorbent polymers can be added to the mixtures [17]. While the super absorbent polymer used in the material provides an increase in strength with internal curing, it is thought that the polymer-based fiber used will increase the strength of the unit element under the bending effect (Fig.2). This type of concrete, which will be tested in the proposed brick or panel design, can reveal many advantages. In panel designs, it can be considered to use air-entraining chemical additives in order to provide thermal insulation by increasing the amount of internal space in the ECC surface layer. Polypropylene fiber can be added to the blend to improve tensile and bending behavior and increase toughness.

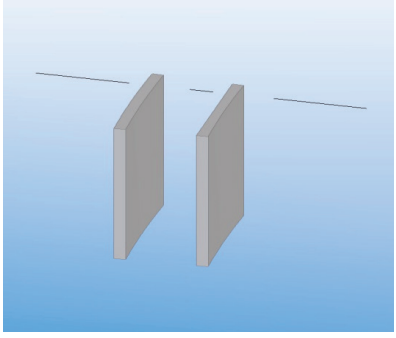

(a) *(b)*

Fig. 2 *ECC Surface Layer (a) and Life Cycle Assessment (LCA) of Concrete Waste (b) [18]*

3.2. **Pumice Insulating Layer**

The inner layer of the panel element should be designed with low thermal conductivity and a feature to provide thermal insulation. Compressed pumice can be used for this layer. Since pumice is a natural material, it provides an additional sustainability advantage to the design in the production of panel elements and after the end of their useful life. Cost optimization will be important in the selection of the materials for the insulation layer. A less costly design can be obtained with pumice. In this selection, the purpose of use and the benefit/cost ratio of the structure, which will consist of panel elements, will be important. However, in any case, the material to be used is a material with high thermal insulation ability and low specific gravity, and it must contain a high rate of voids. In the brick or panel design, cement and water should be added to the pumice to prevent the dispersion of the insulation material between the two surface layers. In addition, super absorbent polymer can be added to the mixture in order to prevent the effects of water and humidity (Fig.3).

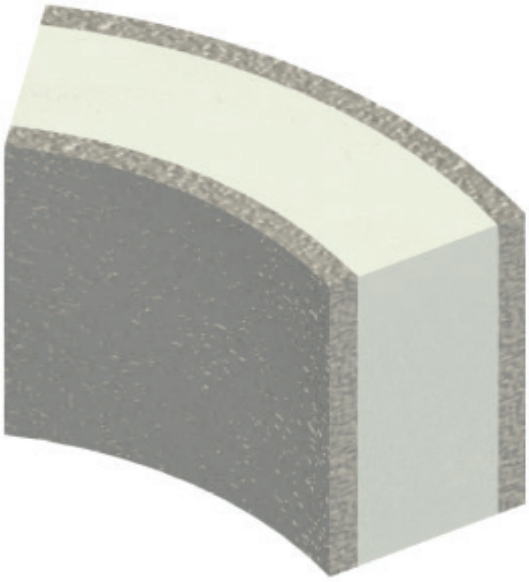

Fig. 3 *ECC Layer + Pumice Insulating Layer [19]*

3.3. **Panel Connection Layer**

Steel profiles and bolts designed on the brick or panel elements can be used for the vertical and horizontal connection of the sustainable modular unit panel elements. Because systems consisting of modular panel elements must have sufficient strength not only in vertical load effects but also in bending moments resulting from horizontal load effects. It is foreseen that the unit panel elements, whose connection details are designed with

stainless steel elements, will have high bearing capacity in terms of axial load, shear force and bending moment. Therefore, with this analytically and experimentally verified design, it will be possible to construct not only one or two storey but also multi-storey structures. However, while choosing the steel connection details and bolt diameters, it is important that the weight of the panel unit element should not exceed 20 kg in terms of practical application. The fact that the carrier system consists of panel + steel connection details will be very advantageous in terms of earthquake resistant designs. However, connecting the panel elements with bolts will provide a practical solution in terms of dismantling the structure to move it to another location. Therefore, the construction or dismantling of the structure can be carried out without a crane (Fig. 4).

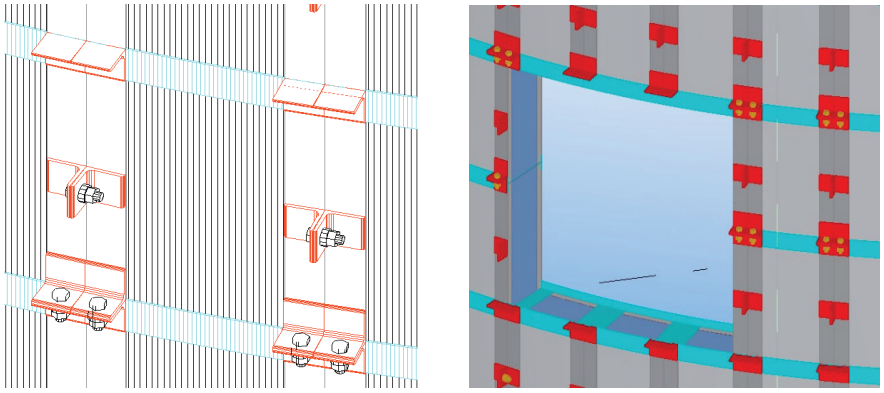

Fig. 4 *Sample of Panel Connection Layer [18]*

3.4. **Sustainable Modular Brick or Panel Element**

In the chapter, modular brick or panel system designs, in which the building construction industry provides solutions to environmental and energy problems, are discussed. The most recent literature studies and solution proposals for these designs have been evaluated comparatively. As a result of this evaluation, the features that innovative modular building systems consisting of concrete waste and sustainable materials, environmentally friendly, high-energy efficiency, resistant to earthquakes and other natural disasters, were presented in the form of suggestions. The most important advantages of structures consisting of unit brick or panel systems can be listed as enabling sustainable designs, modularity, energy efficiency, resistance to natural disasters, reduction of carbon emissions, practical application, and economical solutions. In addition to these features in the article, the evaluation of waste concretes in these designs and bringing them into the economy is included as a suggestion. Each of these features provides solutions to the environmental and energy problems of the building construction industry. However, it is important to combine these features for the most

effective solutions (Fig. 5). The aspects that are open to improvement of these designs, which are an innovative building construction method, are presented as suggestions in the sections of surface, insulation, and connection layers.

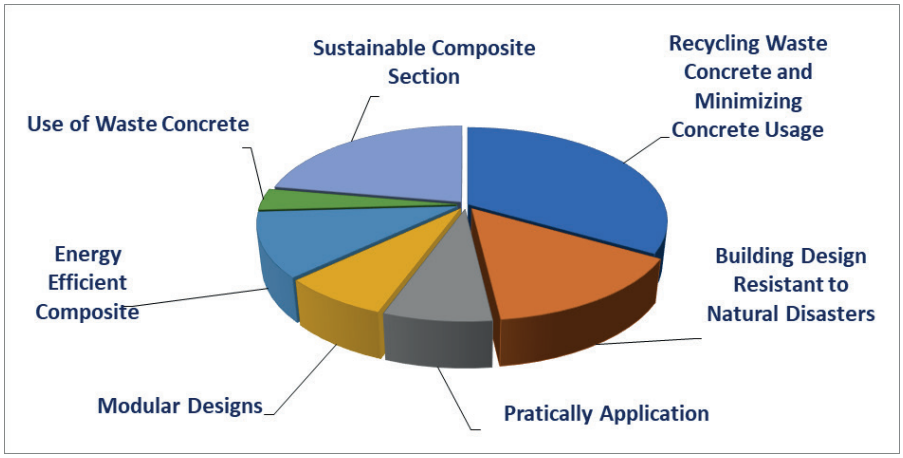

Fig.5 *Solution Definitions*

4. Conclusion

The most important contributions of the book section in the field of environment are the method of using high-performance sustainable materials (ECC Concrete) obtained from the recycling of waste concrete resulting from urban transformation and natural disasters in the construction of new buildings and minimizing the percentage of concrete in the load-bearing modular concrete panel section. The carrier and roof panel elements whose design is recommended have modular features. The construction of the structure can be easily completed with steel connection details and bolts that will be fabricated on the panel element. In this way, a newly constructed building can be dismantled and easily moved to another desired location. This feature emerges as a very useful solution, especially in the construction of new buildings after natural disasters. However, by using the modularity feature, architectural designs for different usage purposes can be easily made. Recommended brick or panel sections; It consists of sustainable and environmentally friendly building materials with high heat and energy efficiency. In panel sections, ECC (Engineered Cementitious Composite) with polymer additives, which will be produced from waste concrete, has high performance and higher heat efficiency than normal concrete. 80% of the section consists of the natural material pumice. Pumice, on the other hand, has a very good thermal insulation capacity as well as its sustainability feature as a building material. The use of waste concrete in panel or brick sections, practical application and minimum labor requirement, modularity, and high

section energy efficiency without requiring additional applications will make a positive contribution to building costs. Moreover, considering the life cycle analyzes of the buildings, the parameters listed above will provide economic gain in the long term. Our design proposal can offer solutions to architectural designs for different uses. In this case, a feature that increases the benefit/cost ratio could be a solution. Our brick or panel system design proposal consisting of sustainable materials; It stands out with its environmentally friendly, innovative, and modular features. Therefore, it is thought to contribute to the UN Sustainable Development Goals.

These suggestions are shown in Fig. 6 as a graphic. In this context, it is aimed that our book chapter will contribute to the topics of sustainable development, sustainable cities, sustainable buildings, urban transformation, environmental protection, energy efficiency, disaster management, and economic building designs.

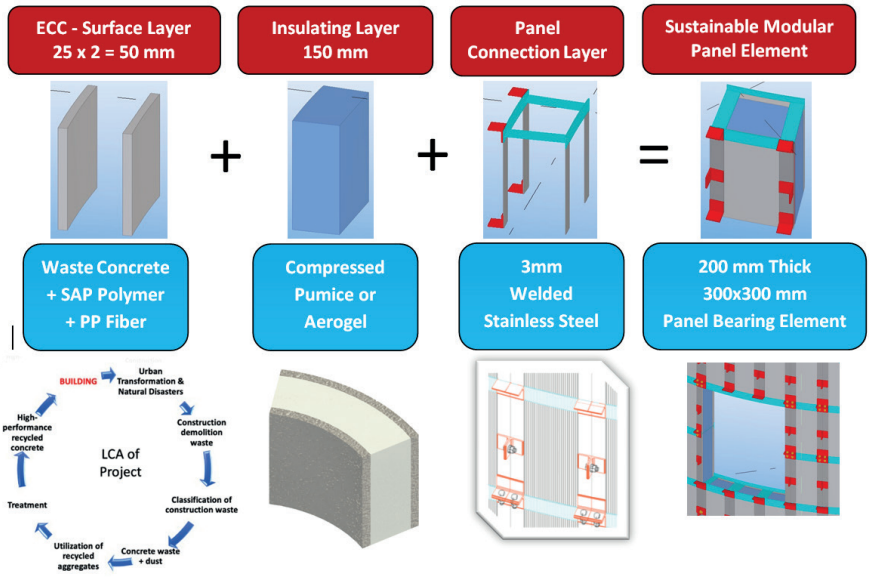

Fig. 6 *Sustainable Modular Building Brick Element*

REFERENCES

[1] Ş. Beniz, Türkiye Çimento Araştırmalarında Çevre Dostu Yaklaşımlar Üzerine Bir İrdeleme, M.Sc., Bursa Uludağ Üniversitesi Fen Bilimleri Enstitüsü, 2022.

[2] K.A. Alawi Al-Sodani, Mix design, mechanical properties and durability of the rubberized geopolymer concrete: A review, Case Studies in Construction Materials 17 (2022) e01480. https://doi.org/10.1016/j.cscm.2022.e01480.

[3] Y.H. Mugahed Amran, M. El-Zeadani, Y. Huei Lee, Y. Yong Lee, G. Murali, R. Feduik, Design innovation, efficiency and applications of structural insulated panels: A review, Structures 27 (2020) 1358–1379. https://doi.org/10.1016/j.istruc.2020.07.044.

[4] Z. Ye, K. Giriunas, H. Sezen, G. Wu, D.-C. Feng, State-of-the-art review and investigation of structural stability in multi-story modular buildings, Journal of Building Engineering 33 (2021) 101844. https://doi.org/10.1016/j.jobe.2020.101844.

[5] W. Pan, Z. Zhang, Benchmarking the sustainability of concrete and steel modular construction for buildings in urban development, Sustain Cities Soc 90 (2023) 104400. https://doi.org/10.1016/j.scs.2023.104400.

[6] S. Lei, F. Wu, S. Liu, L. Liu, W. Lin, Behavior of steel-ECC composite bridges under post-fire conditions, J Constr Steel Res 203 (2023) 107850. https://doi.org/10.1016/j.jcsr.2023.107850.

[7] T.R. Walker, Micro plastics and the UN Sustainable Development Goals, Curr Opin Green Sustain Chem 30 (2021) 100497. https://doi.org/10.1016/j.cogsc.2021.100497.

[8] E. Georgantzia, T. Nikolaidis, K. Katakalos, K. Tsikaloudaki, T. Iliadis, Dynamic Performance Analysis by Laboratory Tests of a Sustainable Prefabricated Composite Structural Wall System, Energies (Basel) 15 (2022) 3458. https://doi.org/10.3390/en15093458.

[9] V. Puri, P. Chakrabortty, S. Anand, S. Majumdar, Bamboo reinforced prefabricated wall panels for low cost housing, Journal of Building Engineering 9 (2017) 52–59. https://doi.org/10.1016/j.jobe.2016.11.010.

[10] H. Tawil, C.G. Tan, N.H.R. Sulong, F.M. Nazri, M.M. Sherif, A. El-Shafie, Mechanical and Thermal Properties of Composite Precast Concrete Sandwich Panels: A Review, Buildings 12 (2022) 1429. https://doi.org/10.3390/buildings12091429.

[11] Y. Li, J. Yao, R. Li, Z. Zhang, J. Zhang, Thermal and energy performance of a steel-bamboo composite wall structure, Energy Build 156 (2017) 225–237. https://doi.org/10.1016/j.enbuild.2017.09.083.

[12] S. Lehmann, Low carbon construction systems using prefabricated engineered solid wood panels for urban infill to significantly reduce greenhouse gas emissions, Sustain Cities Soc 6 (2013) 57–67. https://doi.org/10.1016/j.scs.2012.08.004.

[13] D. Wang, Y. Zhang, Y. Zhu, C. Wu, Y. Zhou, Q. Han, Mechanical performance of sustainable modular prefabricated composite shear panels under cyclic loading, J Constr Steel Res 179 (2021) 106423. https://doi.org/10.1016/j.jcsr.2020.106423.

[14] A. Scioti, M. De Fino, S. Martiradonna, F. Fatiguso, Construction Solutions and Materials to Optimize the Energy Performances of EPS-RC Precast Bearing Walls, Sustainability 14 (2022) 3558. https://doi.org/10.3390/su14063558.

[15] E. Köseömür, F. Birdal, H. Dilbas, Sürdürülebilir Çimento Esaslı Kompozit (ECC) İle Üretilmiş Betonarme Çerçevelerin Yatay Yük Kapasitelerinin Analitik Olarak İncelenmesi, in: SİVAS 2. Uluslararası Bilimsel Araştırmalar ve İnovasyon Kongresi, Sivas, 2023: pp. 801–811.

[16] M. Bravo, J. de Brito, L. Evangelista, J. Pacheco, Superplasticizer's efficiency on the mechanical properties of recycled aggregates concrete: Influence of recycled aggregates composition and incorporation ratio, Constr Build Mater 153 (2017) 129–138. https://doi.org/10.1016/j.conbuildmat.2017.07.103.

[17] H. Dilbas, F. Birdal, C. Parim, M.Ş. Güneş, Mechanical performance improvement of super absorbent polymer-modified concrete, MethodsX 10 (2023) 102151. https://doi.org/10.1016/j.mex.2023.102151.

[18] Trimble Solutions Corporation, Tekla software for students, (2023).

[19] Autodesk, Autodesk Revit Software, (2023).

CHAPTER 7

SUSTAINABLE INNOVATIONS IN SLUDGE DEWATERING FOR ENHANCED WASTE MANAGEMENT EFFICIENCY

Fatma Olcay TOPAC[1]
Sevil CALISKAN ELEREN[2]
Melike YALILI KILIC[3]

1 Prof. Dr., Bursa Uludag University, Faculty of Engineering, Department of Environmental Engineering, 16059, Gorukle, Nilufer-BURSA
2 Asst. Prof. Dr., Bursa Uludag University, Faculty of Engineering, Department of Environmental Engineering, 16059, Gorukle, Nilufer-BURSA
3 Prof. Dr., Bursa Uludag University, Faculty of Engineering, Department of Environmental Engineering, 16059, Gorukle, Nilufer-BURSA

1. INTRODUCTION

Wastewater treatment plants provide an essential service in modern infrastructure, the disposal of sewage and industrial effluents in a manner that will not disrupt ecosystems or threaten public health. In the field of wastewater management, the operational issues surrounding the disposal of a growing mountain of sludge is increasingly becoming an area of concern. Sludge produced in various stages of municipal wastewater treatment facilities includes elements of agricultural value such as macro/micro nutrients and organic compounds. Simultaneously, it contains damaging contaminants such as persistent organic compounds, toxic inorganics, and harmful pathogenic organisms. The composition of the sludge is influenced by the level of contamination in the processed wastewater, the nature of the pollutants present and the techniques used in managing the sludge (Metcalf & Eddy,1991; Rizzardini and Goi, 2014). As these treatment facilities diligently work to remove pollutants and contaminants from incoming wastewater, the resulting byproduct, sludge, poses a significant challenge. This challenge manifests in various aspects, with operational intricacies being a prominent issue. The increase in sludge volume necessitates enhanced processing and disposal mechanisms, demanding additional resources and manpower.

The sludge problem extends beyond environmental ramifications, also affecting the economic sustainability of wastewater treatment plants. The expenses linked to the management of sludge, including transportation, treatment, and disposal, contribute substantially to the overall operational expenses of these facilities. Municipal wastewater sludge is an inherent byproduct of biological wastewater treatment processes, necessitating substantial expenses for its appropriate management, disposal, and treatment. These costs typically constitute around 30–40% of the capital investment and approximately 50% of the operational expenditures for entire wastewater treatment plants (Andreoli et al., 2007). This financial burden underscores the importance of adopting cost-effective and sustainable sludge management strategies.

Within sludge management systems, subsequent to undergoing preliminary treatments like thickening, digestion, or conditioning, the sludge commonly undergoes dewatering prior to progressing to additional processing stages like incineration, composting, or landfill deposition. Sludge dewatering, which involves lowering the sludge's water content to make it easier to handle and dispose of, is an essential phase in the wastewater treatment process. The whole cost of sludge management is directly impacted by how well sludge dewatering works. A higher percentage of water is removed during efficient dewatering, which causes the sludge's volume and weight to decrease. As a result, moving and disposing of the sludge become simpler and less costly (Liu et al., 2016). Efficient sludge dewatering can also contribute to

a more environmentally friendly sludge management process. For example, reduced transportation requirements mean lower carbon emissions, and the ability to utilize sludge in beneficial ways (such as in agriculture) can be more sustainable.

Centrifugation, filter press filtration, vacuum filtration, drying beds, and many other methods are commonly used for sludge dewatering purposes. Nevertheless, the inherent dewaterability of raw sludge is often compromised by the formation of a colloidal structure, primarily shaped by the macromolecular polymers generated by microorganisms. The dewatering efficiency of waste sludge is intricately linked to its rheological characteristics, extracellular polymeric substances (EPS), the size, microstructure, and micromorphology of sluge particles and variations in surface charge density (Wei et al., 2020; Cao et al., 2018). However, among these characteristics, EPS emerges as a critical factor in determining the dewatering properties of sludge; because excessively hydrated EPS binds a huge amount of water. If the cohesive structure of the sludge, known as flocculent structure, undergoes disintegration, and the EPS embedded within the sludge flocs are disrupted during the conditioning process, this would significantly enhance the liberation of bound water and dramatically improve the dewatering capability (Jin et al., 2015). Accordingly various pre-treatment methods, encompassing physical, chemical, biological, and hybrid approaches, have been devised to diminish the volume of sludge, consequently minimizing the need for disposal space and reducing associated costs (Cao et al., 2021).

Continual efforts and innovative strategies are actively being explored to enhance the effectiveness of sludge dewatering, with the objective of mitigating the escalating financial implications linked to the increasing volumes of sludge. This chapter provides information on the water distribution within activated sludge, elucidates the prevailing technologies employed for sludge dewaterability, and, notably, scrutinizes novel methodologies aimed at advancing the efficiency of sludge dewaterability

2. STRUCTURAL CHARACTERISTICS OF SLUDGE FLOCS AND WATER DISTRIBUTION

Sewage sludge is an unavoidable secondary product of wastewater treatment facilities that is overproduced and poses a direct or potential threat to the ecological environment (Ding et al., 2022; Liu et al., 2023).The ratio of COD to sludge is approximately 0.3-1.2 kg TSS/kg COD in the activated sludge process (Zou et al., 2022; Apollo et al., 2023). Owing to variations in wastewater properties and treatment facilities, the resulting sludges exhibit disparate qualities (Wei et al., 2018). Therefore, in order to carry out the required treatment, a thorough understanding of the sludge structure is required.

Activated sludge flocs have a heterogeneous composition and a complex structure. Depending on the changing wastewater composition and operating conditions; size, microstructure, surface properties and density can be very different (Jin et al., 2004). Waste activated sludge typically constitutes a multiphase colloidal system. It includes organic pollutants, colloidal particles, cellular materials (extracellular polymeric substances-EPS), pathogens capable of posing significant pollution risks if not appropriately disposed of, different groups of microorganisms, and various toxic substances such as heavy metals (Yan et al., 2009; Wu et al., 2020) and water.

Chemical, physical, and biological characteristics of sludge are important in sludge dewatering (Cao et al., 2021; Tunçal et al., 2023). Sludge particle size, zeta potential, morphology, rheology, and hydrophobicity are examples of physical characteristics. Two of the primary chemical characteristics of sludge are the distribution of EPS and water in flocs (Tunçal et al., 2023). Biological qualities of sludge are determined by the microorganism type and distribution present in it (Yan et al., 2009). Sludge dewatering performance is strongly affected by the distribution of EPS and water in the sludge.

2.1.Water Classification in Sludge

Water's vapor pressure, entropy, enthalpy, viscosity, and density are all affected differently by the presence of solids in sludge (Vaxelaire and Cezac, 2004). Waste activated sludge usually contains >90% (95-99%) water (Liang et al., 2023; Wei et al., 2018). The types of water in sludge can be categorized into four groups (He et al., 2017) depending on the proximity of the water molecule to the solid part of the sludge (Figure 1):

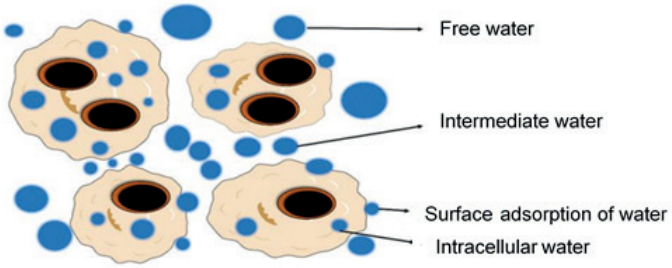

Figure 1. *Form of water in sludge flocs (Liang et al., 2023)*

(i) Free water: It accounts for 65%~85% of the total water content of sludge (about 70%) (Chen et al. 2015). It is not bound to sludge solids. It is not affected by the solid particles in the sludge and its properties do not change (He et al., 2017). It is easier to separate since it does not bind directly to solids (Tunçal et al., 2023).

(ii) Intermediate water: It constitutes 10%~25% of the total water content

of the sludge (about 20%) (Chen et al. 2015). It is the water between the interstitial spaces of sludge flocs and organisms (Liang et al., 2023; Cao et al., 2021). Due to the effect of surface tension, this type of water cannot move freely on the surface of solid-sludge particles. High mechanical forces are needed to separate the interstitial water from the sludge particles because of their strong binding force (Tsang and Vesilind, 1990).

(iii) Surface water (water adsorbed on the surface): It accounts for approximately 7% of the total water content of sludge (Chen et al. 2015). It is surface water retained through adsorption and adhesion on the surface of solid particles and extracellular polymers (He et al., 2017). It is bound to solid particles by capillary forces consisting of adhesion and cohesion forces (Vaxelaire and Cezac, 2004; Lin et al., 2022). This water is difficult to remove mechanically. The structures of extracellular polymers need to be broken in order to extract water (Tunçal et al., 2023).

(iv) Intracellular water: It constitutes approximately 3% of the total water content of the sludge (Chen et al. 2015). It is the intracellular water found in living organisms. It is chemically bound water (Vaxelaire and Cezac, 2004; Ruiz-Hernando et al., 2013). Destroying cell membranes or regulating extracellular polymer structures are necessary for the removal of intracellular water (Zhen et al., 2020).

2.2.Composition of EPS in Sludge

Under certain conditions, microorganisms produce and secrete EPS, a natural polymer, onto the surface of the cell wall. (Cao et al. 2021). EPS possesses a complicated polymer structure primarily composed of macromolecular secretions from microorganisms, encompassing both cellular lysis and hydrolysis products like protein, polysaccharide, humic acid, and DNA. These constituents make up roughly 60-80% of the total mass of sludge. (Zhang et al., 2018; Dai et al., 2018; He et al., 2015). Proteins and polysaccharides are the main components of EPS (Cao et al., 2021). EPS is predominantly composed of compounds resembling proteins (PN, <60%), carbohydrates (PS, 40-95%), lipids (<40%), DNA (<10%), and also encompasses aquatic humic substances and small molecules (Wei et al., 2018). EPS can generate viscous effect to form a highly charged and hydrated gel-like, three-dimensional floc matrix in order to accommodate microorganisms inside the flocs and preserve the structural integrity of the sludge floc (Lin et al., 2022). EPS has a water content of up to 98% (Jin et al., 2004). The sludge particles are negatively charged as they are surrounded by a large amount of EPS, thus forming a stable and electrically excluding colloid system (Dai et al., 2018; Guan et al., 2012). The proteins, polysaccharides, humic acids, as well as phosphate and sulfate radicals contained in EPS constitute its electronegativity (Rodriguez-Chueca et al., 2014).

The effects of EPS fractions on sludge dewaterability depend on the detailed chemical compositions of the EPS. High protein/polysaccharide ratios in EPS composition have a deleterious impact on the dewatering efficiency of sludge (Murthy and Novak, 1999). According to Hyrycz et al. (2022), the hydrophilic protein of EPS can effectively lock bound water in flocs and reduce the sludge dewaterability.

As shown in Figure 2, depending on EPS spatial distribution properties and compactness, from outside to inside; dissolved EPS (S-EPS) can be divided into loosely bound EPS (LB-EPS) and tightly bound EPS (TB-EPS) (Cao et al., 2021). The amount of EPS in sludge greatly affects the stability of the floc and dewatering effectiveness (Mikkelsen and Keiding, 2002).

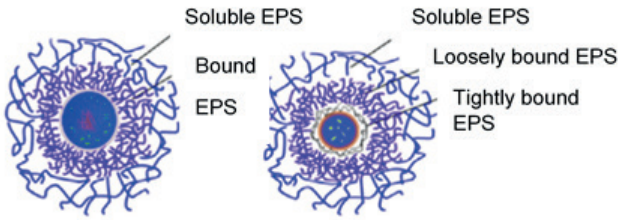

Figure 2. *Structure of EPS (Cao e al., 2021)*

Different components and groups are present in S-EPS, LB-EPS and TB-EPS, resulting in different effects of each EPS layer on sludge dewaterability (Lin et al., 2022). S-EPS is the partial EPS that dissolves in the supernatant and has a high organic content (He et al., 2015). LB-EPS and TB-EPS, both high molecular weight biopolymers, originate from bacterial secretion, extracellular component leakage, cell lysis, hydrolysis, as well as the adsorption of organic matter from the surrounding wastewater(He et al., 2017; Sheng et al., 2010). LB-EPS acts as the primary surface for cell attachment and flocculation. LB-EPS content is negatively correlated with sludge settling and dewatering performance (Yuan et al., 2017). Because of the extremely porous nature of LB-EPS and the substantial presence of bound water, flocs face challenges in approaching and adsorbing to each other. This leads to compromised settleability and dewaterability (Zhang et al., 2018). Cell interactions and binding predominantly take place on the LB-EPS surfaces rather than on those of TB-EPS. Therefore, high LB-EPS content means low dewaterability. Tightly bound EPS (TB-EPS) has a specific shape and is firmly and stably attached to the cell wall (Wingender et al., 1999). The TB-EPS layer contains a significant proportion of bound water, which affects the drying process.

3. ANALYSIS OF EXISTING SLUDGE DEWATERING METHODS

Dewatering, which is applied to reduce the moisture content of sewage sludge, is an essential physical process in sludge treatment (Xia, 2022). As a result of this process, a significant reduction in volume occurs, while at the same time, it helps the mud cake to be easily transportable and the cake to be odorless, and not susceptible to putrefaction (Yüksekdağ et al., 2020). Sludge dewatering is carried out for reasons, such as sludge transportation cost, increase in sludge heating capacity, and volume increase by reducing leachate water (Fester, and Werner, 2023).

3.1. Sludge Drying Beds

Drying beds, which are a natural dewatering method used to dewater sludge, are low in cost. The most commonly used drying beds are the classical type (sand bed). The solids formed after drying in these beds can be removed in landfills or used as soil improvers. However, the disadvantages of the method are that they require large areas, the significant impact of changes in meteorological conditions on the drying properties, the need for manpower to remove the mud cake, and the observation of pests and potential odor formation (Seck et al., 2015; Chen et al., 2021).

3.2. Vacuum Filtration

Vacuum filtration is one of the most commonly used methods for mechanically dewatering sludge. It has disadvantages, such as the complexity of the system, conditioner requirements, and high operating costs (Sultan, 2006). A vacuum filtration setup comprises pumps for sludge feed, apparatus for chemical feed, a tank for sludge conditioning, a rotating filter drum, a conveyor or scraper for sludge cake, a vacuum apparatus, and a filtrate removal system. An image of the drum vacuum filter is given in Figure 3-a (Ryltseva, 2021).

3.3. Belt Filter Press

Sludge is fed continuously in the dewatering process with a belt filter press, one of the mechanical dewatering equipment. The basic principlea are chemical conditioning, gravity drainage, and mechanical pressure application for dewatering by belt filter press. The components of the belt filter press encompass dewatering belts, rollers and bearings, systems for belt tracking and tensioning, controls and drives, along with a belt washing system. (Fester and Werner, 2023). An image of the belt press is given in Figure 3-b (Ryltseva, 2021).

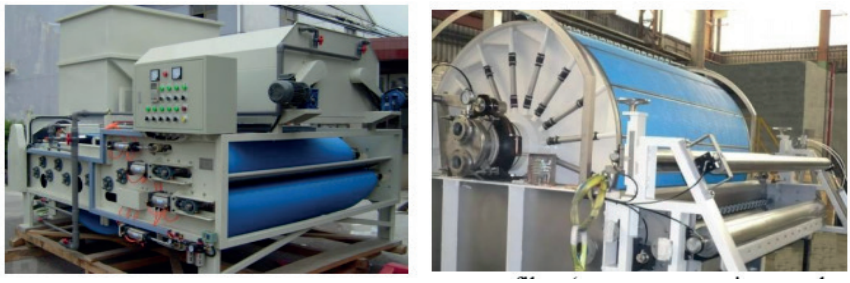

Figure 3. *An image of the filter a-drum vacuum filter, b- the belt filter press*

3.4. Filter Press

The most important difference between the filter press and belt filters, which is one of the mechanical dewatering methods, is that higher pressures are applied to increase the ability of the sludge to dewater (Qi, 2011). Cake formation containing high concentrations of solids, high permeate water quality and high solids retention capacity are among the advantages of this method (Rao, 2022). An image of the filter press is given in Figure 4 (URL-1, 2024).

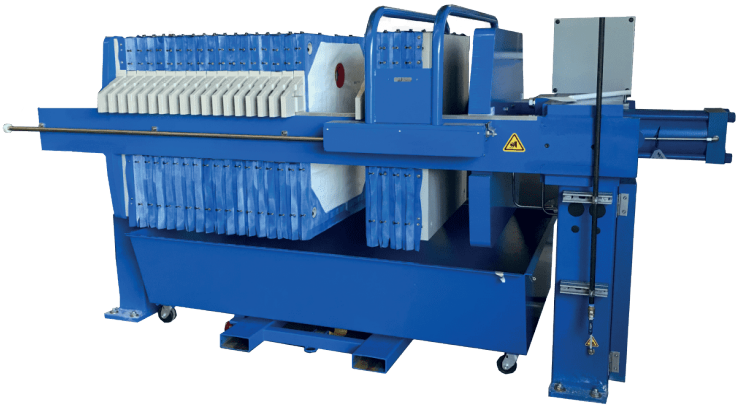

Figure 4. *An image of the filter press*

3.5. Centrifuge

Dewatering by centrifuge is the separation of sludge water under the influence of centrifugal forces and turning it into a denser sludge cake. The permeate containing low-density solids is returned to the plant (Ginisty et al., 2021). From the mud-water mixture containing 1-5% solids, some of the water is separated at the centrifuge outlet to form a mud cake containing 25% solids (Sapmaz, 2022). An image of the centrifuge is given in Figure 5 (Ryltseva, 2021).

Figure 5. *An image of the centrifuge*

4. SUSTAINABLE INNOVATIONS IN SLUDGE DEWATERING

4.1. Fenton Oxidation

According to Luo et al. (2021), the iron-rich mineral increased the amount of Fe^{2+}, which reacts with oxidants in advanced oxidation processes, raising the sludge's dewatering rate.

Tao et al. (2019) used Fe-rich biochar to increase the sludge dewatering rate by Fenton oxidation. When the red mud was added to the process as a functional, the water content of the mud cake decreased by 52%. As a result of the study, the cost of the sludge treatment could be reduced by nearly 29% when using Fe-containing sludge compared with the Fenton sludge conditioning treatment.

In a study conducted by Yu et al. (2019), the water content of sludge, capillary suction time, and specific resistance to filterability were reduced to 65%, 83%, and 95%, respectively, by the Fenton-like oxidation process.

The dewaterability of activated sludge was increased between 40 and 60 min using the electro-fenton process (Chen et.al, 2019). The optimum conditions of the process were 40 mA/cm^2 and pH at 3. When the dewatering filtrate was used five times, the performance of electro-fenton was over 90%. Therefore, this process is effective for sludge dewatering.

4.2. K_2FeO_4 Oxidation

K_2FeO_4 can oxidize various compounds and is used for water, wastewater, and sludge treatment (Cai, 2019; Hu et al., 2020). K_2FeO_4 oxidation destroys the cells and extra-cellular polymeric substances to release bound water (Cao, 2021).

Wu et al. (2018) conducted sludge dewatering experiments by K_2FeO_4 oxidation to improve the dewaterability of sludge. Specific resistance of filtration reduction was obtained as 64% by adding 1 g/g dry solid sludge-derived mesoporous material without pH pre-adjustment.

In another study by Wu et al. (2019), the water content of sludge was reduced from 79% to 68% by using 3.5 g/L K_2FeO_4.

The water content, specific filtration resistance, and capillary suction time at the dosage of 12 mg/g VSS Fe(VI) were decreased from 83%, 9.3×10^{10} s^2/g, and 35.1 s to 76%, 2.6×10^{10} s^2/g and 16.2 s, respectively (Lin et al., 2023).

4.3. Microwave Irradiation

By applying the microwave irradiation to the sludge, the microwave treatment method will accelerate both the moisture evaporation and solid separation processes. The studies of the last several years appear to be directed at assessing the commercialization potential of this technology and the parameters of the microwave operations for utility and wastewater plants. This research intends to find out how microwave treatment can be added to the sludge dewatering process, with the possibility of proving a valuable contribution to the scientific community in determining the ability of microwave treatment to be implemented on an industrial scale.

Microwave irradiation effect on the dewaterability forces measure by specific filtration resistance values and capillary suction time has been investigated in a 2009 study by Yu et al. The findings pointed out that the best dewatering rate was achieved through microwave application at 900 W for 60 seconds. Furthermore, the study showed the crucial influence of the EPS concentration, size of the sludge particles and sludge disintegration level on the noticed variations in the dewaterability of sludge. Under the optimum conditions, the sludge exhibited a disintegration of 1.5-2%, EPS concentration ranging from 1500 to 2000 mg/l, and a particle size distribution of 120-140 μm. Rao et al. (2022) demonstrated in their study how microwave irradiation (MI) caused the water in the sludge to evaporate, reducing the amount of bound water and easing obstructions in the sludge pore channels. The results revealed a significant 19.4% decrease in bound water content, a reduction in the fractal dimension (Df) of the pore structure from 2.955 to 2.867, and an elevation in the Df of pore surface roughness from 2.099 to 2.362 following the application of 700 W microwave power for 5 minutes. This modification was observed to create a more homogeneous pore structure in the sludge, establishing enhanced water flow paths. The study underscored the evident improvement in sludge dewatering performance attributed to microwave irradiation.

In Faruqi et al. study (2021), the dewatering capability of electroplating sludge was examined by utilizing microwave drying technique. From the

obtained results by microwaving at (800 W for 120s) there was a dip in the specific filtration resistance value from 3.54E+09 m/kg to 4.33E+08 m/kg and a fall in the water content from 98.56 wt.% to 94.37 wt.%. Based on the numerical optimization described in the research, it has been determined that the microwave applicaton criteria 800 W and 141 s contact time are optimal in the sense that they provide minimum water content and specific filtration resistance, but they also maximize the extent of solubilizaton.

4.4. Ultrasonic Treatment

It becomes clear that the ultrasonic pretreatment methods are powerful tools to enhance the dewatering and degradability of sludge on efficient and constant basis. When this technique is applied, a more intense modification of the cells is obtained compared to the slow disruption of cells, leading to higher performance of sludge dewatering. In the slurry, the ultrasonic-related cavitation microbubbles get formed when cavitation (application of ultrasonication) is used for sludge treatment. These bubbles then collapse and these regions of high temperatures are created and produce strong zones of shear. The great acidification and increase in salinity may have the significant consequence of the destruction of the EPS matrix. This will consequently break down the polymeric substances and release the bound water. The conducted investigations reveal that many parameters, namely ultrasonic frequency, time, and energy density, determine the effectiveness of sludge dewatering using ultrasonic method.These findings underscore the intricate interplay of multiple parameters in determining the efficacy of the ultrasonic treatment in sludge dewatering processes (Wu et al., 2018; Wolski, 2020).

In the study performed by Qi et al. (2024), the influence of ultrasonic application on the sludge dewatering process was investigated. The data on the sludge sample taken for analysis showed that the best energy density had the value of ultrasonic energy of 9.8 W and the efficient duration of treatment was considered to be 30s. This study clearly pointed out how selecting the right ultrasonic energy density and duration period was critical for better sludge dewatering performance. The carried out study in general shows that the used ultrasonic pre-treatment has a positive effect on the dewatering abilities of the sludge.

In another study, the impact of ultrasonic waves on the dewatering characteristics of sludge was investigated by examining variations in solid contents (SC) and capillary suction time (CST) parameters. The objective was to ascertain the optimal ultrasonic settings for enhancing the sludge dewatering process. The study's findings revealed that under the conditions of 15% sludge subjected to sonication, a treatment time of 5 minutes, and an ultrasonic density of 1 kW/mL, the optimal capillary suction time (CST) for the sludge cake was identified to be 86 seconds. Additionally, the solid

content (SC) in the sludge cake reached its peak at 26.4%. Furthermore, under the optimal conditions of applied ultrasonic treatment, the particle size distributions were determined to be 6.3 μm (d10), 44.2 μm (d50), 24.4 μm (d90), and an average particle size of 28.84 μm (Golbabaei Kootenaei et al., 2022).

Another research study on ultrasonic frequencies and treatment duration focused on water content, soluble chemical oxygen demand, and the distribution of water in sludge were also part of this discovery of the ability of ultrasonic irradiation on the dewatering efficiency of sludge. Following this study, it has been observed that that ultrasonication is a good pretreatment simple method that greatly enhances the sludge dewatering process. The most significant change occurred after pre-treatment with ultrasonic irradiation at the ultrasonic frequency of 30 kHz for two minutes, the water content of the sewage sludge reduced from 93.03% to 86.95% via centrifugal dewatering. It also indicates how ultrasonic pre-treatment can minimize the landfill volume of discarded sewage sludge cake with an ultrasonic pretreated sludge cake volume that is smaller than the volume of the original sludge cake (Mao et al., 2018).

Wolski (2020) conducted a study to investigate the impact of ultrasonic disintegration on the conditioning of sewage sludge. The study examined the amount of free water released and how it relates to the length of treatment and the intensity of ultrasound energy used. The findings demonstrated that ultrasonic energy, at power levels between 0.20 and 0.58 W/ml and doses between 0 and 38700 J/kg of dry matter, can significantly enhance the sludge's ability to thicken due to the dispersive effects of the ultrasonic field. To enhance sludge dewatering, El-Jery et al. (2023) conducted a study where ultrasonic waves at frequencies of 30 kHz and 50 kHz were applied for varying durations (0.5 to 30 minutes). They discovered that a frequency of 30 kHz and a duration of 1 minute yielded the best results. Using these conditions, capillary suction time was reduced by 29% and 22% for 30 kHz and 50 kHz, respectively.

4.5. Thermal Hydrolysis Treatment

Thermal hydrolysis is a sludge pretreatment method that breaks down the tough cell walls of microbes in sludge. It also changes the physical and chemical properties of the sludge, such as the amount of EPS material, the size of the particles, and the overall structure. The process involves heating the sludge to a temperature of 140-180°C for 30-60 minutes under pressure of 6-11 bars. Thermal hydrolysis has been used in municipal wastewater treatment plants since 1995, when it was first implemented in a large-scale plant in Hamar, Norway. The changes induced by thermal hydrolysis disrupt the bonds between sludge flocs and water molecules. By influencing factors that determine the surface charge and structural stability of the sludge, the

applied heat treatment enhances the dewaterability property of the sludge (Kim et al., 2020; Devos et al., 2021).

The efficacy of the thermal pre-treatment was evaluated in a study by Oosterhuis et al. (2014) using laboratory-scale sludge digesters and a pilot-scale thermal hydrolysis process. According to the study's findings, thermally hydrolyzed sludge had 62% less volatile solids than non-hydrolyzed sludge. Furthermore, the study's digesters were shown to be able to handle a solids loading rate that was 2.3 times higher than that of conventional digesters when thermal hydrolysis was present. The biodegradability, viscosity, and dewatering performance of the sludge were shown to be positively impacted by the application of thermal sludge hydrolysis, indicating that this technique could potentially improve the overall efficacy of the sludge treatment process.

A study by Im et al. (2022) examined the thermal hydrolysis of dewatered sludge from a wastewater treatment plant that processes a large volume of water daily. Using a specialized 20-liter reactor with adjustable slope angles, they loaded the reactor with varying amounts (6-10 kg) of sludge and subjected it to thermal hydrolysis for an hour. Notably, the highest CST value was obtained with 7 kg of sludge. Additionally, the time to achieve the desired temperature in the reactor with slope control was determined to be 12 minutes. Furthermore, it was concluded that a mixing speed of 150 rpm yields optimal process efficiency. The impact of remaining oxygen on thermal hydrolysis was found negligible.

An investigation was carried out to determine how the temperature of the thermal hydrolysis pretreatment affected the effectiveness of sludge digestion, the efficiency of dewatering, and the quality of the cake. Higher thermal hydrolysis temperatures often result in a 5%–6% increase in solid reduction and methane yield, according to the results. After dewatering, the higher process temperature is seen to improve cake solids and decrease solids' viscosity. To be more precise, the cake solids percentage in the sludge sample that underwent pretreatment at 130 °C was found to be 27%, whereas at 170 °C, it was found to be 32% (Higgins, et al., 2017).

Through years of industry use, thermal hydrolysis has proven effective as a sludge pretreatment method before anaerobic digestion. It offers benefits such as improved dewatering, increased loading capacity, and higher biogas production and quality. However, further investigation is needed to address the formation of inhibitory compounds like free ammonia and melanoidins that can hinder the process (Ngo et al., 2021).

4.6. Inorganic Coagulant

Inorganic flocculants promote the agglomeration of sludge particles into flocs by charge neutralization and at the same time improve the porosity of

the sludge cake by acting as a skeleton former. Commonly utilized inorganic flocculants include low molecular weight types like $Al_2(SO_4)_3$, $AlCl_3$, $FeCl_3$, $Fe_2(SO_4)_3$, as well as inorganic polymeric coagulants such as polymeric iron sulfate (PFS) and polymeric aluminum chloride (PAC). Inorganic polymeric coagulants typically possess a higher charge density and molecular weight than their low molecular weight inorganic coagulant counterparts (Liang et al, 2023; Wei et al, 2018).

Niu et al. (2013) examined the influence of chemical conditioning on the dewatering properties of sludge, employing three inorganic coagulants: polyaluminum chloride (PACl), high-performance PACl (HPAC), and ferric chloride (FeCl3). It was found that the dewaterability of sludge was significantly improved after chemical conditioning with inorganic flocculants. When sludge inorganic coagulant doses were increased from 5% (g/g DS) to 10%, the specific resistance to filtration decreased from $126x10^{10}$ m/kg to $55.4x10^{10}$ m/kg for PACl, from $39.8x10^{10}$ m/kg to $15.5x10^{10}$ m/kg for HPAC, from $18x10^{10}$ m/kg to $6.82x10^{10}$ m/kg for $FeCl_3$. It was also determined that when $FeCl_3$, PACl and HPAC coagulant dosages were 10% (g/g DS), the total EPS concentration of sludge flocs decreased from 30.1 mg/g DS to 6.5, 17.6 and 18.1 mg/g DS, respectively. The sludge flocs obtained by $FeCl_3$ conditioning were observed to be smaller but denser than those of PACl and HPAC, since Fe^{3+} has a much stronger affinity for EPS.

The sludge dewatering capabilities of two conventional inorganic coagulants (iron or aluminum salts) were examined by Liang et al. (2019). They found that iron coagulants improved the dewaterability of sludge by approximately 28.66% more than aluminum coagulants. It has been demonstrated that iron salts' greater capacity to neutralize charges, their ability to form smaller, more compact flocs, and their stronger acidification effect are the causes of this. In addition, coagulation with iron was reported to be more economical than with aluminum.

In another study carried out by Peng et al. (2024), inorganic (poly aluminum chloride-PAC) and organic (poly dimethyl dialyl ammonium chloride-PDDA) polymeric structures on the dewatering performance of sludge by molecular dynamics (MD) simulations was investigated. It was determined that PAC and PDDA reduced the molecular polarity of biopolymers, caused a decrease in the hydration capacity of EPS and the release of bound water, and increased the dewaterability of sludge. Following PAC treatment, it was found that the amount of water bound to the sludge had dropped by 73.16%. PAC proved to be more efficient than PDDA in disrupting the hydrogen bonds between water molecules and EPS. When compared to biopolymers, PDDA was found to have a better capacity for agglomeration.

4.7. Organic Flocculants

Organic polymer flocculants are still the most widely used methods in sludge conditioning due to their relatively low cost. By forming water drainage pore channels, it can create larger floc sizes, adapt more readily to a wider pH range, and perform well in dewatering applications. PAM (Polyacrylamide) and its derivatives are the most widely used organic polymeric conditioners for sludge dewatering. Polyacrylamide flocculants can be classified as anionic (APAM), cationic (CPAM), amphoteric (AmPAM) and nonionic (NPAM) (Wei et al, 2018).

Wu et al. (2021) evaluated sludge conditioning mechanisms with polyacrylamide (PAM) with different charge densities (19%, 45% and 70%). 70% charge density PAM improved sludge flocculation and filtration performance as a result of increased structural strength. This improvement resulted in the compression of water dispersed among the sludge particles and finally increased dewaterability. Further analysis of the interaction between sludge and PAM (dynamic evaluation by multiple light scattering spectroscopy and dispersive quartz crystal microbalance) showed that the use of high charge density PAM quickly forms flocs with a hard and dense structure that are less affected by hydraulic turbulence. It was also stated that the use of densities above the determined optimum density of PAM may cause clogging of water channels by the PAM solution, increased resistance to water flow and inhibition of removal efficiency.

Tannic acid (TA), a naturally occurring polyphenol compound that is non-toxic, biodegradable, and derived from plant metabolites, can be utilized as a conditioner for sludge dewatering because of its capacity to bond with proteins. Ge et al. (2019) studied five different doses of TA concentrations to condition sludge in 250 ml beakers in the laboratory. Sludge dewaterability was demonstrated by the results, which revealed a considerable reduction in the water content of the dewatered sludge of 13.4% at 200 rpm, 0.15 mmol/gTS TA dosage, and 15 minutes of settling time. In addition, the complex, bridging and precipitating effects of TA on sludge biopolymers were revealed by FTIR and SEM analyses. It has been emphasized that while a lower-cost sludge treatment is carried out by using TA-containing plant wastes, it is important to evaluate the effects of temperature, pH, cation and anion to increase efficiency.

Bioflocculants are considered alternatives to synthetic polymers because they are biodegradable and nontoxic, but may require much higher dosages. However, their use has become increasingly important to reduce the environmental footprint of the dewatering process. Ghazisaidi et al. (2023) investigated the effects of four lignin-based flocculants (LBF) on the dewaterability of biological sludge. Increasing LBF dosages were found

to improve dewatering performance, with the LBF with the highest charge density and molecular weight (7.5% w/w) giving the best results. When using 7.5% w/w LBF, dewatering was greatly improved as the amount of dry cake solids after pressing increased by nearly 50% and the capillary absorption time decreased by approximately 68%. To minimize the usage of LBF while maintaining equivalent performance, the required dosage for LBF could be decreased from 7.5% w/w to 3% w/w through the addition of 0.1 % w/w) of polyacrylamide.

4.8. Acid and Alkali Treatment

Acid or alkaline conditions used in the dewatering of sewage sludge affect the flocculation mechanism, causing hydrolysis of some compounds and changing the surface properties of the sludge flocs. Hydrolysis of EPS and intracellular materials can reduce the surface charge and destabilize the sludge. Disintegration of the polymer structure also causes the release of bound water (She et al., 2017; Raynoud et al., 2012)

He et al. (2017) examined the effects of H_2SO_4 and NaCl addition to sludge on the dewatering performance of sludge in relation to floc distribution and bound water content. Cell lysis under acidic conditions helped release intracellular water and further enhanced the sludge dewatering performance. However, in low dosage alkali conditioning, the sludge's dewaterability was made worse by an increase in the bound water content. Consequently, it has been said that the distribution of water content in EPS and sludge is crucial for the addition of H_2SO_4 and NaCl.

Chen et al. (2020) used oxalic acid (OA) as a single-stage acidification method in the dewatering of sewage sludge. Through experimental studies, oxalic acid was found to be more efficient than treatment with sulfuric acid and hydrochloric acid at the same conditions. The optimum OA dosage (200 mg/g DS) was found to reduce capillary suction time by 78.7% in 30-minute sludge dewatering studies, and this value remained at 58.5% and 56.7% reduction efficiencies for sludge conditioned with H_2SO_4 and HCl, respectively. The decrease in the specific resistance efficiency to filtration also showed a similar trend. The findings indicated that OA exhibited greater efficacy in sludge dewatering compared to the two prevalent inorganic acids. This observation was attributed to potential differences in their abilities to liberate bound water into free water, prompting an examination of bound water contents post-conditioning. As anticipated, the bound water content reduced from 3.32 g/g DS to 2.84 and 2.86 g/g DS following H_2SO_4 and HCl conditioning, respectively. In contrast, OA conditioning led to a significantly greater reduction in this value (1.63 g/g DS). This outcome suggests that OA induces additional destruction of EPS, releasing bound water and enhancing sludge dewaterability.

Ruiz-Hernando ve Ark (2013) evaluated the effectiveness of heat treatment, chemical conditioning with NaOH, and ultrasonic waves in improving secondary sludge dewatering. NaOH doses below 0.2 mol/L have been shown to impair the sludge dewatering process. Alkaline conditioning has been demonstrated to lower the viscosity and thixotropy of the sludge while maintaining a nearly constant average particle size. However, the capillary suction time demonstrated a substantial increase with alkaline conditioning. Consequently, despite the notable decrease in viscosity, this treatment did not elevate the free water content or impede the sludge dewatering process.

4.9. Combined Treatment Methods

The potential benefit of using the chemicals of potassium permanganate (KMnO4) and peroxymonosulfate (PMS) together to improve sludge dewatering performance was examined in the study conducted by Luo et al. (2019). The study's findings indicate that applying PMS and KMnO4 together was far more successful in improving sludge dewaterability than applying these chemicals alone. The research's use of the combined technique resulted in a decrease in the water content of the dehydrated sludge from 78.96% to 70.47% and a reduction in capillary suction time from 73.65 seconds to 24.65 seconds.

In their study, Zhang et al. (2021) proposed a pretreatment method consisting of a combination of acid treatment and microwave irradiation to enhance the dewatering capability of sludge. The particle size analysis as well as the vacuum filtration tests were employed to determine the impact of the method on sludge dewatering. The optimal microwave treatment circumstances was identified as 700 W for 180 s in the study, resulting in a 38.2% reduction in specific filtration resistance under these conditions. The combined acid-microwave method further increased the dewatering ability. At pH 5, it was found that the specific filtration resistance of the sludge decreased by 56.32% compared to the untreated sludge. Furthermore, the SEM images utilized in the study show that the original sludge had a large, voluminous floc structure. The disruption of the floc structure following microwave treatment is verified by SEM images. Following acid-microwave treatment, the floc fragments exhibited a tendency to consolidate and form bigger units. As a result, it was suggested that using the combination approach will improve sludge dewatering efficiency by encouraging the creation of pores.

Menon et al.'s (2020) investigation examined the efficacy of a novel sludge processing method that incorporates ultrasonication together with Fenton and Free Nitric Acid (FNA). The best values for pH, temperature, ultrasonication time, power, and frequency were found to be 5, 30 °C, 15 minutes, 60 watts, and 80 kHz, respectively, based on the results of the studies. Furthermore, it was established that the optimal dosages for FeSO4, H2O2, and FNA were

45 mg/g DS, 250 mg/g DS, and 125 mg/g DS, respectively. Following the procedure, the sludge floc's structure became more porous and had cracks, according to scanning electron microscopy (SEM) analysis. The outcomes of the experiment imply that the elevated mass transfer resulting from the utilization of ultrasonication amplifies the sludge's potential for improved dewatering.

Bien and Bien (2021) studied the physical and chemical methods for sludge dewatering. Zetag 8180 and PIX 113 were used as organic/inorganic chemicals, and the physical method was sonication. The capillary suction time was reduced by sonication and chemical process. According to the results of the study, the max sludge dewatering was obtained with sonicated sludge with PIX113.

In another study conducted by Rashvanlou et al. (2022), the effects of ultrasound and four chemicals (aluminium sulphate (Alum), Iron (III) chloride ($FeCl_3$), cationic polyacrylamide (CPAM), and combined ferric chloride and lime) on sludge dewatering were tested in terms of the capillary suction time, specific resistance to filtration and moisture content. The results show that CPAM and combined chemicals gave higher sludge dewaterability comparing the other two chemicals.

The effect of the combined process of O_3, ferric trichloride/ polyacrylamide ($FeCl_3$/PAM), and sludge ceramsite sand (SCS) for increasing the sludge dewatering was studied by Xia et al. (2023). When comparing the efficiencies of $FeCl_3$ and PAM, $FeCl_3$ was better the PAM. The water content of sludge was reduced from 91% to 65.64%, and the net yield of sludge increased by 73.55%.

He et al., (2024) carried out experiments on sludge dewaterability by PAM coagulation with Fe^{2+}/CaO_2 Fenton-like oxidation. According to the results, the water content of sludge was reduced from 78.6% to 73.1%, and CST from 32.9 to 19.5 by adding PAM before Fe^{2+}/CaO_2.

5. CONCLUSION AND FUTURE RECOMMENDATIONS

The dewatering of waste sludge generated as a result of wastewater treatment, whose quantities are increasing day by day, is one of the crucial steps in sludge management. The reduction in sludge volume through dewatering plays a crucial role in lowering transportation and disposal costs. Mechanical methods such as mechanical presses, vacuum filtration, and centrifuges are frequently favored due to their low energy consumption. However, certain attributes of high-water-content sludge hinder effective water removal, resulting in diminished dewatering efficiency. Notably, the extraction of bound water within the sludge content is recognized as a major challenge in this field. Studies examined within this chapter have

demonstrated that subjecting the sludge to various pre-treatment approaches results in the breakdown of the sludge's flocculent structure, the disruption of EPS, and an increment in the release of bound water. The examined studies indicate that among all the developed methods, integrated approaches can effectively achieve dewatering by optimizing the advantages of each method to the maximum extent. However, it is still unclear which method or methods should be selected for sludges with specific physicochemical properties. To identify the suitable approach, it is essential to conduct research employing cutting-edge machine learning techniques, like artificial neural networks. This will aid in comprehending the intricate and non-linear connections between sludge constituents, rheological characteristics, and dewatering capabilities.

REFERENCES

Andreoli, C.V., Speling, M.V. Fernandes, F. 2007. Sludge treatment and disposal. Biological Wastewater Treatment Series, Vol. 6, IWA Publishing, London.

Apollo, S., Seretlo, M., Kabuba, J. 2023. In-situ sludge degradation and kinetics of a full scale modifed activated sludge system achieving near zero sludge production, Journal of Water Process Engineering, 53, 103864, doi: 10.1016/j.jwpe.2023.103864.

Bie´n, B., Bie´n, J.D. 2021. Conditioning of sewage sludge with physical, chemical and dual methods to ımprove sewage sludge dewatering, Energies, 14, 5079, doi.org/10.3390/en14165079.

Cao, B., Zhang, W., Du, Y., Wang, R., Usher, S. P., Scales, P. J., Wang, D. 2018. Compartmentalization of extracellular polymeric substances (EPS) solubilization and cake microstructure in relation to wastewater sludge dewatering behavior assisted by horizontal electric field: Effect of operating conditions, Water Research, 130: 363-375.

Cao, B., Zhang, T., Zhang, W., Wang, D. 2021. Enhanced technology based for sewage sludge deep dewatering: A critical review, Water Research, 189, 116650, doi:10.1016/j.watres.2020.116650.

Cai, M., Wang, Q., Wells, G., Dionysiou, D.D., Song, Z., Jind, M., Hu, J., Ho, S.H., Xiao, R., Wei, Z. 2019. Improving dewaterability and filterability of waste activated sludge by electrochemical Fenton pretreatment, Chemical Engineering Journal, 362, 525-536, doi.org/10.1016/j.cej.2019.01.047.

Chen, Z., Zhang, W., Wang, D., Ma, T., Bai, R. 2015. Enhancement of activated sludge dewatering performance by combined composite enzymatic lysis and chemical re-flocculation with inorganic coagulants: kinetics of enzymatic reaction and re-flocculation morphology, Water Research, 83, 367-376, doi:10.1016/j.watres.2015.06.026.

Chen, Y., Chen, H., Li, J., Xiao, L. 2019. Rapid and efficient activated sludge treatment by electro-Fenton oxidation, Water Research, 152,181-190, doi.org/10.1016/j.watres.2018.12.035.

Chen, N., Tao, S., Xiao, K., Liang, S. Yang, J., Zhang, L., 2020. A one-step acidification strategy for sewage sludge dewatering with oxalic acid, Chemosphere, 238, 124598, https://doi.org/10.1016/j.chemosphere.2019.124598.

Chen, L., Yanfen Liao, Y., Ma, X. 2021. Economic analysis on sewage sludge drying and its co-combustion in municipal solid waste power plant, Waste Management, 121, 11-22, doi.org/10.1016/j.wasman.2020.11.038.

Dai, Q., Ma, L., Ren, N., Ning, P., Guo, Z., Xie, L., Gao, H. 2018. Investigation on extracellular polymeric substances, sludge flocs morphology, bound water release and dewatering performance of sewage sludge under pretreatment with modified phosphogypsum, Water Research, 142, 337-346, doi: 10.1016/j.watres.2018.06.009.

Devos, P., Haddad, M., Carrère, H. 2021. Thermal hydrolysis of municipal sludge: finding the temperature sweet spot: a review, Waste and Biomass Valorization, 12, 2187-2205. https://doi.org/10.1007/s12649-020-01130-1.

Ding, A., Lin, W., Chen, R., Ngo, H. H., Zhang, R., He, X., Nan, J., Li, G., Ma, J. 2022. Improvement of sludge dewaterability by energy uncoupling combined with chemical re-flocculation: reconstruction of floc, distribution of extracellular polymeric substances, and structure change of proteins, Science of the Total Environment, 816, 151646, doi:10.1016/j.scitotenv.2021.151646.

El Jery A, Kosarirad H, Taheri N, Bagheri M, Aldrdery M, Elkhaleefa A, Wang C, Sammen, SS. 2023. An application of ultrasonic waves in the pretreatment of biological sludge in urban sewage and proposing an artificial neural network predictive model of concentration, Sustainability, 15(17):12875. https://doi.org/10.3390/su151712875.

Faruqi, M.H.Z., Siddiqui, F.Z., Hassan, S.Z. 2021. Optimization of microwave treatment for dewaterability enhancement of electroplating sludge, Journal of Material Cycles and Waste Management, 23, 566-580. https://doi.org/10.1007/s10163-020-01141-z.

Fester, V., Werner, R. 2023. Optimization of polymer dosing for ımproved belt press performance in wastewater treatment plants, advances in slurry technology edited by Trevor Frank Jones, Publisher: intechopen, ISBN 978-1-80356-669-6.

Ge, D., Zhang, W., Yuan, H., Zhu, N., 2019. Enhanced waste activated sludge dewaterability by tannic acid conditioning: Efficacy, process parameters, role and mechanism studies, Journal of Cleaner Production, 241, 118287, https://doi.org/10.1016/j.jclepro.2019.118287.

Ghazisaidi, H., Wang, V., Fatehi, P., Tran, Torsten, H., Meyer, T., Allen, D.G., 2023. Determining the performance of lignin-based flocculants in improving biosludge dewaterability, Journal of Environmental Management, 325, Part B, 116509, https://doi.org/10.1016/j.jenvman.2022.116509.

Ginisty, P., Mailler, R., Rocher, V. 2021. Sludge conditioning, thickening and dewatering optimization in a screw centrifuge decanter: Which means for which result? Journal of Environmental Management, 280, 111745, https://doi.org/10.1016/j.jenvman.2020.111745.

Golbabaei Kootenaei, F., Mehrdadi, N., Nabi Bidhendi, G., Rad, H.A., Hasanlou, H., Mahmoudnia, A. 2022. Improvement of sludge dewatering by ultrasonic pretreatment, International Journal of Environmental Research, 16, 50 https://doi.org/10.1007/s41742-022-00434-5.

Guan, B., Yu, J., Fu, H., Guo, M., Xu, X. 2012. Improvement of activated sludge dewaterability by mild thermal treatment in $CaCl_2$ solution, Water Research, 46, 2, 425-432, doi:10.1016/j.watres.2011.11.014.

He, D.-Q., Wang, L.-F., Jiang, H., Yu, H.-Q. 2015. A Fenton-like process for the enhanced activated sludge dewatering, Chemical Engineering Journal, 272, 128-134, doi:10.1016/j.cej.2015.03.034.

He, D.-Q., Zhang, Y.-J., He, C.-S., Yu, H.-Q. 2017. Changing profiles of bound water content and distribution in the activated sludge treatment by NaCl addition and pH modification, Chemosphere, 186, 702-708, doi:10.1016/j.chemosphere.2017.08.045.

He, D., Zhu, T., Sun, M., Chen, J., Luo, H., Li, J. 2024. Unraveling synergistic mechanisms of polyacrylamide coagulation and Fe^{2+}/CaO_2 Fenton-like oxidation to enhance sludge dewatering, Chemical Engineering Journal, 479, 147576, doi.org/10.1016/j.cej.2023.147576.

Higgins, M.J., Beightol, S., Mandahar, U., Suzuki, R., Xiao, S., Lu, H.W., Le, T., Mah, J., Pathak, B., DeClippeleir, H., Novak, J.T., Al-Omari, A., Murthy, S.N. 2017. Pretreatment of a primary and secondary sludge blend at different thermal hydrolysis temperatures: impacts on anaerobic digestion, dewatering and filtrate characteristics. Water Research, 122, 557-569, https://doi.org/10.1016/j.watres.2017.06.016.

Hu, J., Li, Z., Zhang, A., Mao, S., Jenkinson, I.R., Tao, W. 2020. Using a strong chemical oxidant, potassium ferrate (K_2FeO_4), in waste activated sludge treatment: A review, Environmental Research, 188, 109764, doi.org/10.1016/j.envres.2020.109764.

Hyrycz, M., Ochowiak, M., Krupińska, A., Włodarczak, S., Matuszak, M., 2022. A review of flocculants as an efficient method for increasing the efficiency of municipal sludge dewatering: Mechanisms, performances, influencing factors and perspectives, Science of the Total Environment, 820, 153328, doi:10.1016/j.scitotenv.2022.153328.

Im, S., Kim, H.J., Rho, H., Kim, Y.K. 2022. Investigation of sludge dewatering efficiency in the thermal-hydrolysis reactor at various physical operational factors: Performance and fluid dynamic analysis, Environmental Technology and Innovation, 27, 102457, https://doi.org/10.1016/j.eti.2022.102457.

Jin, B., Wilén, B.-M., Lant, P. 2004. Impacts of morphological, physical and chemical properties of sludge flocs on dewaterability of activated sludge, Chemical Engineering Journal 98, 115-126.

Jin, L., Zhang, G., Zheng, X. 2015. Effects of different sludge disintegration methods on sludge moisture distribution and dewatering performance, Journal of Environmental Sciences, 28, 22-28, https://doi.org/10.1016/j.jes.2014.06.040.

Kim, H. J., Chon, K., Lee, Y. G., Kim, Y. K., Jang, A. 2020. Enhanced mechanical deep dewatering of dewatered sludge by a thermal hydrolysis pre-treatment: Effects of temperature and retention time, Environmental Research, 188, 109746, https://doi.org/10.1016/j.envres.2020.109746.

Liang, J., Zhang, S., Huang, J., Huang, S., Zheng, L., Sun, S., Zhong, Z., Zhang, X. and Yu, X., 2019. Comprehensive insights into the inorganic coagulants on sludge dewatering: comparing aluminium and iron salts, Journal of Chemical Technology and Biotechnology, 94, 1534-155, https://doi.org/10.1002/jctb.5913.

Liang, Y., Wang, R., Sun, W., Sun, Y., 2023. Advances in chemical conditioning of residual activated sludge in China, Water, 15, 345, doi:10.3390/w1502034.

Lin, F., Li, B., 2022. Changes of network structure and water distribution in sludge with the stratified extraction of extracellular polymeric substances, Environmental Science and Pollution Research, 29(32), 48648-48660, doi:10.1007/s11356-022-19075-4.

Lin, W., Guo, J., Zeng, J., Chen, R., Ngo, H.H., Nan, J., Li, Ma, J., Ding, A. 2023. Enhanced sludge dewaterability by ferrate/ferric chloride: The key role of Fe(IV) on the changes of EPS properties, Science of the Total Environment, 858, 159562, dx.doi.org/10.1016/j.scitotenv.2022.159562.

Liu, J., Yang, Q., Wang, D., Li, X., Zhong, Y., Li, X., Deng, Y., Wang, L., Yi, K., Zeng, G. 2016. Enhanced dewaterability of waste activated sludge by Fe(II)-activated peroxymonosulfate oxidation, Bioresource Technology, 206, 134-140, https://doi.org/10.1016/j.biortech.2016.01.088.

Liu, S., Wu, J., Hu, Z., Jiang, M., 2023. Changes in microbial community during hydrolyzed sludge reduction, Frontiers in Microbiology, 14, 1239218, doi:10.3389/fmicb.2023.1239218.

Luo, L., Ge, Y., Yuan, S., Yu, Y., Shi, Z., Zhou, S., Deng, J., 2019. Enhanced dewaterability of waste activated sludge by a combined use of permanganate and Peroxymonosulfate, RSC Advances, 9, 27593. https://doi.org/10.1039/c9ra03781k.

Luo, H., Zeng, Y., He, D., Pan, X. 2021. Application of iron-based materials in heterogeneous advanced oxidation processes for wastewater treatment: A review, Chemical Engineering Journal, 407, 127191, doi.org/10.1016/j.cej.2020.127191.

Mao, H., Chi, Y., Wang, F. Mao, F., Liang, F., Lu, S., Cen, K. 2018. Effect of Ultrasonic Pre-treatment on Dewaterability and Moisture Distribution in Sewage Sludge, Waste and Biomass Valorization, 9, 247-253, https://doi.org/10.1007/s12649-016-9799-3.

Menon, U., Suresh, N., George, G., Ealias, A. M., Saravanakumar, M.P. 2020. A study on combined effect of fenton and free nitrous acid treatment on sludge dewaterability with ultrasonic assistance: Preliminary investigation on improved calorific value, Chemical Engineering Journal, 382, 123035, https://doi.org/10.1016/j.cej.2019.123035.

Metcalf & Eddy, 1991. Wastewater Engineering: Treatment Disposal Reuse, 3rd ed.; McGraw-Hill: New York, NY, USA.

Mikkelsen, L.H., Keiding, K. 2002. Physico-chemical characteristics of full scale sewage sludges with implications to dewatering, Water Research, 36, 10, 2451-2462, doi:10.1016/S0043-1354(01)00477-8.

Murthy, S.N., Novak, J.T., 1999. Factors affecting floc properties during aerobic digestion: implications for dewatering, Water Environment Research, 71, 197-202.

Ngo, P. L., Udugama, I. A., Gernaey, K. V., Young, B. R., Baroutian,S. 2021. Mechanisms, status, and challenges of thermal hydrolysis and advanced thermal hydrolysis processes in sewage sludge treatment, Chemosphere, 281, 130890, https://doi.org/10.1016/j.chemosphere.2021.130890.

Niu, M., Zhang, W., Wang, D., Chen, Y., Chen, R., 2013. Correlation of physicochemical properties and sludge dewaterability under chemical conditioning using inorganic coagulants, Bioresource Technology, 144, 337-343, https://doi.org/10.1016/j.biortech.2013.06.126.

Oosterhuis, M., Ringoot, D., Hendriks, A., Roeleveld, P. 2014. Thermal hydrolysis of waste activated sludge at Hengelo Wastewater Treatment Plant, The Netherlands. Water Science and Technology, 70(1): 1-7. https://doi.org/10.2166/wst.2014.107.

Peng, S., Wang, Z., Li, L., Ai, J., Li, L., Liao, G., Wang, D., Peng, S., Zhang, W., 2024. Molecular dynamic modeling of EPS and inorganic/organic flocculants during sludge dual conditioning, Science of The Total Environment, 906, 167719, https://doi.org/10.1016/j.scitotenv.2023.167719.

Qi, Y., Thapa, K.B., Hoadley, A.F.A. 2011. Application of filtration aids for improving sludge dewatering properties A review, Chemical Engineering Journal, 171, 373-384, doi:10.1016/j.cej.2011.04.060.

Qi, Y., Chen, J., Xu, H., Wu, S., Yang, Z., Zhou, A., Hao, Y. 2024. Optimizing sludge dewatering efficiency with ultrasonic Treatment: Insights into Parameters, Effects, and microstructural changes, Ultrasonics Sonochemistry, 102, 106736, https://doi.org/10.1016/j.ultsonch.2023.106736.

Rashvanlou, R.B., Pasalari, H., Moserzadeh, A.A., Farzadkia, M. 2022. A combined ultrasonic and chemical conditioning process for upgrading the sludge dewaterability, International Journal of Environmental Analytical Chemistry, 102(7), 1613-1626, doi.org/10.1080/03067319.2020.1739668.

Rao, B., Su, J., Xu, S., Pang, H., Xu, P., Zhang, Y., Zhu, J., Tu, H. 2022. Thermal and non-thermal mechanism of microwave irradiation on moisture content reduction of municipal sludge, Water Research, 226, 119231, https://doi.org/10.1016/j.watres.2022.119231.

Rao, B., Wang, G., Xu, P. 2022. Recent advances in sludge dewatering and drying technology, Drying Technology, 40(15), 3049-3063, doi.org/10.1080/07373937.2022.2043355.

Raynaud, M., Vaxelaire, J., Olivier, J., Dieudé-Fauvel, E., Baudez, J.-C., 2012. Compression dewatering of municipal activated sludge: Effects of salt and pH, Water Research, 46, 14, 4448-4456, https://doi.org/10.1016/j.watres.2012.05.047.

Rizzardini, C.B., Goi, D. 2014. Sustainability of domestic sewage sludge disposal, Sustainability, 6, 2424-2434.

Rodríguez-Chueca, J., Mediano, A., Ormad, M.P., Mosteo, R., Ovelleiro, J.L. 2014. Disinfection of wastewater effluents with the Fenton-like process induced

by electromagnetic fields, Water Research, 60, 250-258, doi:10.1016/j.watres.2014.04.040.

Ruiz-Hernando, M., Martinez-Elorza, G., Labanda, J., Llorens, J. 2013. Dewaterability of sewage sludge by ultrasonic, thermal and chemical treatments, Chemical Engineering Journal, 230, 102-110, doi:10.1016/j.cej.2013.06.046.

Ryltseva, Y. 2021. Express-method of determining the water-yielding capacity of natural water sludge in modern dewatering Technologies, IOP Conf. Series: Materials Science and Engineering, 1030, 012108, doi:10.1088/1757-899X/1030/1/012108.

Sapmaz, S. 2022. Arıtma Çamurlarının Bertarafında Kullanılan Kurutma Sistemlerinin Enerji Verimliliğinin Değerlendirilmesi, Kocaeli Üniversitesi Fen Bilimleri Enstitüsü, Doktora Tezi, Kocaeli.

Seck, A., Gold, M., Niang, S., Mbéguéré, M., Diop, C., Strande, L. 2015. Faecal sludge drying beds: increasing drying rates for fuel, resource recovery in Sub-Saharan Africa, Journal of Water Sanitation and Hygiene for Development, 05.1, 72-80, doi: 10.2166/washdev.2014.213.

Sheng, G.P., Yu, H.Q., Li, X.Y., 2010. Extracellular polymeric substances (EPS) of microbial aggregates in biological wastewater treatment systems: a review, Biotechnology Advances, 28, 882-894.

Sultan, H. 2006. Çamurun Hamsudan Mekanik Olarak Ayrıştırma Sistemi Tasarımı, Yüksek Yıldız Teknik Üniversitesi, Fen Bilimleri Enstitüsü, Lisans Tezi, İstanbul.

Tao, S., Yang, J., Hou, H., Liang, S., Xiao, K., Qiu, J., Hu, J., Liu, B., Yu, W., Deng, H. 2019. Enhanced sludge dewatering via homogeneous and heterogeneous Fenton reactions initiated by Fe-rich biochar derived from sludge, Chemical Engineering Journal, 372, 966-977, doi.org/10.1016/j.cej.2019.05.002.

Tsang, K.R., Vesilind, P.A., 1990. Moisture Distribution in Sludges. Water Science and Technology, 22 (12), 135-142, doi:10.2166/wst.1990.0108.

Tunçal, T., Mujumdar, A.S.,2023. Modern techniques for sludge dewaterability improvement, Drying Technology, 41:3, 339-351, doi:10.1080/07373937.2022.2092127.

URL-1. 2024. https://www.elliscorp.com/solutions/water-solutions/filter-press/

Vaxelaire, J,. Cézac, P. 2004. Moisture distribution in activated sludges: A review, Water Research, 38, 9, 2215-2230, doi:10.1016/j.watres.2004.02.021.

Wei, H., Gao, B., Ren, J., Li, A., Yang, H. 2018. Coagulation/flocculation in dewatering of sludge: A review, Water Research, 143, 608-631, doi:10.1016/j.watres.2018.07.029.

Wei, L., Xia, X., Zhu, F., Li, Q., Xue, M., Li, J., Sun, B., Jiang, J., Zhao, Q. 2020. Dewatering efficiency of sewage sludge during Fe^{2+}-activated persulfate oxidation: Effect of hydrophobic/hydrophilic properties of sludge EPS. Water Research, 181: 115903.

Wingender, J., Neu, T.R., Flemming, H.C. 1999. Microbial Extracellular Polymeric

Substances: Characterization, Structures and Function, Springer-Verlag, Berlin, Heidelberg (Chapter 3).

Wolski, P. 2020. The effect of ultrasonic disintegration on sewage sludge conditioning, Desalination and Water Treatment, 199, 99-106.

Wu, B., Su, L., Dai, X., Chai, X. 2018. Development of sludge-derived mesoporous material with loaded nano CaO_2 and doped Fe for re-utilization of dewatered waste-activated sludge as dewatering aids, Chemical Engineering Journal, 335, 161-168, dx.doi.org/10.1016/j.cej.2017.10.015.

Wu, S., Zheng, M. Dong, Q. Liu, Y., Wang, C. 2018. Evaluating the excess sludge reduction in activated sludge system with ultrasonic treatment, Water Science and Technology, 77, 2341-2347.

Wu, J., Tao Lu, T., Bi, J., Haoran Yuan H., Chen, Y. 2019. A novel sewage sludge biochar and ferrate synergetic conditioning for enhancing sludge dewaterability, Chemosphere, 237, 124339, doi.org/10.1016/j.chemosphere.2019.07.070.

Wu, B., Dai, X., Chai, X. 2020. Critical review on dewatering of sewage sludge: infuential mechanism, conditioning technologies and implications to sludge re-utilizations, Water Research, 180, 115912.

Wu, W., Ma, J., Xu, J., Wang, Z., 2021. Mechanistic insights into chemical conditioning by polyacrylamide with different charge densities and its impacts on sludge dewaterability, Chemical Engineering Journal, 410, 128425, https://doi.org/10.1016/j.cej.2021.128425.

Xia, J., Ji, J., Hu, Z., Rao, T., Liu, A., Ma, J., Sun, Y. 2022. Application of Advanced Oxidation Technology in Sludge Conditioning and Dewatering: A Critical Review, International Journal of Environmental Research and Public Health, 19, 9287, doi.org/10.3390/ijerph19159287.

Xia, T., Zhang, X., Chen, D., Gao, Z., Ji, Y., Xia, J., Wang, L. 2023. Effects of ceramsite derived from sewage sludge combined with the O_3–$FeCl_3$/PAM process on the dewatering of waste-activated sludge and investigation of dewatering mechanisms, Water Science and Technology, 88(2), 367-380, doi: 10.2166/wst.2023.224.

Yan, S., Subramanian, S.B., Tyagi, R.D., Surampalli, R.Y., 2009. Wastewater sludge characteristics, R.D.Tyagi, R.Y. Surampalli, S.Yan, T.C. Zhang, C.M. Kao, B.N. Lohan (Ed.), Sustainable Sludge Management: Production of Value Added Products, American Society of Civil Engineers, Virginia, pp. 6-36.

Yuan, D., Wang, Y., Qian, X. 2017. Variations of internal structure and moisture distribution in activated sludge with stratified extracellular polymeric substances extraction, International Biodeterioration & Biodegradation, 116, 1-9, doi:10.1016/j.ibiod.2016.09.012.

Yu, Q., Lei, H., Yu, G., Feng, X., Li, Z., Wu, Z. 2009. Influence of microwave irradiation on sludge dewaterability, Chemical Engineering Journal, 155, 1-2, 88-93, https://doi.org/10.1016/j.cej.2009.07.010.

Yu, W., Wen, Q., Yang, J., Xiao, K., Zhu, Y., Tao, S., Lv, Y., Liang, S., Fan, W., Zhu, S., Liu, B., Hou, H., Hu, J. 2019. Unraveling oxidation behaviors for intracellular and extracellular from different oxidants (HOCl vs. H_2O_2) catalyzed by ferrous iron in waste activated sludge dewatering, Water Research, 148, 60-69, doi. org/10.1016/j.watres.2018.10.033.

Yüksekdağ, M., Gökpınar, S., Yelmen, B. 2020. Atıksu Arıtma Tesislerinde Arıtma Çamurları ve Bertaraf Uygulamaları, Avrupa Bilim ve Teknoloji Dergisi, (18), 895-904.

Zhang, H., Lu, X., Song, L., Zhang L. 2018. Effects of Loosely Bound EPS Release and Floc Reconstruction on Sludge Dewaterability, Water Air Soil Pollution, 229, 27, doi:10.1007/s11270-017-3683-z.

Zhang, X., Ye, P., Wu, Y., Guo, Z., Huang, Y., Zhang, X., Sun, Y., Zhang, H. 2021. Research on Dewatering Ability of Municipal Sludge under the Treatment of Coupled Acid and Microwave, Geofluids, Article ID 7161815, https://doi.org/10.1155/2021/7161815.

Zhen, Z., Jinxiang, Y., Renhui, D. 2020. A Review on the Physical Dewatering Methods of Sludge Pretreatment in Recent Ten Years, IOP Conference Series: Earth and Environmental Science, 455, 012189.

Zou, X., He, J., Zhang, P., Pan, X., Zhong, Y., Zhang, J., Wu, X., Li, B., Tang, X., Xiao, X., Pang, H. 2022. Insights into carbon recovery from excess sludge through enzyme-catalyzing hydrolysis strategy: environmental benefts and carbon-emission reduction, Bioresource Technology, 351, 127006, doi: 10.1016/j.biortech.2022.127006.

CHAPTER 8

FFF-BASED 3D PRINTING OF METALS: A BRIEF REVIEW

Sinan YILMAZ[1]

1 Assist. Prof. Dr., Kocaeli University, Mechanical and Material Technologies, Kocaeli/Turkey, sinan.yilmaz@kocaeli.edu.tr, ORCID: 0000-0001-7107-5454.

1. INTRODUCTION

All engineering products indeed have their origins in the design process. Design in mechanical engineering is a critical process in which factors such as the product's lifespan, cost, ergonomics, functionality, and degree of impact on the environment must be considered.

The ability of a design to meet these specified criteria is directly associated with the material chosen. For a machine component to ensure environmental conditions and loads during operation over the anticipated period, it must possess mechanical, physical, and chemical properties suitable for the task. Furthermore, the manufacturability of the chosen material, specifically its formability/shaping capability, is a crucial criterion in material selection. Therefore, engineering encompasses the interconnected processes of design, material selection, and manufacturing activities. Therefore, the manufacturing process should also be taken into consideration while choosing materials. For instance, welding a machine requiring a tight seal necessitates choosing a weldable material. On the other hand, tight tolerances and low surface roughness on a machine part suggest machining as the preferred process.

Conventional manufacturing methods include different manufacturing techniques such as forming, casting, welding, and machining. Regardless of the chosen method among these, machining is typically employed as a final step for the manufactured part, whether it involves cutting runners in casting, eliminating burrs in forging, or refining surface roughness. This circumstance results in adverse economic and ecological implications, leading to both time losses and supplementary costs arising from process expenditures and waste materials.

Consequently, Additive Manufacturing (AM) methods offer innovative technologies that could potentially substitute traditional techniques. They enable the swift layer-by-layer production of intricate components without requiring molds, extra machining, or sophisticated and costly machinery.

Therefore, AM methods constitute a revolutionary manufacturing technology known as 3D printing, encompassing techniques such as Stereolithography (SL), Selective Laser Sintering (SLS), Laminated Object Manufacturing (LOM), Laser Engineering Net Shaping (LENS), Electron Beam Melting (EBM). The principles, materials, pros, and cons of AM methods are listed in Table 1. In addition to the mentioned methods, another technique within the scope of AM is the Fused Filament Fabrication (FFF), also called as Fused Deposition Modeling (FDM). Unlike the other methods mentioned, FFF, or FDM, is the most widely used AM method with a broad spectrum of applications ranging from hobbyist activities to industrial production, and from education to architecture (Wong & Hernandez, 2012).

Table 1. Classification of Additive Manufacturing Techniques (Pazhamannil et al., 2022).

Method	Procedure Designation	Process	Materials	Pros and Cons
Material extrusion	Fused filament Fabrication (FFF)	Solidification of a continuous filament, wound onto a spool, by melting it through a nozzle onto a plane.	• Thermoplastics • Composites • Metals	• Cheaper and effortless • Large variety of materials • Poor mechanical behavior • Relatively rough surface • Nozzle clogging
Vat photopolymerization	• Stereolithography (SL) • Continuous liquid interface production (CLIP)	• Photopolymer in a container • UV Laser/digital light projector	Photopolymers	• High resolution • Difficulty of resin cleaning • Relatively small dimensions • Limited material variety
Material jetting	Multi-jet modeling (MJM)	Ink-jet type	Liquid polymers	• Detailed geometry • Ability to print one layer at a time • Poor mechanical behavior
Binder jetting	Binder jet 3D Printing (BJ-3DP)	• Powder on build plate • Drops on demand	• Metals • Ceramics • Sand	• Material variety • High speed • High cost
Sheet lamination	Laminated object manufacturing (LOM)	• Binding of sheets with adhesive material • Laser cutting	• Paper • Plastic • Metal (less common)	• Fast and cheap • No support required • Low surface quality • Delicate parts
Powder bed fusion	• Selective laser sintering (SLS) • Selective laser melting (SLM) • Electron beam melting (EBM)	• Powder on the build plate • High energy laser/ electron	• Powders of polymer or metal	• Flexibility • Zero waste • Post processing necessity • Laborious and time-consuming manufacturing process
Direct energy deposition	• Laser engineered net shaping (LENS) • Electron beam additive manufacturing (EBAM)	• Metal in wire or powder form • Melting via a concentrated, high-intensity heat source	Metals	• Functional parts • Minimal waste • Low speed and high cost • Anisotropic and heterogeneous
Pellet extrusion	Material extrusion (MEX)	• Granules are propelled through single or twin-screw extrusion pathways. • Melting and blending	• Thermoplastic	• Easy • Reduced degradation • Melting rate sensitivity

2. FUSED FILAMENT FABRICATION

The method called FFF entails passing a thermoplastic polymer filament with a uniform diameter (1.75/2.85 mm) through a heated nozzle up to the material's melting temperature, solidifying one layer at a time onto a plane (build plate), to obtain three-dimensional solid objects (see Figure 1). That's why it's also called as 3D printing (Yilmaz et al., 2024).

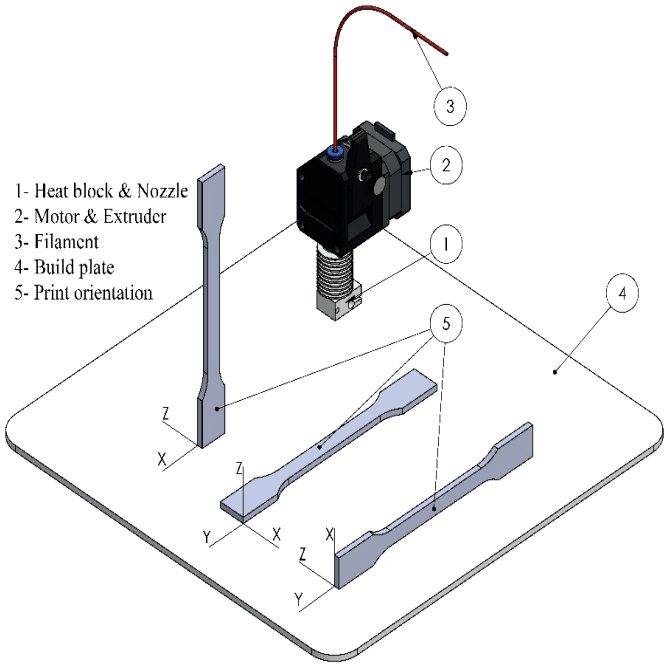

Figure 1. Schematic illustration of FFF (Yilmaz et al., 2023)

According to the flowchart in Figure 2, the FFF method initiates with acquiring the solid model of the design. As mentioned earlier, since the method needs solidified layer at a time, the CAD file of the object should be accessed via a software which positions it to be segmented into planes to determine the process parameters, and then sends it to the FFF machine (3D printer). As previously mentioned, in the manufacturing method using 3D printing, since each layer needs to be solidified individually, the CAD file of the object is opened with software that divides it into planes to determine coordinates (that's why it's called a slicer), and then manufacturing parameters are set. Subsequently, it needs to be sent to an FFF machine (3D printer) to execute the G-codes.

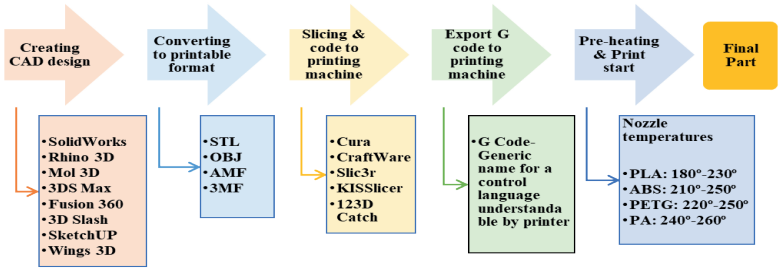

Figure 2. FFF flowchart (Rajendran et al., 2023)

There are many parameters affecting the final parts' surface roughness, dimensions, and strength in the 3D printing. Besides the material used as filament, the most important ones include temperature, speed, layer height, infill ratio, and infill pattern (Kurose et al., 2020; Salem Bala et al., 2016). Frequently utilized filament materials in FFF are PLA (Polylactic Acid) and ABS (Acrylonitrile Butadiene Styrene) (Kiendl & Gao, 2020). Although these materials are often preferred in terms of cost and process ease, unfortunately they cannot be used as functional machine elements due to their low strength. Therefore, the use of advanced engineering materials such as Polyphenylene Sulfide (PPS), Polyetherimide (PEI), Polyetheretherketone(PEEK) is considered in FFF method for applications requiring high strength and long lifespan. However, these materials come with limitations in terms of cost and process. Therefore, for the fabrication of parts with enhanced strength in polymer based FFF method, the most effective solution often involves the use of composite or blended forms of materials such as PLA, ABS, Polietilentereftalat (PET) ve Polyamide (PA), which have lower strength than advanced engineering polymers but are easier to process (Yilmaz, 2023).

However, whether in composite or blended form, polymers inherently have low melting temperatures and, more importantly, low T_g (glass transition temperature) values. Therefore, the effective use of these materials is not possible in applications involving high temperatures. At this point, the metal based FFF method, where metal particles are turned into filament with a binding polymer and then 3D printed, holds great potential for enabling durable and long-lasting manufacturing.

3. METAL 3D PRINTING IN FFF

Metal FFF method is a technology that enables the manufacturing of complex-shaped and functional metal-based parts using 3D printing. In this method, metal powders are mixed with a binding polymer to form a filament, which is then melted layer by layer using a 3D printer to fabricate the desired metal part. The filament used in the method contains a high percentage (50-

90%) of metal particles, and after FFF, the binding polymer is removed from the structure through various methods (debinding), making it possible to manufacture nearly 100% metal-based parts. This technology allows for the rapid prototyping and small-scale production of intricate geometries of metal parts without the need for complex and expensive equipment/machinery. The flowchart of the metal based FFF method is provided in Figure 3.

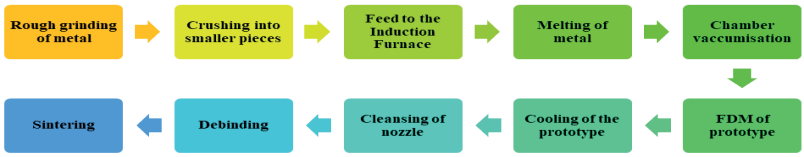

Figure 3. FFF Metal 3D printing flowchart (Kumar Singh & Chauhan, 2016)

In the FFF method, the temperature reached typically ranges between 450-500 degrees Celsius, so metal does not melt in metal based FFF. Only the binder material (polymer, wax, or an additive) melts to hold the metal particles together and achieve the desired geometry. Therefore, additional processes are required after 3D printing. The first of these is debinding, carried out to remove the polymer from the structure. As debinding is the process that most complicates metal based FFF and has the greatest impact on the geometry of the manufactured part, it is the most critical stage in 3D printing. The debinding process is divided into three categories: catalytic, chemical, and thermal (Quarto et al., 2021). Among these, the chemical debinding process is the fastest and most efficient. The essence of the method lies in using a solution selected according to the chemical structure of the polymer used as a binder in the filament (Kukla et al., 2016). As seen in Figure 4, the part is referred to as "green part" before debinding and "brown part" afterwards. After debinding, a process called "sintering" is carried out at a temperature close to the melting temperature of the metal, which ensures the fusion of metal particles together. The sintering process is the most critical stage that determines the strength of the final product. Since the method is still in its early stages of development, there is limited literature studying FFF metal printing in scientific publications. In these studies, stainless steel is commonly used as the filament material (Liu et al., 2020; Obadimu & Kourousis, 2023; Sargini et al., 2021). In addition to stainless steel, there are also studies using titanium, copper, and other metals as filament (Nurhudan et al., 2021; Tosto et al., 2022).

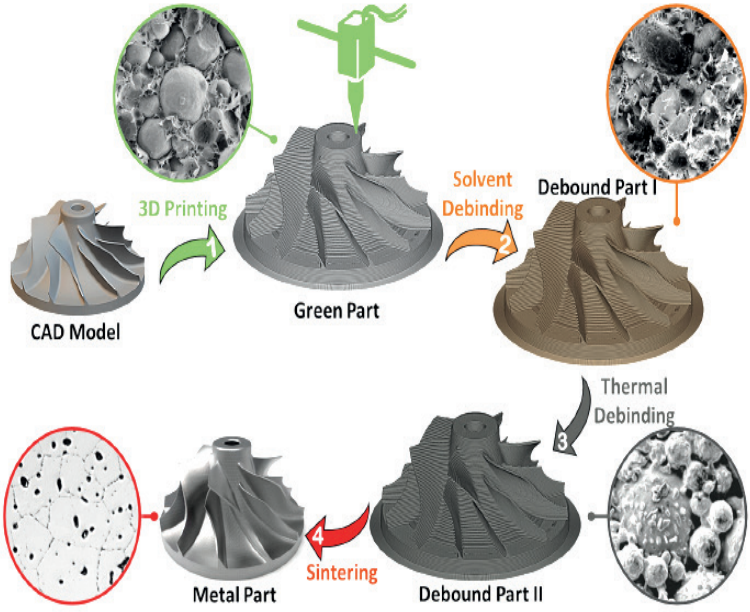

Figure 4. Schematic illustration of debinding process for FFF based 3D printed metals (Li et al., 2023)

4. CONCLUSIONS

Additive Manufacturing (AM) is a next-generation technology where objects with complex geometries can be manufactured with high dimensional and surface precision, without or with minimal waste material. The method with the highest potential within AM, which encompasses a variety of different methods, is the fused filament fabrication (FFF) method. It provides a wide range of applications by enabling manufacturing with simple equipment and affordable consumable. While originally designed and developed as a method focused on manufacturing parts from thermoplastic materials, FFF has seen the emergence of the use of metal-based filaments in response to increasing engineering demands in recent years. In this review, AM methods have been briefly categorized and explained, with a concise overview provided on part manufacturing using metal-based filaments with the FFF method. The process has been summarized outlining the key stages leading to the production of the final product.

REFERENCES

Kiendl, J., & Gao, C. (2020). Controlling toughness and strength of FDM 3D-printed PLA components through the raster layup. *Composites Part B: Engineering*, *180*, 107562. https://doi.org/10.1016/j.compositesb.2019.107562

Kukla, C., Duretek, I., Schuschnigg, S., Gonzalez-Gutierrez, J., & Holzer, C. (2016). Properties for PIM feedstocks used in fused filament fabrication. *World PM 2016 Congress and Exhibition*, *November*.

Kumar Singh, A., & Chauhan, S. (2016). Technique to Enhance FDM 3D Metal Printing. *Bonfring International Journal of Industrial Engineering and Management Science*, *6*(4), 128–134. https://doi.org/10.9756/bijiems.7574

Kurose, T., Abe, Y., Santos, M. V. A., Kanaya, Y., Ishigami, A., Tanaka, S., & Ito, H. (2020). Influence of the layer directions on the properties of 316l stainless steel parts fabricated through fused deposition of metals. *Materials*, *13*(11). https://doi.org/10.3390/ma13112493

Li, S., Deng, H., Lan, X., He, B., Li, X., & Wang, Z. (2023). Developing cost-effective indirect manufacturing of H13 steel from extrusion-printing to post-processing. *Additive Manufacturing*, *62*(October 2022), 103384. https://doi.org/10.1016/j.addma.2022.103384

Liu, B., Wang, Y., Lin, Z., & Zhang, T. (2020). Creating metal parts by Fused Deposition Modeling and Sintering. *Materials Letters*, *263*, 127252. https://doi.org/10.1016/j.matlet.2019.127252

Nurhudan, A. I., Supriadi, S., Whulanza, Y., & Saragih, A. S. (2021). Additive manufacturing of metallic based on extrusion process: A review. *Journal of Manufacturing Processes*, *66*(December 2020), 228–237. https://doi.org/10.1016/j.jmapro.2021.04.018

Obadimu, S. O., & Kourousis, K. I. (2023). Microscopic and mesoscopic/macroscopic structural characteristics of material extrusion Steel 316L: influence of the fabrication process. *International Journal of Structural Integrity*, *14*(2), 314–321. https://doi.org/10.1108/IJSI-07-2022-0100

Pazhamannil, R. V., N., J. N. V., P., G., & Edacherian, A. (2022). Property enhancement approaches of fused filament fabrication technology: A review. *Polymer Engineering \& Science*, *62*(5), 1356–1376. https://doi.org/https://doi.org/10.1002/pen.25948

Quarto, M., Carminati, M., & D'Urso, G. (2021). Density and shrinkage evaluation of AISI 316L parts printed via FDM process. *Materials and Manufacturing Processes*, *36*(13), 1535–1543. https://doi.org/10.1080/10426914.2021.1905830

Rajendran, S., Palani, G., Kanakaraj, A., Shanmugam, V., Veerasimman, A., Gądek, S., Korniejenko, K., & Marimuthu, U. (2023). Metal and Polymer Based Composites Manufactured Using Additive Manufacturing—A Brief Review. *Polymers*, *15*(11), 1–19. https://doi.org/10.3390/polym15112564

Salem Bala, A., bin Wahab, S., & binti Ahmad, M. (2016). Elements and Materials Improve the FDM Products: A Review. *Advanced Engineering Forum*, *16*, 33–51. https://doi.org/10.4028/www.scientific.net/aef.16.33

Sargini, M. I. M., Masood, S. H., Palanisamy, S., Jayamani, E., & Kapoor, A. (2021). Additive manufacturing of an automotive brake pedal by metal fused deposition modelling. *Materials Today: Proceedings*, *45*(xxxx), 4601–4605. https://doi.org/10.1016/j.matpr.2021.01.010

Tosto, C., Bragaglia, M., Nanni, F., Recca, G., & Cicala, G. (2022). Fused Filament Fabrication of Alumina/Polymer Filaments for Obtaining Ceramic Parts after Debinding and Sintering Processes. *Materials*, *15*(20). https://doi.org/10.3390/ma15207399

Wong, K. V., & Hernandez, A. (2012). A Review of Additive Manufacturing. *ISRN Mechanical Engineering*, *2012*, 1–10. https://doi.org/10.5402/2012/208760

Yilmaz, S. (2023). Comprehensive analysis of 3D printed PA6.6 and fiber-reinforced variants: Revealing mechanical properties and adhesive wear behavior. *Polymer Composites*, *45*(2), 1446–1460. https://doi.org/10.1002/pc.27865

Yilmaz, S., Eyri, B., Gul, O., Karsli, N. G., & Yilmaz, T. (2023). Investigation of the influence of salt remelting process on the mechanical, tribological, and thermal properties of 3D-printed poly(lactic acid) materials. *Polymer Engineering and Science*, *64*(1), 17–30. https://doi.org/10.1002/pen.26526

Yilmaz, S., Gul, O., Eyri, B., Karsli, N. G., & Yilmaz, T. (2024). Analyzing the Influence of Multimaterial 3D Printing and Postprocessing on Mechanical and Tribological Characteristics. *Macromolecular Materials and Engineering*, *Early View*. https://doi.org/10.1002/mame.202300428

CHAPTER 9

APPLICABILITY OF RAINWATER HARVESTING IN AN EXAMPLE PUBLIC BUILDING

Melike YALILI KILIC[1]
Zeynep YILDIRIM[2]

1 Prof. Dr., Bursa Uludag University, Engineering Faculty, Department of Environmental Engineering, Gorukle, Nilufer, BURSA
2 Bursa Uludag University, Engineering Faculty, Department of Environmental Engineering, Gorukle, Nilufer, BURSA

1. INTRODUCTION

The increasing world population causes the importance of water resources to increase daily. This rapid increase in the world population has a negative impact on natural resources. Despite the rapidly increasing need for water, the decreasing amount of accessible water resources day by day due to reasons such as global warming, climate change, deforestation, destruction of basin areas and unconscious use of water resources makes water the most important agenda item in the world (URL-1, 2016).

Besides daily needs, water is also an essential resource in agriculture, energy, industry, tourism, and transportation. The total volume of water on earth is 1.4 billion km^3. 2.5% of the world's water is freshwater resources, and 97.5% is saltwater. 68.7% (24 million km^3) of the freshwater amount is found in Antarctica and the Arctic as ice and snow, and 30.1% (8 million km^3) is found as groundwater (DSİ, 2022). This situation makes access to fresh water difficult. Therefore, effective use of water becomes essential.

Due to the rapid increase in the need for water, the importance of rainwater harvesting, an alternative method to water resources, has been increased daily. Rainwater harvesting is a practice in which rainwater is collected with artificial water collection systems and used for drinking, domestic, and irrigation. It provides excellent benefits in solving water shortages, primarily experienced in places with low rainfall (Özben, 2022). Harvested rainwater is used as agricultural irrigation water, industrial process water, for washing vehicles, workplace cleaning, and toilet flushing. After undergoing the necessary purification, rainwater can also be used as drinking water. Approximately 100 million people worldwide use water collected from rainwater harvesting practices for drinking and non-drinking water use (Kara and Baykurt, 2022).

This study included literature on rainwater harvesting, and the use of rainwater collected from the roof of a public building in toilet reservoirs in the Kestel district of Bursa province was investigated. In addition, the cost of the rainwater collection system to be implemented in this building and the depreciation period of the system have been calculated.

2. RAINWATER HARVESTING

Rainwater harvesting is the collection and accumulation of surface runoff and precipitation water and the provision of water required for plant-animal production and domestic consumption (Kantaroğlu, 2011; Abd-el-Kader et al., 2023). Water harvesting from the roof surface, one of the rainwater harvesting methods, is the collection of rainwater falling on the roof surface and accumulating it in a tank on the ground surface or an underground tank with the help of gutters (Pamuk Mengü and Akkuzu, 2008). An example of storing rain collected from roofs is given in Figure 1.

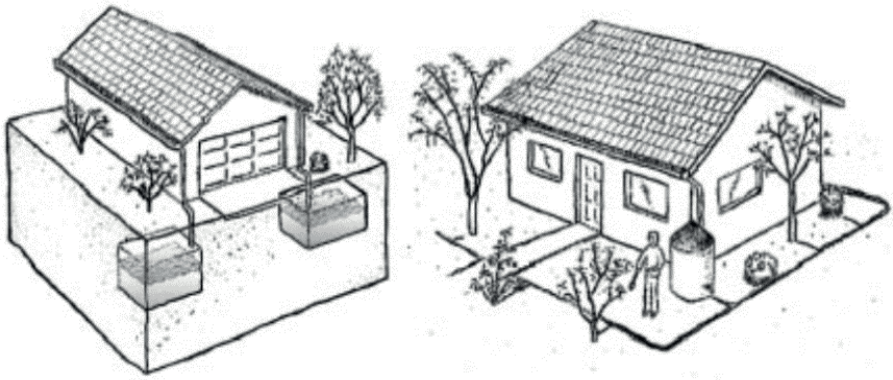

Figure 1. *Storage of rain collected from roofs (Kantaroğlu, 2011).*

Rainwater collected from the roofs of buildings can be brought to drinking water quality by adequate purification. Purified rainwater is used in washing machines and toilet tanks inside and in places such as garden irrigation and car washing outside the building (Eren et al., 2016). Rainwater can be used for drinking water after filtration, chlorination, and disinfection (Kantaroğlu, 2011).

Rainwater is collected in two ways: underground in cisterns and above ground in tanks. Although both methods have advantages and disadvantages, factors such as rainfall regime, storage size, materials used and their costs, and labor force are evaluated when deciding which system to use (Alpaslan et al., 2008).

Cistern systems are an ideal option for areas where underground and surface water resources are scarce but receive good rainfall and for settlements that do not have water supply infrastructure (Alpaslan, 1992). Cisterns are generally used in rural areas, arid regions, coastal areas, and scattered settlements. Cisterns consist of four components.

Components that make cistern systems;

- Collecting rainwater from building roofs or surfaces,
- Providing gutter and transmission system,
- Collecting rainwater in tanks,
- It is purified and delivered into the building (DSİ, 2022).

3. MATERIAL AND METHODS

The study was planned in Kestel district, located on 42,900 hectares at 40° 9 latitude and 29° 12 longitude in the east of Bursa. The district's

population is 70,865 people, and it is a position that receives immigrants from all seven regions of Turkey, consisting of 7 centers and 28 outskirts. In addition to continuing to develop by making great strides in the region's industrial and agricultural fields, air, water, and environmental pollution also bring problems such as increased need for energy, decreased natural resources, rapidly growing population, and traffic congestion. Although it is a region rich in water resources, the unconscious use of resources and population growth due to agriculture and industry poses a danger in the coming years. Within the scope of the study, a public building located in a park with green areas in the district center and whose roof has a large surface area was selected.

The family park, which also includes the Kestel Municipality additional service building, covers an area of 15000 m^2 (Figure 2). The park has green areas, walking paths, a small cafeteria, playgrounds for children, and camellias. It consists of a men's and women's toilet and a small prayer room for men and women. The municipal additional service building, from which rainwater is planned to be collected, consists of a 7% sloped roof.

Figure 2. *A view of family park (URL-2, 2024)*

7,923 m^2 of this area consists of green areas, and there is a town hall next to the park. Rainwater harvesting will be done from the roof of the municipal annex building. According to the rainwater collection method, the water flowing toward the slope is collected. The gutters and stone masonry structures that follow the leveling curves allow more extended filtration and storage of water. Infrastructure and drainage works are planned to be carried out, and rainwater will be stored underground and used in the toilet reservoir in the square. Rainwater tank volume will be calculated based on the annual rainfall

amount. Storage is planned in a plastic water tank made of polyethylene raw material. It will then be pumped up for toilet cistern use.

The region where rainwater harvesting will take place is in a humid and temperate climate zone, and an area of 24,588 hectares consists of forests. In general, the terrain is mountainous and 155 meters above sea level. Apart from the residential areas and forests, the entire land is agricultural, with an agricultural area of 15,652 hectares. Due to the existence of around 300 establishments along with extensive industries such as construction, manufacturing, and weaving, the district receives immigration and develops (URL-3, 2024).

It is of great importance to determine the rainfall amount correctly when making calculations in rainwater harvesting applications. When receiving data, it is necessary to select the nearest station. According to the data of the Bursa Provincial Directorate of Meteorology, precipitation data for the central district of Bursa according to periodic measurements between 1980 and 2022 were obtained from the institution (Table 1), (URL-4, 2024). According to the data, the average annual rainfall is 707.4 mm. When we look at the climate data in Bursa, The month with the highest average temperature is determined as August, and the month with the lowest is January. The annual average number of rainy days is 112.5 days, December is the month with the most rainfall, and August is the month with the least rainfall. When determining the amount of water to be generated in rainwater harvesting, data such as filter efficiency coefficient, rainfall conditions of the location, and the area to be harvested are required.

Roof coefficient: It is the coefficient that should be used depending on the type of roof material. It explains that not all rainwater falling on the roof can be recycled. The coefficient of 0.90 is accepted for glass and metal roof types.

Filter efficiency coefficient: The efficiency coefficient of the filter that rainwater collected from the roof first passes through to separate it from solid materials. It is specified as 0.9 by German standards (DIN, 1989) (Table 2).

Calculations regarding the rainwater to be collected from the roof are given below (Tema, 2017).

Rain collection area: This is the total area where rainwater can be collected.

Precipitation amount: It is the sum of annual precipitation with data received from the General Directorate of Meteorology (Table 1).

Table 1. *Temperature and precipitation data for Bursa city (1928-2022) (URL-4, 2024)*

Bursa	January	Febraury	March	April	May	June	July	August	September	October	November	December	Yearly
Temperature average (°C)	5,4	6,2	8,3	12,9	17,7	22,0	24,5	24,3	20,3	15,6	11,1	7,4	14,6
Average number of rainy days	14,85	13,41	12,55	11,22	9,02	6,16	3,06	2,92	5,12	8,96	11,04	14,20	112,5
Average monthly rainfall amount (mm)	89,1	75,9	69,9	61,5	50,6	35,4	22,0	18,4	43,7	65,9	75,7	99,3	707,4

4. RESULTS

The middle part of the roof of the building where the work will be done is made of glass, and the other parts are made of metal.

Area of Roof: 29,65 * 45,65 = 1353,52 m^2

Rainwater efficiency = Rain catchment area * rainfall amount * filter efficiency coefficient * roof coefficient

Table 2. *Amount of rainwater to be collected from the roof*

Roof type	Roof area (m^2)	Roof Coefficient	Annual Rainfall Amount	Filter Coefficient	Amount of Rainwater to be Harvested (m^3)
Metal, glass	1353,52	0,9	707,4	0,9	775,558

Rainwater Yield: 775.558,84 L = 775,558 m^3 $year^{-1}$

The rainwater potential collected from the roof throughout the year is 775,558 m^3. Considering the information obtained from the Bursa Provincial Directorate of Meteorology, It was determined that the highest rate of 37% could be collected in winter, 26% in spring and autumn, and 11% in summer (Figure 3).

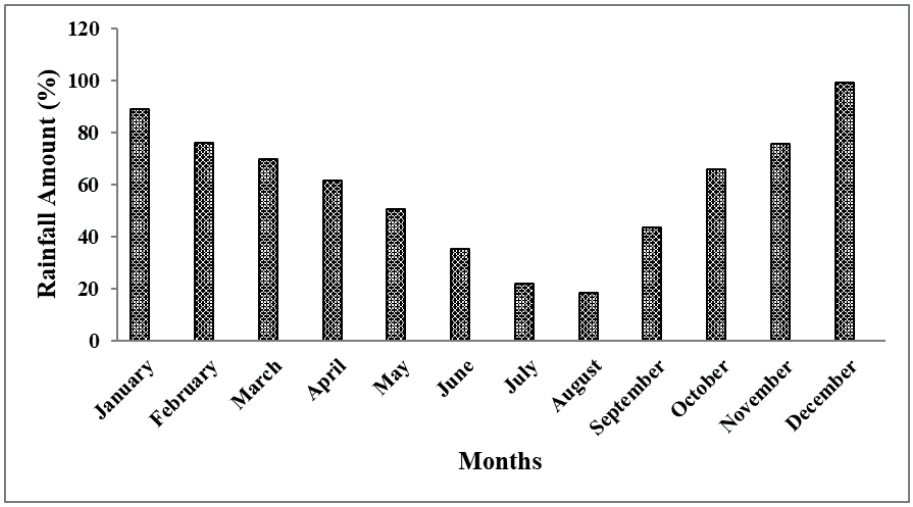

Figure 3. *Amount of rainwater to be collected by month*

4.1. Calculation of the Amount of Water Required for Toilet Cisterns

Toilets consume 8 liters of water for each flush. There are 8 toilets in the park: 3 for women, 3 for men, and 1 for the disabled. According to the information received from the Kestel Municipality Directorate of Technical Affairs for each toilet, it is expected that 30-40 people will use one toilet per day, taking into account the use of the toilets in the square before. An average of 35 people were taken as a reference in the calculation. If approximately 35 people use a toilet a day, for 8 toilets (35 * 8 = 280) 280 people use the toilets a day. Citizens are expected to consume approximately 2240 liters of water per day for toilet tanks.

Daily Water Need: 280 * 8 = 2240 L/day

Monthly Water Need: 30 * 2240 = 67200 L/year = 67,200 m^3/month

Annual Water Need: 365 * 1680=817600 L/year = 817,600 m^3/year

4.2. Calculation of Warehouse Volume

Rainwater falling on the roof surface is collected and stored by transferring it to an above-ground tank or an underground tank with the help of gutters. Warehouse building materials are made of reinforced concrete, fiberglass, or stainless steel. If used as drinking water, filtration, chlorination, and disinfection or boiling are required. Building the warehouse completely underground will be more efficient both in terms of aesthetics and better utilization of the area. Considering reasons such as cost and labor, the more advantageous plastic rainwater tank will be preferred. It is planned to use a plastic water tank produced from polyethylene raw material. The storage

volume of the system was calculated considering the month of December when there is maximum precipitation.

December: 99,3 mm

Storage volume = rainfall amount * roof area * 0.90

99,3 L m^{-2} * 1353,52 * 0.90 = 120 964,08 L = 120,964 m^3 tank volume required.

The price of 1 water tank of 20 tons is 1287,68 $ (URL-5, 2024).

6 warehouses of 20 tons are required.

4.3. Cost of Rainwater Harvesting System Equipment

Since rainwater will be collected in a total area of approximately 1500 m^2 in this study, it is planned to use two filters, one of 1000 m^2 and the other of 500 m^2. One 900-watt submersible pump will be needed to pump the water upwards (Table 3).

Table 3. *Cost of rainwater harvesting system equipment (URL-6, 2024)*

Equipment	Unit	Features	Cost ($)
Vortex rainwater filter (area of 1000 m^2)	Flow 25.6 L/second	Stainless steel/self-cleaning type	501,26
Vortex rainwater filter (area of 500 m^2)	Flow 12.8 L/second	Stainless steel/self-cleaning type	286,43
Submersible pump	Power-900 W	Stainless clean water submersible pump	99,55

4.4. Depreciation Period of Rainwater Harvesting System

The cost of the rainwater collection system consists of the equipment required for the rainwater collection system, rainwater filter, submersible pump, and rainwater tank. The cost of the equipment is given in Table 4. Here, the cost of the rainwater collection system is calculated as 8613,36 $.

Table 4. *Rainwater tank cost (URL-7, 2024)*

Rainwater tank	Cost ($)
20 Ton plastic water tank (6 pieces)	7726,13
Rainwater filter (3 pieces)	787,69
Submersible pump	99,55
Total	**8613,36**

In the study, which has a total annual water consumption of 817,600 m^3 for the toilet reservoir, water consumption can be met from rainwater. The

annual amount of water saved is 775,558 m^3 and the water sales price of Bursa Water and Sewerage Administration (BUSKİ) for official institutions is $1.15, including wastewater fee (URL-8, 2024).

Annual saved amount;

Toilet Cistern; 817,600 m^3* 1,15 $ m^3 = 936,75 $

Depreciation period of the system:

Total system cost / annual cost saved

8613,36 / 936,75 = 9,19 year

5. CONCLUSIONS

Pollution and unconscious use of water resources, misuse of water in the agricultural sector, climate change, increasing population, and increased water consumption due to industrialization make it difficult for countries to access fresh water. With global warming and dry summer seasons in recent years, the need for freshwater increases daily. For this reason, protecting water resources and saving water is very important. With the increasing need for freshwater resources, interest in methods such as rainwater harvesting is increasing daily. Rainwater harvesting practices are an alternative source to mains water. Aiming to develop a strategy that will provide maximum benefit from rainwater, the water harvesting method helps provide the water required for consumption by collecting and accumulating rainwater and runoff water.

In this study, the potential of rainwater collected from the roof of a public building with a surface area of 1353.52 m^2 in the Kestel district of Bursa province to meet the water needs to be used in toilet reservoirs was examined. For this purpose, using the monthly rainfall data of Bursa province, the amount of rainwater to be collected from the roof of the building was calculated as 775,558 m^3 annually. The annual water needed to be used in toilet reservoirs, which is planned to be met with collected rainwater, was found to be 817,600 m^3 year-1. It has been determined that the rainwater collected in practice can be used to meet the water needs of the toilet reservoir.

Additionally, taking the month of December with maximum precipitation as a reference, the tank volume of the system was calculated as 120,964 m^3. According to the volume calculation, 6 warehouses of 20 tons are required. The total cost of the rainwater collection system to be built is calculated as 8613,36 $. The water requirement for the toilet reservoir is obtained from rainwater and 936,75 $ can be saved annually. When the cost of the rainwater collection system applied in the sample project and the annual saved network water cost were compared, the depreciation period of the system was found to be 9.19 years.

Based on all these calculations, it is concluded that the rainwater collection system applied to the sample public building is advantageous. Nowadays, when there is a water shortage and water supply causes great costs, both cheap and practical systems such as rainwater harvesting should be widespread. It is thought that by disseminating these systems, ecological balance will be preserved, sustainable development will be achieved and water resources will be used more efficiently.

REFERENCES

1. Abd-el-Kader, M.M., El-Feky, A.M., Saber, M., AlHarbi, M.M., Alataway, A., Alfaisal, F.M. 2023. Designating appropriate areas for flood mitigation and rainwater harvesting in arid region using a GIS-based multi-criteria decision analysis, Water Resources Management, 37(3), 1083-1108, doi.org/10.1007/s11269-022-03416-6.
2. Alpaslan, N., 1992. Turistik yerleşimlerin su ihtiyacı için sarnıç seçeneğinin irdelenmesi, Datça Çevre Sorunları Sempozyumu Bildiriler Kitabı, Datça, 1992.
3. DIN 1989. Regenwassernutzungsanlagen. Deutsches Institut Normung DIN: 1989, German.
4. DSİ, 2022. Devlet Su İşleri. https://www.dsi.gov.tr/Sayfa/Detay/754. Erişim tarihi.20.11.2022.
5. Eren, B., Aygün A., Likos, S., Damar, A.İ., 2016. Yağmur suyu hasadı: sakarya üniversitesi esentepe kampüs örneği, International Symposium on Innovative Technologies in Engineering and Science (ISITES), 3-5 November, Antalya.
6. Kantaroğlu, Ö. 2011. Yüksek performanslı binalarda su stratejileri, Tesisat Mühendisliği Dergisi, 17(22), 34-38.
7. Kara B, Baykurt G. 2022. Using the scs curve number method for rainwater harvesting: a case study from Yenipazar, Turkey, International Journal of Advances in Engineering and Management, 4(4), 1204-1216, doi: 10.35629/5252-040412041216.
8. Özben, O.M. 2022. havza bazlı yağmur suyu hasadı potansiyelinin belirlenmesi: Denizli Serinhisar İlçesi Örneği, Pamukkale Üniversitesi, Fen Bilimleri Enstitüsü, Yüksek Lisans Tezi.
9. Pamuk Mengü G, Akkuzu E., 2008. Küresel su krizi ve su hasadı teknikleri, Adnan Menderes Üniversitesi Ziraat Fakültesi Dergisi, 5(2): 75-85.
10. Saha, A., Ghosh, M., Chandra Pal, S. 2021. Identifying suitable sites for rainwater harvesting structures using runoff model (scs-cn), remote sensing and GIS techniques in upper kangsabati watershed, West Bengal, India. Editors: Adhikary PP, Shit PK, Santra P, Bhunia GS, Tiwari AK, Chaudhary BS. Geostatistics and Geospatial Technologies for Groundwater Resources in India, 119-150, Cham, Zug, Switzerland, Springer Cham.
11. *Tema, 2017*. TEMA - Geleceğin suyu. http://sutema.org/ resources/Document/FileName/2015-12-01_22-11-14-692%20GeleceginSuyu.pdf [Erişim: 20 Aralık 2017].
12. Alpaslan, N., Tanık, A., Dölgen, D. 2008. Türkiye'de su yönetimi sorunlar ve öneriler, TÜSİAD Yayın No: 2008-09.
13. URL-1, 2016. https://esa.un.org/unpd/wup/.../wup2014-highlights.Pdf Erişim Tarihi: 01.03.2024.
14. URL-2, 2024. https://www.kestel.bel.tr Erişim Tarihi: 01.03.2024.

15. URL-3, 2024. https://tr.wikipedia.org/wiki/Kestel Erişim Tarihi: 03.03.2024.
16. URL-4, 2024. https://www.mgm.gov.tr/veridegerlendirme/il-ve-ilceler-istatistik.aspx?m=BURSA Erişim Tarihi: 03.03.2024.
17. URL-5, 2024. https://www.plastiksudeposu.com.tr/en-ucuz/20-tonluk-plastik-su-deposu-beyaz?utm_source=Google%20Shopping&utm_campaign=Google%20Product&utm_medium=cpc&utm_term=2094&srsltid=AfmBOoo5zcB7N-WHqh6afAiS0iPV_FItmHtbtcSlptSowP0KQgdoO6q0dVk Erişim Tarihi: 05.03.2024.
18. URL-6, 2024. https://www.tankplast.com/yfvr-0200 Erişim Tarihi: 05.03.2024.
19. URL-7, 2024. https://www.hirdavatcesitleri.com/urun/sgs5372-30-metre-temiz-su-cekme-dalgic-pompa-900- watt?gad_source=4&gclid=Cj0KCQiA84CvBhCaARIsAMkAvkJCnoqQ4OzMCG0HaO70fzmPbj6y34d-t8rPgmn6Z3YiSF_LISp0-NUaAkBREALw_wcB Erişim Tarihi: 08.03.2024.
20. URL-8, 2024. http://www.buski.gov.tr/tr/abonerehberi/kategori_17 Erişim Tarihi: 08.03.2024.

CHAPTER 10

METADATA MANAGEMENT BENEFITS IN THE TURKISH BANKING SECTOR

Cemal GÜMÜŞ[1]
İsmail CANSIZ[2]

1 Assistant Professor Scsoft Bilişim Teknolojiler, Business Development and Project Management, Haliç and Altınbaş University, Part-time Lecturer. cemal.gumus@scsoft.com.tr, Orcid No: 0009-0004-3629-1388
2 İsmail Cansız, Scsoft Bilişim Teknolojileri, Enterprise Architecht, ismail.cansiz@scsoft.com.tr

1. INTRODUCTION

This study aimed to examine the definition of metadata and the benefits of metadata management in the financial sector. Metadata is created to represent relevant data in detail and clearly, and different research areas such as sample data definitions and options are used for various applications. An unambiqous explanation of metadata is vital for further use. It is possible to see different evaluations regarding the definition. The main purpose of metadata is to provide quick access to the needed information, easy finding and discovery of resources.

While keywords within descriptions are referred to as "meta tags," metadata serves a broader purpose. It functions as a system for organizing digital information, ensuring its long-term storage and accessibility.

Utilizing metadata empowers users to locate resources by pinpointing relevant criteria and offering spatial information. In the realm of digital marketing, metadata facilitates the organization and presentation of content, thereby maximizing the effectiveness of marketing activities. This leads to increased brand visibility and improved "findability" of content. Diverse metadata standards are employed across various disciplines. For example, a web page's metadata might encompass details about the programming language, creation tools, and other structural aspects.

1.1 Definition and Purpose:

Within the domain of computer science, the term "metadata" has been identified as exhibiting a high degree of ambiguity, susceptible to reinterpretations based on the specific context (Guerra E, 2013). However, a prevailing understanding has emerged, defining metadata as a formal representation of data that serves to delineate and describe information in a standardized and stable manner (Löpprich Martin, 2014).

1.1.1 Various Definitions of Metadata:

Small atomic units (table fields, attributes of form questions, records) that define and constrain a specific object (Kim HH, 2019). It describes the data type, range, or set of possible values (N., 2016). Single units can be combined into complex elements (Corradi L, 2012). Metadata can be based on terminologies, controlled vocabularies and taxonomies (Daniel C, 2014) Centralized storage for metadata is possible through both data dictionaries and metadata repositories (Cunningham SG, 2016), empowering machines with comprehensive, actionable metadata for independent data handling. (Lyttleton O, 2011). Information that explains different side of a data asset, rising its usability throughout its life cycle (Gartner, 2024). While the common definition of metadata as "data about data" seems simple, it encompasses a vast array of information. It delves into technical and business processes, data rules and limitations, and both logical

and physical data architectures. Beyond describing the data itself, metadata extends to the concepts it represents (e.g., business processes, applications, code, infrastructure) and their relationships. This comprehensive understanding of data, systems, and workflows empowers organizations to evaluate data quality and manage databases and applications effectively. From processing and maintenance to integration, security, auditing, and governance, metadata plays a vital role, as highlighted by the Dmbok (Deborah Henderson, 2017). Various types of data–location, date, or card catalog item (Microsoft, 2023). Machine recognizable information about web resources or other things (Berners-Lee, 2009). Defining a data model for the meta model is a critical initial step after solidifying the metadata strategy and understanding business needs. This foundational structure allows for the creation of various meta model types, each serving a specific purpose. High-level conceptual models focus on illustrating system connections, while lower-level attributional models delve deeper into the characteristics of elements and processes within a specific model. Beyond its role in organizing information architecture, the meta model itself becomes a valuable asset – a centralized repository for metadata. It functions as both a planning tool and a communication channel for capturing requirements, while simultaneously housing information about the data, the building blocks, their properties, and the relationships between them.

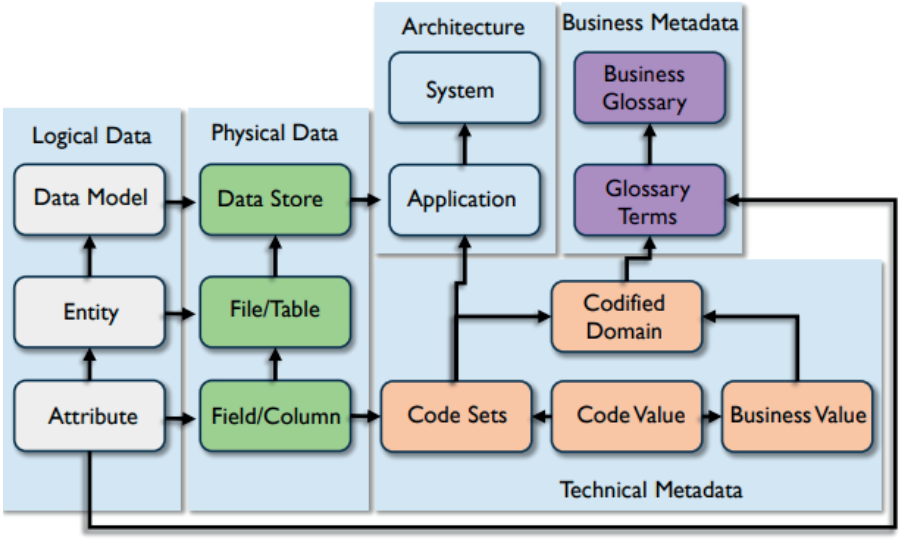

Figure 1: *Sample Metadata repository meta model. The boxes represent the high-level major entities, which contain the data.*

Source 1: *DMBOK Second Edition, p.441*

1.1.2 Purpose

Huang's research sheds light on the multifaceted nature of metadata, highlighting its critical role in various data management tasks. One key area is information retrieval, where metadata, particularly semantic annotations, acts as a fuel for machine-powered searches. By providing a richer layer of descriptive information, these annotations enable more precise matching of queries, ultimately delivering more relevant and on-demand results. In data integration and core dataset definition, metadata plays a foundational role. It acts as a bridge, establishing a common language by defining and aligning the underlying structure of the data. This alignment is essential for enabling secondary use of the data, such as in clinical research where datasets from various sources need to be seamlessly combined. Beyond these core functionalities, metadata has been employed for purposes like automating data quality control processes and even building ontologies – structured representations of knowledge within a specific domain (Huang G, 2017).

Effective metadata management applications transform raw data into a comprehensive and understandable resource. This rich context empowers banks to improve data quality and relevance, ultimately unlocking its full business value. As data volume and distribution increase, metadata becomes even more crucial. It facilitates several key processes: data exploration, understanding data relationships, tracking data usage, and evaluating value and risks associated with data use. These functionalities establish metadata management as central to effective data governance, supporting strategic goals and driving digital transformation within banks.

Far from being static repositories, metadata management solutions reach new heights when empowered by artificial intelligence and machine learning. These "active" solutions can be enhanced with human expertise and seamlessly integrated with data analysis tools and other applications. This powerful combination unlocks the potential to extract even deeper insights from the data. Consequently, the entire data management ecosystem – processes, applications, and systems – becomes more intelligent and adaptable.

2. LITERATURE REVIEW

The concept of metadata, essentially data about data, traces its roots back centuries. While the librarians of the ancient Great Library of Alexandria wouldn't have called them such, the small labels attached to scrolls functioned as some of the earliest examples of metadata, providing context and facilitating information retrieval. Fast forward to libraries of a few decades ago, and we see another iteration of this concept – the card catalog, another form of metadata used to organize and access information. The formalization of metadata for computer systems came much later, with Stuart McIntosh and David Griffel of MIT pioneering the idea of a digital "metalanguage" in 1967.

This vision laid the groundwork for the sophisticated metadata management systems used today (David Griffel, 1967).

The 1980s witnessed a surge in formalizing metadata practices. In 1979, the International Press Telecommunications Council (IPTC) took a pioneering step by outlining metadata bases and attributes specifically designed for images. This groundwork paved the way for their later development of the Information Interchange Model (IIM) in the early 1990s. This file architecture, with its embedded metadata properties, could be applied to various media formats, including images, text, and more. The IIM significantly streamlined the exchange of news content between national and international news outlets. While diverse metadata systems and standards emerged, efforts were also underway to categorize these systems. A landmark contribution came in 1994 with the paper "Metadata: A User's View" by Francis P. Bretherton and Paul T. Singley. They proposed two distinct forms of metadata:

- **Guide Metadata:** This type assists researchers in locating specific elements within data, typically using keywords (meta tags) based on natural language.

- **Structural/Control Metadata**: This category focuses on the internal structure and management of data, exemplified by tagging database objects like tables, columns, keys, and indexes.

These advancements laid the foundation for the robust metadata management systems we rely on today. (Bretherton, 1994).

The early 2000s witnessed significant developments in metadata management. In 2001, Adobe introduced the Extensible Metadata Platform (XMP). While similar in purpose to the earlier IPTC standard, XMP leveraged two key technologies: Extensible Markup Language (XML) and Resource Description Framework (RDF). XML provided a structured format for encoding instructions that display text, while RDF offered a versatile digital language for representing information. This combination in XMP enabled applications to capture metadata during content creation and embed it directly within the file itself, as well as within content management systems. This streamlined approach made it easier to record and manage essential information like titles, authors, keywords, and copyright details in a user-friendly format. Following closely in 2002, Ralph Kimball, in his book "The Data Warehouse Toolkit," offered a comprehensive definition of metadata: "all information that describes and characterizes the structures, operations, and contents of the DW/BI system." This definition emphasized the critical role of metadata in understanding and managing data warehouse and business intelligence systems (Ralph Kimball, 2013). In 2003, to take the development of metadata to the next level, Priscilla Caplan divided Metadata schemes into different categories to reflect key aspects of functionality (Priscilla Caplan, 2005).

Metadata and Marketing: The year 2007 marked a turning point for metadata in the realm of marketing. Prior to this, Google's search engine relied heavily on a pre-determined list of links, some paid and some organic. With the expansion of its platform to include a wider range of content formats like news, images, and videos, Google introduced a new focus on metadata. This shift emphasized the importance of metadata for website owners, as it became a crucial factor in search engine optimization (SEO) and ensuring content discoverability. Essentially, websites needed to adopt new metadata practices to make their information readily searchable and relevant within the evolving Google search landscape (Kandregula, 2020). Modern marketing thrives on metadata, a powerful tool that guides users to websites. Effective metadata enhances web content searchability, leading to increased website traffic. Marketers can optimize metadata online, maximizing content reach. Accurate and organized metadata is crucial for building a discoverable website. Furthermore, metadata significantly impacts SEO – it's a factor in Google's search process and is displayed on Search Engine Results Pages (SERPs). Optimizing metadata with relevant keywords and conversion-focused language can significantly increase website traffic.

The European Union's General Data Protection Regulation (GDPR), enforced in May 2018, ushered in a new era of data privacy. This regulation mandates that any EU customer data that could potentially identify individuals must be anonymized or entirely deleted. While the data itself might be retained for Big Data research, it can no longer be used to track specific users. To comply with GDPR, businesses need to develop a far deeper understanding of their data holdings than ever before (Informatica, 2024).

Metadata Management Study: Effective metadata management requires a comprehensive approach that encompasses the entire spectrum of data within an organization. This breadth is two-fold. Firstly, it involves the ability to gather metadata from a wide range of sources, both on-premises and in the cloud. Secondly, it necessitates managing four distinct metadata categories:

- **Technical Metadata**: This category focuses on the technical underpinnings of data, including database structures, data transformation processes, quality control checks, and any relevant mappings and codes.

- **Business Metadata**: This type of metadata delves into the business context of the data. It includes glossary terms, management processes, and metadata that provides context for applications and business use cases.

- **Operational and Architectural Metadata**: This category encompasses information related to how data is used and managed within systems. It includes runtime statistics, timestamps, volume metrics, log information, and details about system location.

- **Usage Metadata**: This final category captures how users interact with data. It can include user ratings, reviews, and access patterns.

Building a robust common metadata foundation relies on four above categories. Smart metadata management applications leverage various functionalities to empower this foundation:

- **Collection**: These applications can scan and gather metadata from diverse sources across an organization, encompassing both cloud-based and on-premises systems like data lakes, data warehouses, databases, file systems, and data integration tools. This comprehensive collection ensures high data availability for data analysis and data science initiatives.

- **Curation**: Beyond simply collecting metadata, these tools empower the creation of a rich business context. This is achieved by documenting the data's business meaning through the inclusion of glossary terms, key concepts, relationships, and associated processes. Additionally, they facilitate the collection of user input through ratings, reviews, and certifications, aiding in the evaluation of data asset usefulness for other users.

- **Inference**: Smart applications go a step further by applying intelligence to uncover hidden connections within the collected metadata. This includes inferring data source lineage, identifying data similarities, and ranking datasets based on their potential value for various user types and purposes.

3. BENEFITS OF METADATA MANAGEMENT IN THE BANKING SECTOR

The purpose of metadata management is to effectively manage, organize and make sense of data assets in the financial sector. It facilitates and accelerates access to data by disclosing, classifying and tracking data assets with metadata. It provides access to accurate and reliable data by improving data quality, thus strengthening decision-making processes. Additionally, it can improve data management processes in the financial sector, meet compliance requirements and minimize data-driven risks. It supports organizations in making data-based strategic decisions through the effective use of data assets. It paves the way for institutions to realize the artificial intelligence transformation of their business processes and contributes to the process.

Metadata Management is to ensure that metadata is managed accurately and efficiently in order to effectively manage and use the data assets of an organization or institution in the financial sector. With metadata management implemented in a bank, it facilitates access to data, improves data quality and strengthens data management processes by identifying, classifying, cataloging and monitoring data assets.

3.1 Issues Overcome in the Application of Metadata Management in the Banking Sector

Data Complexity and Management Challenges: Organizations can often encounter complexity when managing data assets from different sources. Data in different formats, with different terminologies, and in different systems can be difficult to bring together and manage effectively.

Challenges in Data Access: Fast and efficient access to data can be difficult due to missing or disorganized metadata. It can make it difficult for users to access the data they want and slow down their decision-making processes. These difficulties can be overcome with metadata management.

Data Quality Issues: Inaccurate, incomplete, or outdated metadata can degrade data quality. Poor data quality can also affect decision-making processes and reduce reliability.

Compliance and Security Concerns: Challenges in complying with compliance requirements and ensuring data security can impact data management processes and put organizations at risk. One of the main purposes of metadata management is to manage data assets more effectively, facilitate access to data, improve data quality and meet compliance requirements by addressing the above-mentioned problems. In this way, organizations understand their data better, access it faster and use it more reliably.

Solutions implemented to make metadata management beneficial in the financial sector can be listed below.

Metadata cataloging and standardization: Cataloging data assets and standardizing metadata. In standard metadata, it makes it easier to identify, classify and associate data entities.

Automation-supported metadata management: Automatically updating and managing metadata using automation tools. Automatic updating ensures continuous monitoring of data assets and refresh of information.

Data-aware dynamic cataloging interfaces: Users can discover data according to their needs through dynamic cataloging interfaces that enable users to access data more easily and effectively.

Data quality management processes: Helps prevent inaccurate or incomplete metadata and improve data quality by using special processes and tools to improve the data quality of metadata.

Data security and compliance controls: Specific tools and processes are used for data security and compliance controls. In this way, it controls access to data and meets compliance requirements.

User participation and feedback integration: Platforms and feedback mechanisms that encourage users to contribute to metadata ensure that users contribute to data and the correct metadata is created.

Automation and AI-supported metadata management: Ensures continuous monitoring and updating of data assets along with automatic updating and management of metadata using machine learning and automation tools. With these methods, data management processes can be improved.

3.2 Other Benefits Provided By Metadata Management In The Banking Sector:

The use of metadata management provides institutions with safe and fast access to data. Gains achieved through its application in the financial sector:

Better management and usability of data assets: With metadata cataloging and standardization solutions, data assets are better identified, classified and linked. This provides a better understanding of data assets, making them easier to manage and use.

Fast and easy access to data: Access to data is accelerated with dynamic cataloging interfaces and user-friendly platforms. Users can access the data they want more easily and quickly, which speeds up data discovery and analysis processes.

Data security and compliance: With data security tools and compliance controls, data security is ensured and compliance requirements are met. This reduces the organization's risks and increases sensitivity to compliance.

Data analytic and business intelligence improvements: Accurate and up-to-date metadata ensures that data analytic and business intelligence solutions are based on more solid foundations. This enables deeper and more reliable analysis.

Reduction in data storage and management costs: More organized and accurate management of data assets helps reduce unnecessary data storage costs and control data management costs.

Adapting to changing business needs: Flexible metadata management allows the business to quickly adapt to changing needs. Integration of new data sources or business processes becomes faster and easier.

Development of data-driven culture: Successful implementation of projects can contribute to the development of a data-driven culture. Data-driven decision-making processes become more important across the business.

Increasing data quality and accuracy: Correction of missing or inaccurate metadata is ensured through data quality management processes. This improves data quality and strengthens data-based decision-making.

Increasing user participation and data sharing: User participation increases with platforms that enable users to contribute metadata. At the same time, data sharing becomes easier and data sharing between different departments or users is encouraged.

4. STATE OF ART

Metadata management is an important element for all sectors, especially banks, that work data-oriented. Currently, various techniques and technologies are used in the field of metadata management in Türkiye, at national and international levels, and new technologies have been developed.

Many institutions and organizations use automation tools to support metadata management. Automation simplifies the processes of collecting, classifying and updating metadata. These systems monitor data assets, detect changes and automatically update them as required. Automation enables data processes to be managed more effectively and access to data is accelerated. Additionally, machine learning and Artificial Intelligence (AI) technologies contribute greatly to metadata management.

4.1 Methods Used in Metadata Application Development

Metadata automation has been increasingly used in the banking sector, like many other sectors, in recent years. Technology companies show interest in metadata application development within the scope of R&D activities. The methods used by a technology company to implement metadata management in a bank in Turkey are examined as follows.

- Using the ISO-11179 standard in the metadata registry.
- Data profiling, data recognition templates statistical methods in Classifying and Labeling data assets.
- JSON schema validation method in the development of Schema Independent infrastructure.
- REST (Application Program Interfaces) API, request and response messages in JSON format and HTTP response codes in the development of APIs.
- In retrieving metadata from Databases, connecting to the relevant databases with the ADO.NET connection object.
- In dynamic form creation, a JSON form object containing the form structure will be created through type definitions. Creating forms using this object.
- Use of Graph diagram and Tree structure in visualizing metadata.

- Data connector will be used to access databases. 8. Ensuring periodic data collection with scheduled jobs in detecting and updating metadata data.
- Manual Data Dictionary creation and Automatic creation of Data Dictionaries from the Database.
- Use of open source libraries to create diagrams in creating ER Diagrams. Use of UML, Crow's Foot, Barker, Chen IDEF1X notations in diagrams.

4.2 Metadata Architecture in the Bank

PostgreSQL was used as metadata DB which includes many capabilities for maintaining schema-independent data. In this application, the jsonb feature of the database is used. The trigram index structure was used to index variable data. Dynamic Type System infrastructure has been designed for schema-independent structure. With this structure, it is aimed to dynamically meet different metadata needs that may arise later. Connectors have been developed for commonly used databases so that metadata can be collected from different data sources and recorded in the repository.

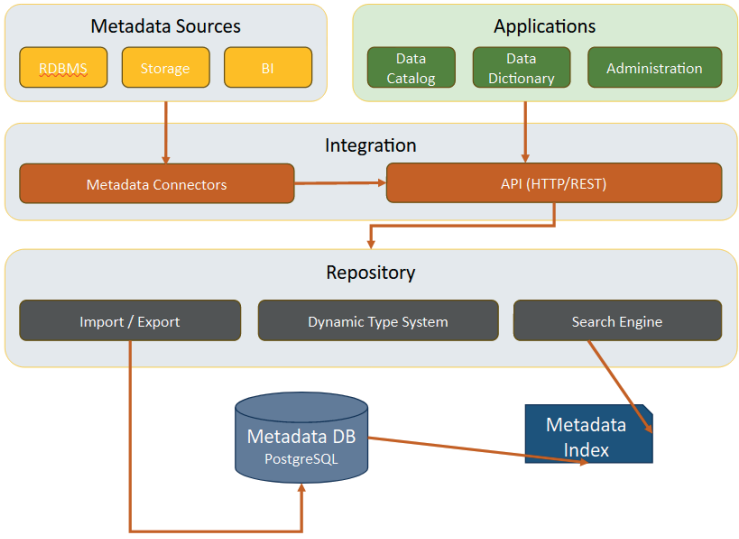

Figure 2: *Metadata Architecture Implemented in a Bank*

There are four types under the Type Definition Service in a schema-independent structure.

- Enum: It is used for lists containing finite values. It serves the same purpose as enum (enumeration) in programming languages. An example enum is defined as follows:

- Entity: It is used to define the metadata that is desired to be kept in the system. It corresponds to the class definition in programming languages. An example entity is defined as follows:
- Relationship: It is used to define the relationships between entities.
- Classification: It is used to classify entities.

An example of Enum is defined as follows:

```
 {
"MetaTypeName": "enum",
 "TypeDefName": "GENDER_ENUM",
 "Description": "Person genders",
 "DefaultValue": "Male",
 "ElementDefs": [
  {
   "Value": "Male"
  },
  {
   "Value": "Female"
  }
 ]
}
```

- An example entity is defined as follows:

```
{
 "MetaTypeName": "entity",
 "TypeDefName": "Person",
 "Description": "Person entity definition",
 "AttributeDefs": [
  {
   "Name": "FirstName",
   "TypeName": "string",
   "IsOptional": false
  },
```

```
    {
      "Name": "LastName",
      "TypeName": "string",
      "IsOptional": false
    },
    {
      "Name": "Gender",
      "TypeName": "GENDER_ENUM",
      "IsOptional": true
    },
    {
      "Name": "BirthDate",
      "TypeName": "date",
      "IsOptional": true
    }
  ]
}
```


Instance Service: Provides management of instance records for entity, enum, classification and relationship types defined in the system.

Search Service: It is the service used to query metadata.

Admin UI: It is the application that contains the application's management screens. New type definitions (enum, entity, etc.) definitions, authorization, etc. Contains functions.

Applications: Contains application modules such as Data Catalog and Data Dictionary.

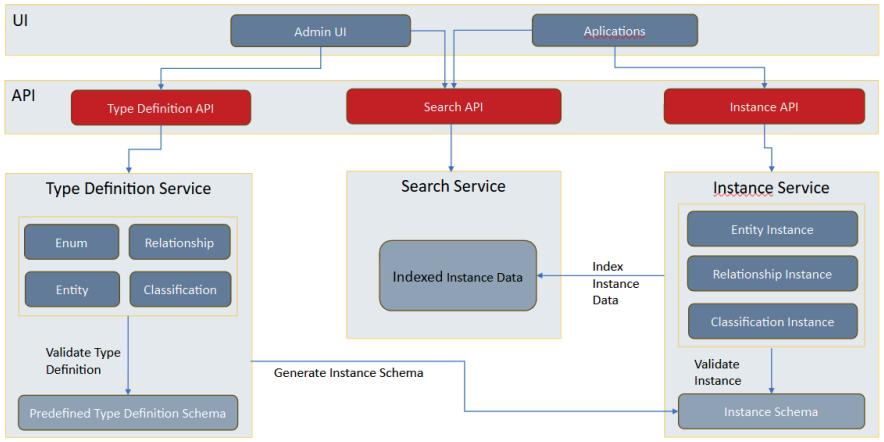

Figure 3: *Metadata Application Technical Design in a Bank*

Figure 4 shows the process from creation to deletion or exclusion of metadata. Lifecycle steps are managed in metadata management.

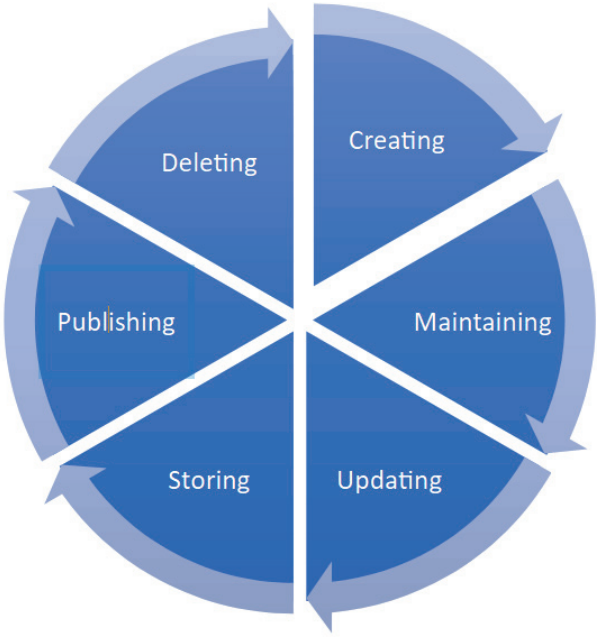

Figure 4: *Metadata Lifecycle*

5. CONCLUSION

More effective use of existinginfo through metadata management in the banking sector in Türkiye contributes to the correct and strategic decision-making processes of corporate managers by easily accessing accurate and meaningful data. For data analysts and data scientists working in the financial sector, access to data is accelerated, data quality increases, and it is vital for them to reach more accurate results thanks to the accuracy of metadata.

Access to accurate and reliable data ensures that your analyzes are built on stronger and more solid foundations. Decision makers and senior management in the banking sector have access to accurate and meaningful data, which directly affects their strategic decision-making processes. Together with properly managed metadata, it can provide reliable data to senior decision makers, allowing them to make more accurate strategic decisions. Operational business units and employees who carry out daily business are among the ultimate beneficiaries of easy access and use of data. Accurate metadata makes cross-unit data sharing easier. Customer Services and Marketers have an important place in the financial sector. Access to customer data significantly impacts customer relationships and marketing strategies. With metadata management, units provide faster access to more accurate and meaningful data. Business units that do business intelligence and analytical reporting can present accurate data to business intelligence applications and provide more meaningful, accurate data to users who do analytical reporting.

Effective metadata management unlocks significant advantages for banks. Data scientists benefit from a streamlined process, allowing them to dedicate more time to analyzing data and extracting valuable insights that drive business growth. Data teams experience faster project delivery cycles thanks to the efficiency and repeatability fostered by robust metadata practices. Additionally, these practices can lead to cost reductions by minimizing data redundancy, ultimately lowering storage expenses.

REFERENCES

Admins a Progress Report, Center for International Studies, Massachutes Institute of Technology, David Grafel and Stuart McIntosh, 1967

Ashish N, Dewan P, Toga AW. The GAAIN Entity Mapper: An Active-Learning System for Medical Data Mapping. Front Neuroinform. 2015;9:30. doi: 10.3389/fninf.2015.00030. doi: 10.3389/fninf.2015.00030.

Bretherton, F.P. and Singley, P.T.. (1994). Metadata: A user's view. Proceedings of the 7th International Conference on Scientific and Statistical Data Management. 166 - 174. 10.1109/SSDM.1994.336950.

Corradi L, Porro I, Schenone A, Momeni P, Ferrari R, Nobili F, Ferrara M, Arnulfo G, Fato MM. A repository based on a dynamically extensible data model supporting multidisciplinary research in neuroscience. BMC Med Inform Decis Mak. 2012 Oct 08;12:115. doi: 10.1186/1472-6947-12-115. https://bmcmedinformdecismak.biomedcentral.com/articles/10.1186/1472-6947-12-115

Cunningham SG, Carinci F, Brillante M, Leese GP, McAlpine RR, Azzopardi J, Beck P, Bratina N, Bocquet V, Doggen K, Jarosz-Chobot PK, Jecht M, Lindblad U, Moulton T, Metelko. Nagy A, Olympios G, Pruna S, Skeie S, Storms F, Di Iorio CT, Massi Benedetti M. Core Standards of the EUBIROD Project. Defining a European Diabetes Data Dictionary for Clinical Audit and Healthcare Delivery. Methods Inf Med. 2016;55(2):166–76. doi: 10.3414/ME15-01-0016.15-01-0016

Daniel C, Sinaci A, Ouagne D, Sadou E, Declerck G, Kalra D. Standard-based EHR-enabled applications for clinical research and patient safety: CDISC-IHE QRPH-EHR4CR & SALUS collaboration. AMIA Joint Summits on Translational Science; April 7-11; San Francisco. 2014. p. 19.

DATA MANAGEMENT BODY OF KNOWLEDGE Second Edition, Technics Publications, New Jersey. 2017 DAMA International.

Gartner, https://www.gartner.com/en/information-technology/glossary/metadata Retrieved: Feb 2024

Griffel D, McIntosh S. Center for International Studies. Admins-A Progress Report. Massachusetts Institute of Technology, Jan, 1967.

Guerra E, Fernandes C. A Qualitative and Quantitative Analysis on Metadata-Based Frameworks

Usage. 13th International Conference in Computational Science and Its Applications – ICCSA 2013; June 24-27; Ho Chi Minh City, Vietnam. 2013.

Huang G, Yuan M, Li C, Sun Q. Research on ontology generation and evaluation method in oil field based on the MDR. JCM. 2017 Nov 24;17(4):665–676. doi: 10.3233/jcm-170751.

Informatica. https://www.informatica.com/resources/articles/what-is-metadata-management.html Retrieved: Feb 2024).

Kim HH, Park YR, Lee KH, Song YS, Kim JH. Clinical Metadata ontology: a simple classification scheme for data elements of clinical data based on semantics. BMC Med Inform Decis Mak. 2019 Aug 20;19(1):166. doi: 10.1186/s12911-019-0877-x.

Löpprich Martin, Jones J, Meinecke M, Goldschmidt H, Knaup P. A reference data model of a

metadata registry preserving semantics and representations of data elements. Stud Health Technol Inform. 2014;205:368–72.

Lyttleton O, Wright Alexander, Treanor Darren, Lewis P. Using XML to encode TMA DES metadata. J Pathol Inform. 2011;2:40. doi: 10.4103/2153-3539.84233. http://www.jpathinformatics.org/article.asp?issn=2153-3539;year=2011;volume=2;issue=1;spage=40;epage=40;aulast=Lyttleton

Microsoft, Introduction to managed metadata, Article published on Sep, 2023 https://learn.microsoft.com/en-us/sharepoint/managed-metadata?redirectSourcePath=%252fen-us%252farticle%252fIntroduction-to-managed-metadata-a180fa28-6405-4679-9ec3-81d2028c4efc Retrieved: Feb 2024

Tim Berners-Lee, https://www.w3.org/DesignIssues/Metadata.html Published Jan 1997 Retrieved: Feb 2024

Priscilla Caplan and Rebecca Guenther, Practical Preservation: The PREMIS Experience, Library Trends, Vol. 54, No. 1, Summer 2005

Ralph Kimball and Margy Ross The Data Warehouse Toolkit: The Definitive Guide to Dimensional Modeling 3rd Edition, Willey 2013.

Sowmya Kandregula, An Introduction to Metadata Management on December 16, 2020. Retrieved: Feb2024 https://www.dataversity.net/an-introduction-to-metadata-management/

CHAPTER 11

ON THE ALL-SATELLITE AND SINGLE-SATELLITE TECHNIQUES FOR GNSS CLOCK PRODUCTS COMPARISON

Sermet ÖĞÜTÇÜ[1]
Behlül Numan ÖZDEMİR[2]
Ülkünur KORAY[3]

1 Necmettin Erbakan University, Geomatics Engineering, Turkey
2 Konya Technique University, Geomatics Engineering, Turkey
3 Necmettin Erbakan University, Geomatics Engineering, Turkey

1. Introduction

Most of the geodetic applications require precise satellite orbit and clock products (Karadeniz et al., 2022; Konukseven et al., 2022; Erdem and Demirel, 2021). Precise satellite orbit includes the three-dimensional Earth Centered Earth Fixed (ECEF) coordinates of the satellite. Precise clock product includes the clock biases of the satellites with respect to the Analysis Center (AC) specific reference time (Yao et al., 2017). 12 ACs are responsible to produce orbit and clock products for GNSS. Not all ACs produce each GNSS (GPS, GLONASS, Galileo, BeiDou) orbit/clock products. Among them, GeoForschungsZentrum (GFZ), Wuhan University (WHU) and CODE produce the orbit/clock products for each GNSS constellation. For more detailed information, the reader is referred to Analysis Center Coordinator (ACC) official web site (https://igs.org/acc/).

Due to the different methods for orbit integration and clock estimates among the ACs, small to large differences can be observed between the ACs orbit/clock products (Hou et al., 2022; Li et al., 2019; Steigenberger and Montenbruck, 2020). In addition to the applied methods, time constraint differences are also playing an important factor for the quality difference between the products. Final, rapid, ultra-rapid, and real-time products (Bahadur and Nohutcu, 2020; Ogutcu, 2020) are generally produced based on the time constraint of ACs. Some studies also focus on the clock and orbit differences between the final, rapid, ultra-rapid, and real-time products (Li et al., 2015; Li et al., 2022; Byram and Hackman, 2015; Zhao et al., 2023).

To robustly investigate the target products' quality with respect to the reference products, the orbit (radial, along-track, cross-track) and clock differences should be computed correctly. Contrary to the resolved radial, along-track, and cross-track orbit differences, the clock differences cannot be computed directly between the products due to the systematic bias known as ACs-specific clock datum differences (Guo et al., 2023). Timescale differences

between the ACs or the products, such as IGS Rapid Time (IGRT) and IGS Final Time (IGST), from the same AC are mainly caused by the different reference clocks used by the ACs or products. Most of the clock files include the reference clock information in the header section. These reference clocks are the IGS sites equipped with high precision external receiver clocks with different classification, such as hydrogen maser, rubidium, and cesium (Mikoś et al., 2023). Besides the reference clock difference, the ACs-specific clock datum still might be different due to the processing strategies, such as the combination of GNSS system, cutoff angle and the other processing strategies that can affect the clock estimate. Therefore, even if the same reference clocks are used among the ACs, different datum definition of the clock estimates may still exist.

If this systematic bias is ignored in the clock comparison, several meters to tens of meters spurious differences can be observed between the ACs. The reference clock of the ACs can be changed within adjacent days, as a result, it also affects the day-boundary discontinuities (DBDs) (Rovira-Garcia et al., 2021). The clock difference between the ACs is also important for the clock corrected radial component due to the strong correlation between the radial component and clock estimate.

To remove the time-scale difference between the ACs, single-satellite method, one of the first adapted method, is widely used by most literature (Zhang et al., 2011; Shi et al., 2015; Guo et al., 2016; Montenbruck et al., 2015; Zhao et al., 2021). In this method, a reference satellite should be chosen in the corresponding GNSS constellation. However, selecting a reference satellite is generally a non-trivial task, but due to the no specific convenient method, selecting a reference satellite is generally applied arbitrarily. The other method, known as all-satellite method, proposed by Yao et al, 2017 (Yao et al., 2017). In this method, all available satellites in the same epoch are chosen to participate the contribution. Therefore, the prerequisite for choosing a reference satellite is eliminated. The details of these methods are given in the Method section.

Yao et al, 2017 show that the proposed all-satellite method reduced the drawbacks of the single-satellite method using GPS clock data, especially considering the selection of the best satellite as a reference and inconsistent results between the different reference satellite selections. Yao et al, 2017 also emphasize that a reference satellite that has the highest clock offset precision should be chosen for the single-satellite method for the best realistic result. However, which criteria should be considered for the precision of clock offset data for the single-satellite method was not given. Except for GPS clock data, GLONASS, Galileo, and BeiDou clock data were also not investigated in terms of the clock difference using the single-satellite and all-satellite methods.

In this study, one week of clock data in 2021 (DOY:024-030) from GFZ and WHU ACs are investigated in terms of the clock comparison using the single-satellite and all-satellite methods. The effect of clock fitting precision, overlapped hadamard deviation and frequency accuracy on the reference satellite selection in the single-satellite method are also investigated.

2. Method

GNSS_PRODUCTS_DIFF software developed by the authors was used within the scope of this study. The main functionality of this software is computing the orbit (radial/along-track/cross-track) and clock differences between the products. The software is capable to read GPS, GLONASS, Galileo, and BeiDou (BDS-2 and BDS-3) orbit and clock data from precise ephemeris and clock files. For clock comparison, single-satellite and multiple-satellite methods were integrated in the software.

The computation of the single-satellite method can be explicitly expressed as follows:

$$\Delta_{product\_1}^{satellites} = dt_{product\_1}^{ref\_satellite} - dt_{product\_1}^{satellites} \quad (1)$$

$$\Delta_{product\_2}^{satellites} = dt_{product\_2}^{ref\_satellite} - dt_{product\_2}^{satellites} \quad (2)$$

$$\nabla\Delta^{satellites}_{product,1,2} = \Delta^{satellites}_{product\_1} - \Delta^{satellites}_{product\_2} \quad (3)$$

where Δ and $\nabla\Delta$ denote the single-difference (SD) and double-difference (DD) operators for each epoch. $dt^{ref\_satellite}_{product\_1}$ and $dt^{ref\_satellite}_{product\_2}$ denote the clock bias value of the chosen reference satellite (for example G01) in each product i.e., GFZ and WHU. $dt^{satellites}_{product\_1}$ and $dt^{satellites}_{product\_2}$ denote the clock bias values of all available satellites except for the reference satellite. After the DD operator, ACs-specific time-scale bias is removed, but other biases (which are constant in a continuous arc for all satellites) from the processing strategy differences between the ACs and the noises of the clock solutions remain. Therefore, for the clock comparison, standard deviations of the DD clock biases are reflecting the real compliance between the products. Since the RMS of DD clock biases includes the unavoidable biases between the products, the RMS is not used as an indicator (Wang et al., 2018). Moreover, the remaining biases are usually lumped to the receiver clock estimate in Precise Point Positioning (PPP) (Alçay and Atiz, 2021; Uçarli et al., 2021). Therefore, the higher the standard deviation values between the clock products, the more difference in the estimated coordinates in PPP.

In the all-satellite method, instead of choosing one reference satellite, all satellites in the corresponding epochs are selected as a reference. The computation of the all-satellite method can be explicitly expressed as follows:

$$\delta_{product\_1,2} = \left[\sum_{j=1}^{s}\left(dt^{satellites}_{product_1}\right) - \sum_{j=1}^{s}\left(dt^{satellites}_{product_2}\right)\right]/s \quad (4)$$

$$\delta^{satellite}_{dt} = dt^{satellites}_{product_1} - dt^{satellites}_{product_2} - \delta_{product\_1,2} \quad (5)$$

where s is the number of satellites, $\delta_{product\_1,2}$ is the datum difference between the two products, and the standard deviation of $\delta^{satellite}_{dt}$ reflects the real compliance between the products. As seen from the all-satellite method, the prerequisite for choosing a reference satellite is eliminated. Moreover, the effect of choosing the reference satellite on the computed differences in the

single-satellite method are also removed. For a more detailed description of the methods, the reader is referred to Yao et al, 2017 (Yao et al., 2017).

Yao et al, 2017 expressed that a reference satellite that has the highest clock offset precision should be chosen to avoid unrealistic difference between the products. However, there is no convenient and practical way for choosing the reference satellite in according with the precision criteria. Additionally, which precision criteria should be considered has not been explored in detail in the existing literature.

In the results section, the results of the standard deviation of clock differences are given concerning each available reference satellite in the single-satellite method. When choosing the reference satellite, three criteria related to the clock biases – namely, fitting residuals, overlapped hadamard deviation and frequency accuracy – are investigated. In addition to that, the differences from the all-satellite method are also given for each GNSS in the results section.

3. Results

As shown in Equation 1-2-3, the standard deviation results of the differences between the clock products are based on the choice of the reference satellite in the single-satellite method. To investigate how the results are changing with respect to the different reference satellite, each available satellite for each GNSS is used as the reference satellite in the single-satellite method. Figure 1 shows the average standard deviation of the epoch-wise clock differences between GFZ and WHU associated with each reference satellite (PRN numbers in the bottom of the plots) for DOY 024. For the convenient interpretation, the clock differences were converted to the distances (cm).

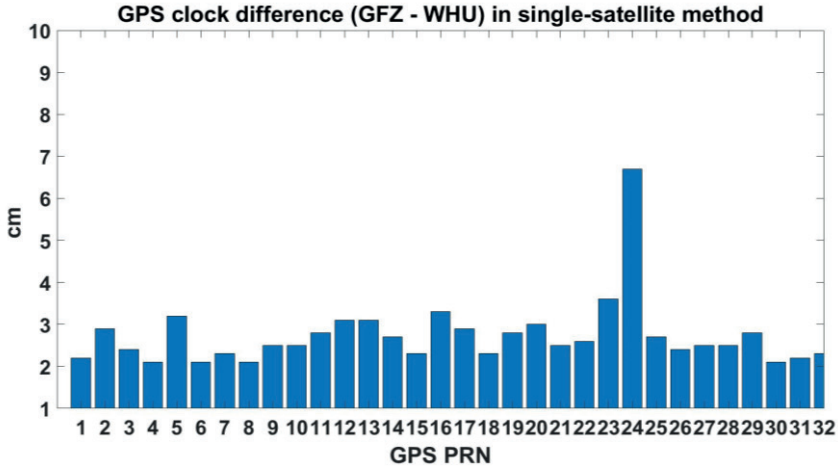
GPS clock difference (GFZ - WHU) in single-satellite method
cm
GPS PRN
1 2 3 4 5 6 7 8 9 10 11 12 13 14 15 16 17 18 19 20 21 22 23 24 25 26 27 28 29 30 31 32

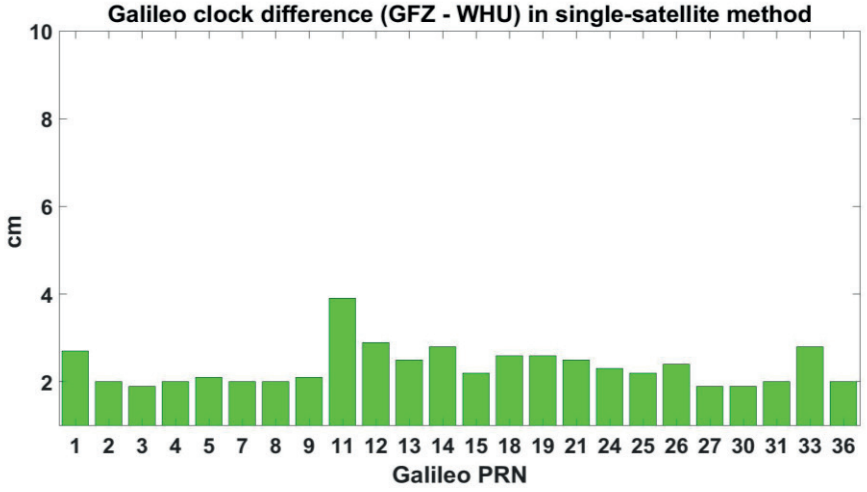
Galileo clock difference (GFZ - WHU) in single-satellite method
cm
Galileo PRN
1 2 3 4 5 7 8 9 11 12 13 14 15 18 19 21 24 25 26 27 30 31 33 36

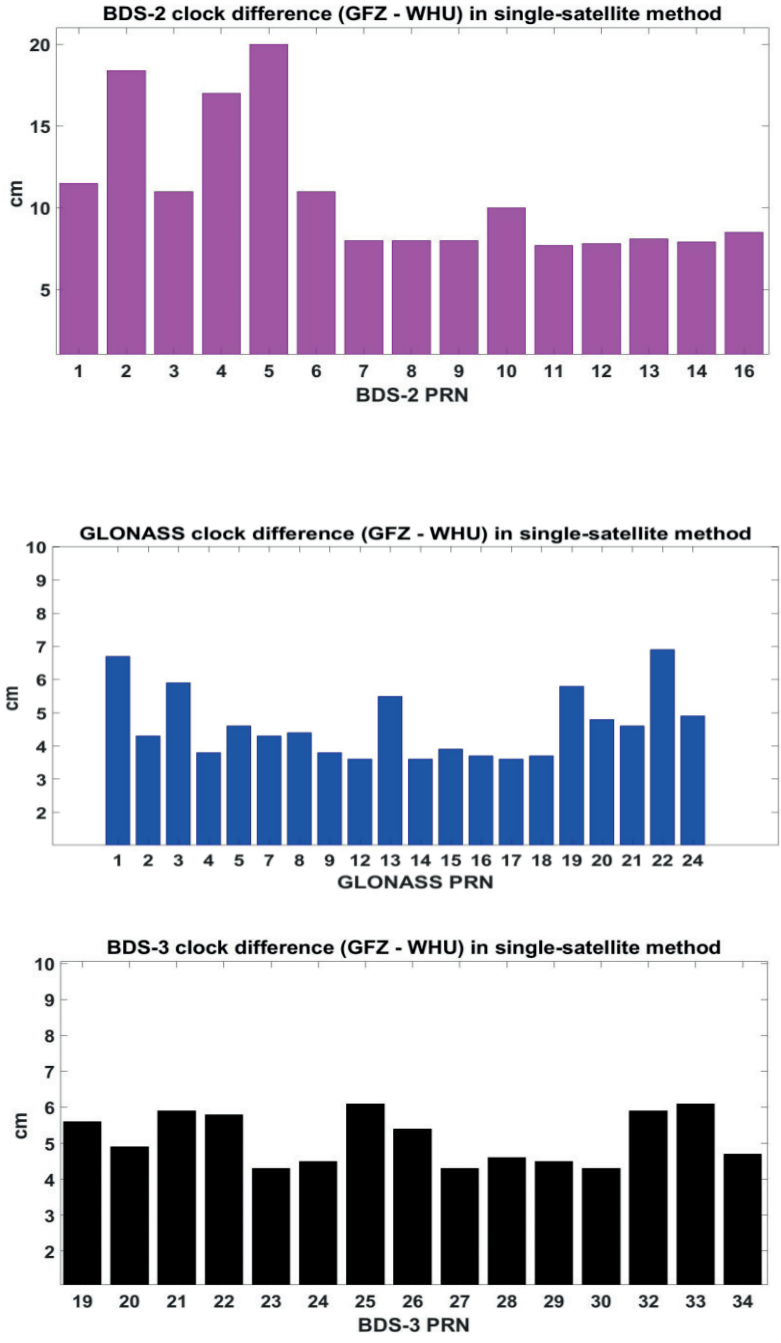

Figure 1. Average standard deviation of the clock differences for DOY 024 w.r.t. each reference satellite in single-satellite method.

As shown in Figure 1, changing the reference satellite affects the results to some extent in the single-satellite method. The results also showed that choosing some satellite as a reference satellite significantly deviated the results from the average value. Fluctuations in the results are rather less for GPS and Galileo compared to GLONASS and BDS. Since the BDS-2 clock differences between GFZ and WHU are much higher than the other GNSS, the vertical scale was set to 20 cm for BDS-2.

To investigate which precision criteria of the reference satellites affects the results, overlapped hadamard deviation, fitting precision, and frequency accuracy [Maciuk et al., 2021] criteria for clock biases are investigated for each GNSS. The overlapped hadamard deviation which is not affected by the linear frequency drift for the clock bias data is defined as (Chen et al., 2021):

$$H\sigma^2(\tau) = \frac{1}{6\tau^2(N-3m)}\sum_{i=1}^{N-3m}(x_{i+3m} - 3x_{i+2m} + 3x_{i+m} - x_i)^2 \quad (6)$$

where $H\sigma^2(\tau)$ is the overlapped hadamard variance, x_i is the satellite clock offset at the epoch time, N is the number of clock biases, m is the smoothing factor, τ is the sampling interval. The square root of the hadamard variance, which is called hadamard deviation, represents the frequency stability.

The frequency accuracy describes the degree of consistency of the actual frequency with respect to the nominal value. It can be defined as (Pan, 2020):

$$K_T = \frac{\sum_{i=1}^{N}(x_i-\bar{x})*(t_i-\bar{t})}{\sum_{i=1}^{N}(t_i-\bar{t})^2} \quad (7)$$

where K_T denotes the frequency accuracy, $\bar{x}$ denotes the mean value of the clock biases, t_i is the second of the corresponding epoch, $\bar{t}$ is the mean second of all epochs.

A quadratic polynomial model containing the phase, frequency, and frequency drift is usually used to evaluate precision index of the satellite clock. The following quadratic polynomial model can be expressed as follows (Cao et al., 2023):

$$x_i = a_0 + a_1(t_i - t_0) + a_2(t_i - {t_0}^2) + \varepsilon_i \quad (8)$$

where a_0, $a_1$and a_2 denote the phase, frequency, and frequency drift of the clock offset fitted by the least-square adjustment, t_i and t_0 denote the observation epoch and reference epoch, ε_i denote the fitting residual.

Since the biggest clock difference was computed while taken GPS G24 as a reference satellite in the single-satellite method, GPS G24 satellite was taken as an example for investigating the hadamard deviation, frequency accuracy, and fitting residuals.

In order not to take up unnecessarily large space in the article, only fitting residuals of GFZ were given for each GNSS. Since GFZ and WHU results are very close to each other, only GFZ results are given. Figure 2 shows the fitting residuals results for DOY 024 in 2021.

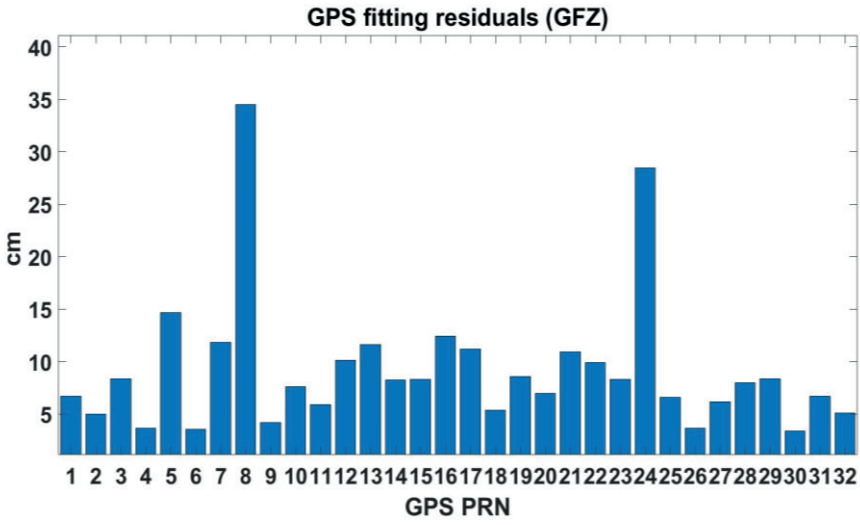

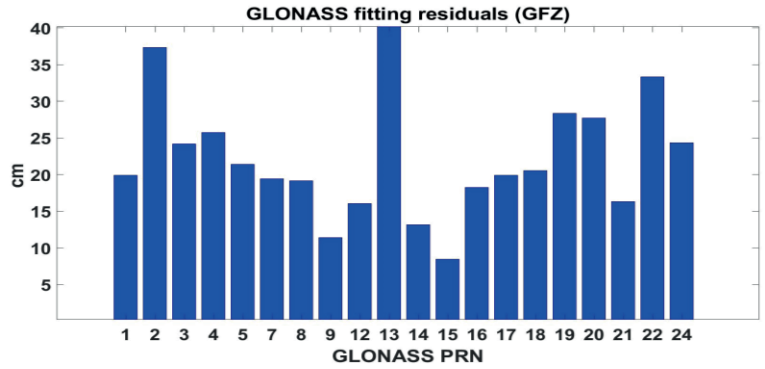
GLONASS fitting residuals (GFZ)
cm
40
35
30
25
20
15
10
5
1 2 3 4 5 7 8 9 12 13 14 15 16 17 18 19 20 21 22 24
GLONASS PRN

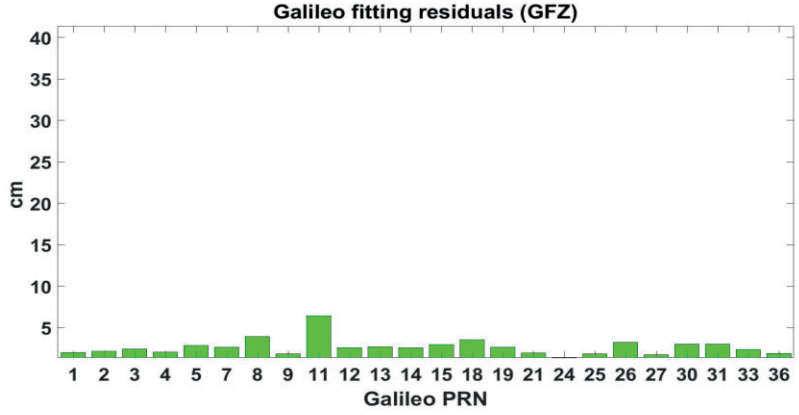
Galileo fitting residuals (GFZ)
cm
40
35
30
25
20
15
10
5
1 2 3 4 5 7 8 9 11 12 13 14 15 18 19 21 24 25 26 27 30 31 33 36
Galileo PRN

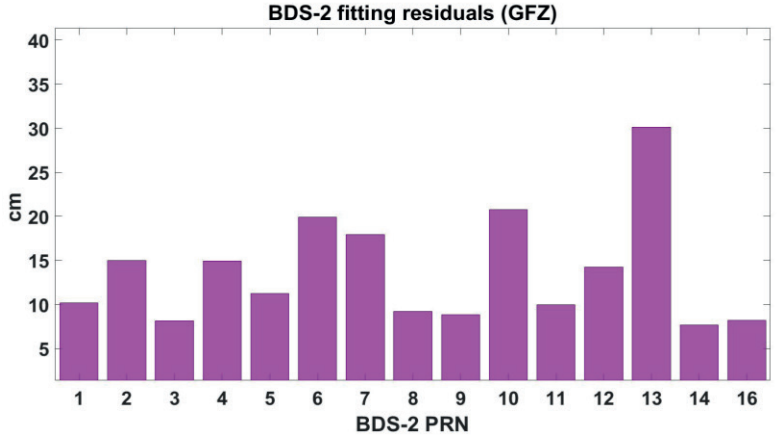
BDS-2 fitting residuals (GFZ)
cm
40
35
30
25
20
15
10
5
1 2 3 4 5 6 7 8 9 10 11 12 13 14 16
BDS-2 PRN

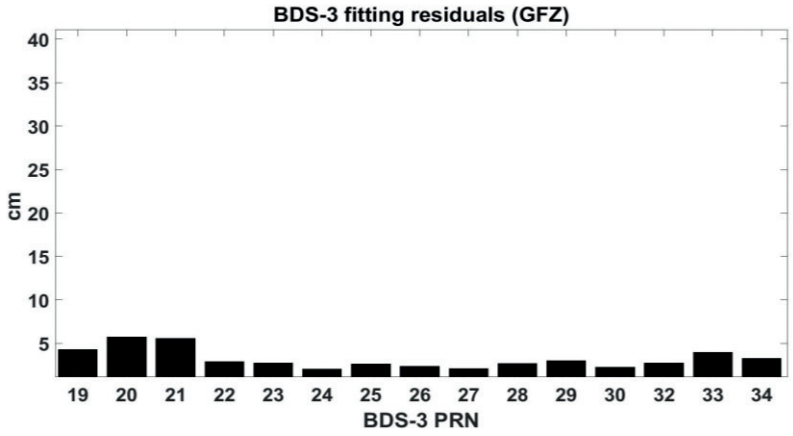

Figure 2. The results of the fitting residuals for each GNSS (DOY:024 in 2021)

As seen from the results of the fitting residuals, the results vary among the GNSS constellations. For GPS, the fitting results of PRN 08 and 24 are significantly higher than other GPS satellites. The main reason behind these differences is the stability of the different types of satellite clock oscillators. Cesium (Cs) clock is operating for GPS 08 and 24, which its stability is lower than the rubidium (Rb) and Passive Hydrogen Maser (PHM). The other GPS satellites have Rb clocks. Since all BDS-3 and most of the Galileo satellites have PHM (Pirti et al., 2021), theirs fitting residuals are lower compared to GPS, GLONASS, and BDS-2. All GLONASS satellites have Cs clock, which has the poorest stability among the atomic clocks. That is why the highest fitting residuals were observed for GLONASS satellites (Cao et al., 2021; BEZCİOĞLU et al.). Rb clocks are also operating for all BDS-2 satellites.

The results of the hadamard deviation are similar to the fitting residuals i.e., the lower the quality of the satellite clock oscillators, the higher the hadamard deviation. For GPS 08 and 24 satellites, the hadamard deviation was computed around 1.32×10^{-13}, the average value for other GPS satellites was computed 4.66×10^{-14}, which is roughly one magnitude lower than the value

of GPS 08 and 24. The same is true for other GNSS constellation, but the differences of hadamard deviations among the satellites are more evident for GLONASS and BDS-2 (Öğütcü et al., 2022). When the results of the frequency accuracy are investigated, no correlation was found with respect to the fitting accuracy and hadamard deviation. Therefore, the results of the frequency accuracy are omitted for the rest of the manuscript.

When the results of the single-satellite method and the results of fitting accuracy are investigated, it can be seen that choosing the reference satellite which has the high stability or low stability doesn't not directly affect the clock differences in the single-satellite method. For example, GPS 08 has the lowest fitting accuracy, but when chosen as a reference satellite, clock differences in the single-satellite method are relatively small compared to other reference satellites. For GLONASS, PRN 13 has the lowest fitting accuracy, when it is chosen a reference satellite, the clock differences are lower than some GLONASS satellites. For BDS-2, PRN 13 has the lowest fitting accuracy, yet when chosen as a reference satellite the clock differences are lower than most BDS-2 satellites. Therefore, the results proved that no direct relationship between the clock differences and the stability of the chosen reference satellites.

Table 1 shows the mean values, computed using one week of GFZ clock data, of the fitting residuals and overlapped hadamard deviation for each GNSS constellation. Since the GFZ and WHU results are very close to each other, only the results from GFZ are given due to save the space of the manuscript.

Table 1. The results of fitting residuals and hadamard deviation

Items	Fitting residuals (cm)	Hadamard deviation
GPS	9.6	5.47×10^{-14}
GLONASS	24.0	1.25×10^{-13}
Galileo	3.0	1.80×10^{-14}
BDS-2	12.0	4.87×10^{-14}
BDS-3	5.1	2.49×10^{-14}

As seen from Table 1, the fitting residuals and hadamard deviation show the strong correlation with respect to the quality of the satellite clock oscillators. Table 2 shows the mean standard deviation of clock differences, using one week of clock data, of the single-satellite and all-satellite methods for each GNSS constellation.

Table 2. The standard deviation results of the single-satellite and all-satellite methods (unit: cm)

Items	Single satellite	All satellite
GPS	2.6	1.8
GLONASS	5.2	3.5
Galileo	2.8	1.9
BDS-2	11.0	7.3
BDS-3	6.4	4.3

When computing the daily single-satellite results, each satellite was taken as a reference satellite for each GNSS. Then, the average of one week's result was computed. For all-satellite results, since all satellites are chosen as a reference satellite in a single step, one clock difference result was computed daily for each GNSS.

As seen from the results, the all-satellite method always produced a smaller clock difference compared to the single-satellite method for each GNSS, which means that ACs-specific clock datum differences can be better removed (in terms of the standard deviation) by the all-satellite method. Except for the mean values, daily results also showed that the all-satellites method always produces smaller daily difference among the multiple daily results of the

single-satellite method using each satellite as a reference satellite. The minimum and maximum clock differences were computed for GPS and BDS-2 satellites, respectively, for each method.

4. Conclusion

In this study, the single-satellite and all-satellite methods for the clock comparison were investigated using the one week of clock data from GFZ and WHU ACs. For the single-satellite method, the relationship between the clock difference and the three clock stability parameters of the chosen reference satellite – namely, the clock fitting precision, overlapped hadamard deviation and frequency accuracy – was investigated. The results showed that the stability parameters of the chosen reference satellite have no direct effect on the clock differences. Therefore, a prerequisite, such as choosing the reference satellite with the highest precision for smaller clock differences, is not necessary in the single-satellite method. The clock differences in the single-satellite method depend on the chosen reference satellite. For some chosen reference satellite, the standard deviation of the clock differences is quite high among the other chosen reference satellite.

When the all-satellite method is investigated, it was seen that clock differences of the all-satellite method are smaller than the single-satellite method for each day and GNSS constellation. This proves that ACs-specific clock datum differences can be better removed by the all-satellite method in terms of the standard deviation. Moreover, the necessity of choosing a reference satellite is removed in the all-satellite method.

In essence, when two clock products are compared, the all-satellite method always guarantees the smallest and most realistic standard deviation of the clock differences.

Conflicts of interest

The authors declare no conflicts of interest.

Acknowledgement

The authors thank Salih ALCAY and Huseyin DUMAN for reading and making valuable comments.

References

1. Alçay, S., & Ömer, A. T. İ. Z. (2021). Farklı yazılımlar kullanılarak gerçek zamanlı hassas nokta konum belirleme (RT-PPP) yönteminin performansının incelenmesi. Geomatik, 6(1), 77-83.
2. Bahadur, B., & Nohutcu, M. (2020). Real-time single-frequency multi-GNSS positioning with ultra-rapid products. Measurement Science and Technology, 32(1), 014003.
3. BEZCİOĞLU, M., Tayyib, U. C. A. R., & YİĞİT, C. Ö. Investigation of the capability of multi-GNSS PPP-AR method in detecting permanent displacements. International Journal of Engineering and Geosciences, 8(3), 251-261.
4. Byram, S., & Hackman, C. (2015, April). Multi-GNSS ultra-rapid orbit and clock products from the USNO. In Proceedings of the ION 2015 Pacific PNT Meeting (pp. 151-156).
5. Cao, Y., Huang, G., Xie, S., Xie, W., Liu, Z., & Tan, Y. (2023). An evaluation method of GPS satellite clock in-orbit with periodic terms deducted. Measurement, 214, 112765.
6. Cao, Y., Huang, G., Xie, W., Xie, S., & Wang, H. (2021). Assessment and comparison of satellite clock offset between BeiDou-3 and other GNSSs. Acta geodaetica et geophysica, 56, 303-319.
7. Chen, J., Zhao, X., Hu, H., Ya, S., & Zhu, S. (2021). Comparison and assessment of long-term performance of BDS-2/BDS-3 satellite atomic clocks. Measurement science and technology, 32(11), 115021.
8. Erdem, N., & Demirel, A. (2021). The current state of use of satellite-based positioning systems in Turkey. Intercontinental Geoinformation Days, 3, 46-49.
9. Guo, J., Wang, C., Chen, G., Xu, X., & Zhao, Q. (2023). BDS-3 precise orbit and clock solution at Wuhan University: status and improvement. Journal of Geodesy, 97(2), 15.
10. Guo, J., Xu, X., Zhao, Q., & Liu, J. (2016). Precise orbit determination for quad-constellation satellites at Wuhan University: strategy, result validation, and comparison. Journal of Geodesy, 90, 143-159.
11.Hou, Y., Wang, H., Wang, J., Ma, H., Ren, Y., Li, P., & Wang, Y. (2022). Studies and Analysis of Combining BDS-3/GNSS Ultra-Rapid Orbit Products from Different IGS Analysis Centers. Remote Sensing, 14(23), 6122.

12.Karadeniz, B., Pehlivan, H., & Arı, B. (2023). Examination of the Performance of Precise Point Positioning Technique with Real-Time Products on Smartphones. Advanced Geomatics, 3(1), 33-39.

13.Konukseven, Ceren, Sermet Öğütcü, and Salih Alçay. "GNSS Frequency Availability Analysis." Advanced Geomatics 2.1 (2022): 14-16.

14. Li, X., Ge, M., Dai, X., Ren, X., Fritsche, M., Wickert, J., & Schuh, H. (2015). Accuracy and reliability of multi-GNSS real-time precise positioning: GPS, GLONASS, BeiDou, and Galileo. Journal of geodesy, 89(6), 607-635.

15. Li, X., Wang, Q., Wu, J., Yuan, Y., Xiong, Y., Gong, X., & Wu, Z. (2022). Multi-GNSS products and services at iGMAS Wuhan Innovation Application Center: strategy and evaluation. Satellite Navigation, 3(1), 20.

16. Li, X., Zhang, K., Ma, F., Zhang, W., Zhang, Q., Qin, Y., ... & Bian, L. (2019). Integrated precise orbit determination of multi-GNSS and large LEO constellations. Remote Sensing, 11(21), 2514.

17. Maciuk, K., Kudrys, J., Skorupa, B., & Malkin, Z. (2021). Testing the product quality of Galileo and GPS on-board oscillators. Measurement, 167, 108261.

18. Mikoś, M., Kazmierski, K., & Sośnica, K. (2023). Characteristics of the IGS receiver clock performance from multi-GNSS PPP solutions. GPS Solutions, 27(1), 55.

19. Montenbruck, O., Steigenberger, P., & Hauschild, A. (2015). Broadcast versus precise ephemerides: a multi-GNSS perspective. GPS solutions, 19, 321-333.

20.Ogutcu, S. (2020). Performance assessment of IGS combined/JPL individual rapid and ultra-rapid products: Consideration of Precise Point Positioning technique. International journal of engineering and geosciences, 5(1), 1-14.

21.Öğütcü, S., Shakor, A., & Farhan, H. (2022). Investigating the effect of observation interval on GPS, GLONASS, Galileo and BeiDou static PPP. International journal of engineering and geosciences, 7(3), 294-301.

22. Pan, X. (2020, June). Performance evaluation and analysis of Galileo satellite clock in orbit. In China Satellite Navigation Conference (CSNC) 2020 Proceedings: Volume II (Vol. 651, p. 422). Springer Nature.

23. Pirti, A., Hoşbaş, R. G., Şenel, B., Köroğlu, M., & Bilim, S. (2021). Galileo uydu sistemi ve sinyal yapısı. Geomatik, 6(3), 207-216.

24. Rovira-Garcia, A., Juan, J. M., Sanz, J., González-Casado, G., Ventura-Traveset, J., Cacciapuoti, L., & Schoenemann, E. (2021). Removing day-boundary discontinuities on GNSS clock estimates: methodology and results. Gps solutions, 25(2), 35.

25. Shi, J., Xu, C., Li, Y., & Gao, Y. (2015). Impacts of real-time satellite clock errors on GPS precise point positioning-based troposphere zenith delay estimation. Journal of Geodesy, 89(8), 747-756.

26.Steigenberger, P., & Montenbruck, O. (2020). Consistency of MGEX orbit and clock products. Engineering, 6(8), 898-903.

27. Uçarli, A. C., Demir, F., Serdar, E. R. O. L., & Alkan, R. M. (2021). Farklı GNSS uydu sistemlerinin hassas nokta konumlama (PPP) tekniğinin performansına etkisinin incelenmesi. Geomatik, 6(3), 247-258.

28. Wang, Z., Li, Z., Wang, L., Wang, X., & Yuan, H. (2018). Assessment of multiple GNSS real-time SSR products from different analysis centers. ISPRS international journal of geo-information, 7(3), 85.

29. Yao, Y., He, Y., Yi, W., Song, W., Cao, C., & Chen, M. (2017). Method for evaluating real-time GNSS satellite clock offset products. GPS Solutions, 21, 1417-1425.

30. Yao, Y., He, Y., Yi, W., Song, W., Cao, C., & Chen, M. (2017). Method for evaluating real-time GNSS satellite clock offset products. GPS Solutions, 21, 1417-1425.

31. Zhang, X., Li, X., & Guo, F. (2011). Satellite clock estimation at 1 Hz for realtime kinematic PPP applications. GPS solutions, 15, 315-324.

32. Zhao, W., Dai, X., Lou, Y., Peng, Y., & Xu, X. (2023). Evaluation of strategies for the ultra-rapid orbit prediction of BDS GEO satellites. Geo-spatial Information Science, 26(1), 16-30.

33. Zhao, Y., Cheng, C., Li, L., Wang, R., Liu, Y., Li, Z., & Zhao, L. (2021). BDS signal-in-space anomaly probability analysis over the last 6 years. GPS Solutions, 25, 1-12.